ALLOY CATALYSTS WITH MONOLITH SUPPORTS FOR METHANATION OF COAL-DERIVED GASES. FINAL TECHNICAL PROGRESS REPORT, APRIL 22, 1975--AUGUST 22, 1977

BRIGHAM YOUNG UNIV., PROVO, UTAH

06 SEP 1977

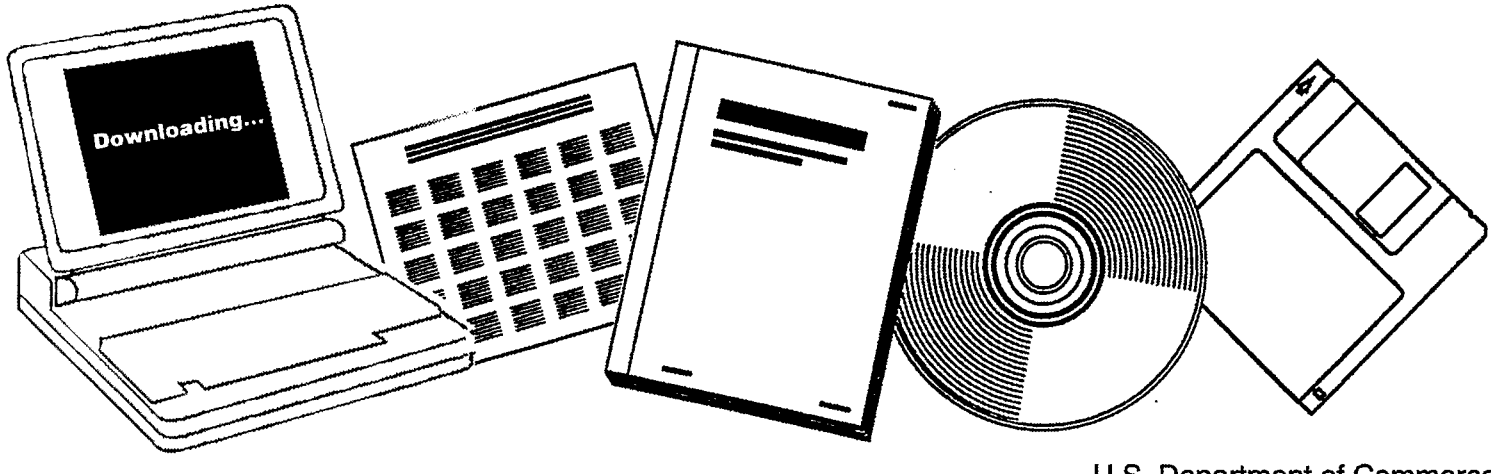

One Source. One Search. One Solution.

NTIS

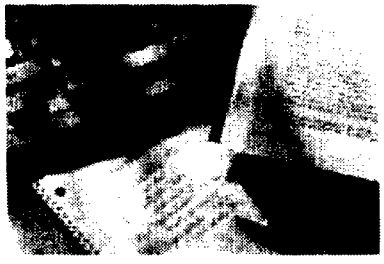

Providing Permanent, Easy Access to U.S. Government Information

National Technical Information Service is the nation's largest repository and disseminator of government-initiated scientific, technical, engineering, and related business information. The NTIS collection includes almost 3,000,000 information products in a variety of formats: electronic download, online access, CD-ROM, magnetic tape, diskette, multimedia, microfiche and paper.

Search the NTIS Database from 1990 forward

NTIS has upgraded its bibliographic database system and has made all entries since 1990 searchable on **www.ntis.gov.** You now have access to information on more than 600,000 government research information products from this web site.

Link to Full Text Documents at Government Web Sites

Because many Government agencies have their most recent reports available on their own web site, we have added links directly to these reports. When available, you will see a link on the right side of the bibliographic screen.

Download Publications (1997 - Present)

NTIS can now provides the full text of reports as downloadable PDF files. This means that when an agency stops maintaining a report on the web, NTIS will offer a downloadable version. There is a nominal fee for each download for most publications.

For more information visit our website:

www.ntis.gov

U.S. DEPARTMENT OF COMMERCE
Technology Administration
National Technical Information Service
Springfield, VA 22161

FE-1790-9
Distribution Category UC-90c

ALLOY CATALYSTS WITH MONOLITH SUPPORTS FOR METHANATION OF COAL-DERIVED GASES

Final Technical Progress Report
For Period April 22, 1975 to August 22, 1977

Calvin H. Bartholomew

Brigham Young University
Provo, Utah 84602

Date Published -- September 6, 1977

PREPARED FOR THE UNITED STATES
ENERGY RESEARCH AND DEVELOPMENT ADMINISTRATION

Under Contract No. EX-76-S-01-1790

FOREWORD

This report summarizes technical progress during the first two years and a four month contract extension period (April 22, 1975 to August 22, 1977) of a study conducted for the Energy Research and Development Administration (ERDA) under Contract No. EX-76-S-01-1790. The principal investigator for this work was Dr. Calvin H. Bartholomew; Dr. Paul Scott was the technical representative for ERDA.

The following students contributed to the technical accomplishments and to this report: Graduates - Blaine Barton, Kyung Sup Chung, Erek Erekson, Richard Fowler, George Jarvi, Don Stowell, Richard Turner, and Gordon Weatherbee, and Undergraduates - Ken Atwood, Ray Eelsing, Scott Engstrom, Kevin Mayo, Don Mustard, and Norman Shipp. Elaine Alger and Scott Folster provided typing and drafting services. The assistance of Professor Charles Pitt (Department of Mining, Metallurgical and Fuels Engineering, University of Utah) in providing us with x-ray diffraction data is gratefully acknowledged. For the Auger and ESCA data the assistance of Dr. Bernard J. Wood of SRI and of Dr. Joseph Andrade and Dr. Robert N. King of the Surface Analysis Laboratory of th University of Utah is likewise acknowledged.

TABLE OF CONTENTS

LIST OF TABLES

LIST OF FIGURES

ABSTRACT

Catalytic activities for methanation of carbon monoxide have been determined for alumina-supported cobalt, nickel, ruthenium, and bimetallic combinations of nickel with cobalt, iron, molybdenum oxide, palladium, platinum, rhodium, and ruthenium before and after exposure to low concentrations of hydrogen sulfide in hydrogen. The catalyst samples were prepared by impregnation techniques and characterized by means of hydrogen and carbon monoxide chemisorption, x-ray diffraction, Auger Spectroscopy, and ESCA. Activity tests at 225 and 250°C and 1 atm show the order of specific activity to be Co > Ni-Co > Ni > Ni-MoO_3 > Ni-Pt > Ni-Ru; after 12-24 hours exposure to 10 ppm H_2S the order of activity is Ni-Co > Co > Ni-MoO_3 > Ni > Ni-Pt > Ni-Ru. The specific activities based on catalytic surface area of Ni-Co, Ni-Ru, and Ni-MoO_3 actually increase after exposure to H_2S. The six most promising catalyst compositions in both pellet and monolithic form were reactor tested to determine (i) conversion-temperature behavior at 1 and 25 atm, (ii) effects of reactant steam, carbon deposition, and *in situ* exposure to H_2S on catalytic activity, and (iii) differences in methane production for pellet and monolithic catalysts having different support geometries. The conversion-temperature data show that the rate of methane production on nickel is increased two-three fold at high conversions and four-five fold at low conversions by increasing the reaction pressure from 1 to 25 atm. Addition of reactant steam dramatically increases carbon dioxide production while decreasing methane production. In carbon deposition tests at 400-450°C ($H_2/CO = 2$) alumina-supported Ni, Ni-Co, Ni-Pt, Ni-Rh, and Ni-Ru lose 30-50% of their activity after 7-10 hours, while Ni-MoO_3/Al_2O_3 is completely deactivated. Monolithic-supported nickel is significantly more active for methane production than pellet-supported nickel. These and other significant results are presented and discussed. An account of technical communications with other workers and visits to other laboratories is also included.

I. OBJECTIVES AND SCOPE

A. Background

Natural gas is a highly desirable fuel because of its high heating value and nonpolluting combustion products. In view of the expanding demand for and depletion of domestic supplies of clean fuels, economic production of synthetic natural gas (SNG) from coal ranks high on the list of national priorities.

Presently there are several gasification processes under development directed toward the production of SNG. Although catalytic methanation of coal synthesis gas is an important cost item in each process, basic technological and design principles for this step are not well advanced. Extensive research and development are needed before the process can realize economical, reliable operation. Specifically, there appear to be important economical advantages in the development of more efficient, stable catalysts.

From the literature (1,2), three major catalyst problems are apparent which relate to stability: (i) sulfur poisoning, (ii) carbon deposition with associated plugging, and (iii) sintering. Our understanding of these problems is at best sorely inadequate, and the need to develop new and better catalyst technology is obvious. Nevertheless, there has been very little reseach dealing with new catalyst concepts such as bimetallic (alloy) or monolithic-supported catalysts for methanation. This study deals specifically with sulfur poisoning, carbon deposition, and the effects of support (monolith and pellet) geometry on the performance of alloy methanation catalysts.

B. Objectives

The general objectives of this research program are (i) to study nickel and ruthenium alloy catalysts in the search for catalysts resistant to poisoning and carbon deposition and (ii) to investigate the effects on catalytic efficiency of support (monolith and pellet) geometry. The work was divided into five tasks, most of which were to be completed in the first two years:

Task 1. Prepare pellet- and monolithic-supported nickel and ruthenium methanation catalysts by impregnation with metal salts of nickel, ruthenium, iron, platinum, etc. followed by reduction in hydrogen. Measure hydrogen and carbon monoxide chemisorption uptakes before and after exposure to hydrogen sulfide. Examine metallic phases of these catalysts by x-ray diffraction for chemical composition

and particle size.

Task 2. Design and construct a continuous flow laboratory reactor system capable of 25-1000°C and 1-25 atm to be used for screening methanation catalysts and investigating effects of sulfur poisoning on methanation activity.

Task 3. Screen catalysts prepared in Task 1 using a reactor system constructed in Task 2 to determine methanation catalyst activity before and after exposure to 10 ppm H_2S.

Task 4. Compare the most promising catalysts based on the results of Tasks 1 and 3 for steady-state catalytic activity on different pellet and monolith supports of different hole sizes and geometries under various operating conditions, i.e., temperature, pressure, H_2/CO ratio and H_2S level.

Task 5. Maintain close communication with organizations doing similar research such as the Bureau of Mines, Bituminous Coal Research, Institute of Gas Technology, and others.

C. Technical Approach

The main features of the technical approach used to accomplish the above outlined tasks are reviewed here.

Task 1: Catalyst preparation and characterization. Alumina pellets and extruded monolithic ceramic supports (provided by Corning Glass Works) coated with high surface area alumina were impregnated with nickel nitrate and alloying metal salt. Metals alloyed with nickel included cobalt, iron, molybdenum, rhodium, ruthenium, platinum, and palladium. Ruthenium was used in combination with nickel, cobalt and palladium. Approximately equimolar quantities of base metals were used in combination with nickel or other base metals; relatively small amounts of noble metal were used in combination with base metals. Catalyst samples were dried in vacuum at 70-100°C, reduced at 500°C in flowing hydrogen, and carefully passivated with 1% air in preparation for further testing. A dedicated reduction apparatus was used to reduce and passivate large batches of pellets and monolithic catalysts. Alloy catalysts were initially prepared in pellet form for chemisorption, x-ray diffraction, and reactor screening measurements. Only the more promising catalysts were prepared in monolithic form.

Hydrogen and carbon monoxide chemisorption uptakes were measured using a conventional volumetric apparatus before and after exposure of each catalyst to 10 ppm H_2S over a period of several hours in a dedicated poisoning apparatus. X-ray diffraction measurements were carried out to determine the active metallic phases and metal crystallite

size where possible.

Task 2: Laboratory reactor construction. Our continuous-flow reactor system was designed for either differential or integral activity testing to 400 psig and 1000°C. Use of calibrated mass flow meters enabled variations in feed composition. Reactant and product gases were analyzed by means of gas chromatography.

Task 3: Reactor screening of alloy catalysts. Catalyst samples were screened on the basis of steady-state methanation activity (reaction rate based upon catalyst mass or surface area) measured in a differential flow reactor at atmospheric pressure and 225 and 250°C at a H_2/CO ratio of 4.0. Both freshly-reduced catalysts and catalyst samples exposed in a separate poisoning system to 10 ppm H_2S over a period of 6-18 hours were tested.

Task 4: Catalyst geometry testing and design. The most promising catalysts based on the results of screening were tested for activity and conversion as a function of pressure, temperature, H_2/CO ratio, and H_2S concentration. The effects of water addition to the feed stream were also investigated. Conversion of carbon monoxide to methane during *in situ* exposure to low levels of hydrogen sulfide and at low H_2/CO ratios was used as a measure of stability toward sulfur poisoning and carbon deposition. A comparison of steady-state conversions for monolithic supports of different hole sizes and geometries was made to determine the role of catalyst geometry in methanation. This task was not scheduled for completion until the end of 1977 (as outlined in the proposal).

Task 5: Technical visits and communication. Close communication was maintained with industrial and academic researchers working in methanation catalysis. The principal investigator attended coal and catalysis meetings, visited other laboratories, and received several visitors.

II. EXECUTIVE SUMMARY

A project progress summary is presented in Figure 1 and accomplishments and results are summarized below. Figure 1 shows that Tasks 1, 2, 3, and 5 were completed either on or ahead of schedule. Task 4, Catalyst Testing and Design, will be completed in December 1977 as part of the renewal of this contract.

Accomplishments during the contract period are best summarized according to task:

Task 1. Over 25 alumina pelleted-supported and over 40 monolithic-supported catalysts were prepared with the following metal combinations: Co, Ni, Ni-Co, Ni-Fe, Ni-MoO_3, Ni-Pd, Ni-Pt, Ni-Rh, Ni-Ru, Ru-Co, and Ru-Pd. Hydrogen chemisorptive uptakes were measured for all samples. Also, hydrogen and carbon monoxide uptakes were measured before and after 12-24 hours exposure to 10 ppm H_2S for 15 of these catalysts. Many of the catalysts were further characterized by chemical analysis, x-ray diffraction, electron microscopy, Auger electron spectroscopy and ESCA.

Hydrogen adsorption at 25°C was found to be a reliable means of measuring metal surface area, whereas carbon monoxide adsorption was fraught with complexities. After exposure of nickel-containing catalysts to H_2S, hydrogen chemisorption decreased and carbon monoxide increased both in proportion to the amount of H_2S adsorbed. Thus hydrogen adsorption can be used to measure the extent of sulfur poisoning of nickel catalysts; carbon monoxide is not recommended. The catalysts prepared in this study have generally higher metal surface areas than commercial methanation catalysts and are thermally stable to 450°C.

Task 2. The construction of a single-pass tubular reactor was completed during the fourth quarter, and several minor additions and modifications were made during the fifth and sixth quarters. This reactor is capable of integral or differential operation with variable feed gas compositions and steam injection. The temperature range is 25-1000°C, and the pressure range is 1-25 atm. Gas flows are measured to 1% accuracy by calibrated mass flow meters and gas analysis performed using NDIR and gas chromatography.

A 1 inch I.D. stainless steel reactor can be used to test either pelleted or monolithic catalyst samples at pressure up to 25 atm. Several glass reactors were constructed for differential activity testing of powdered, pelleted, or monolithic samples in the presence of H_2S at low pressures.

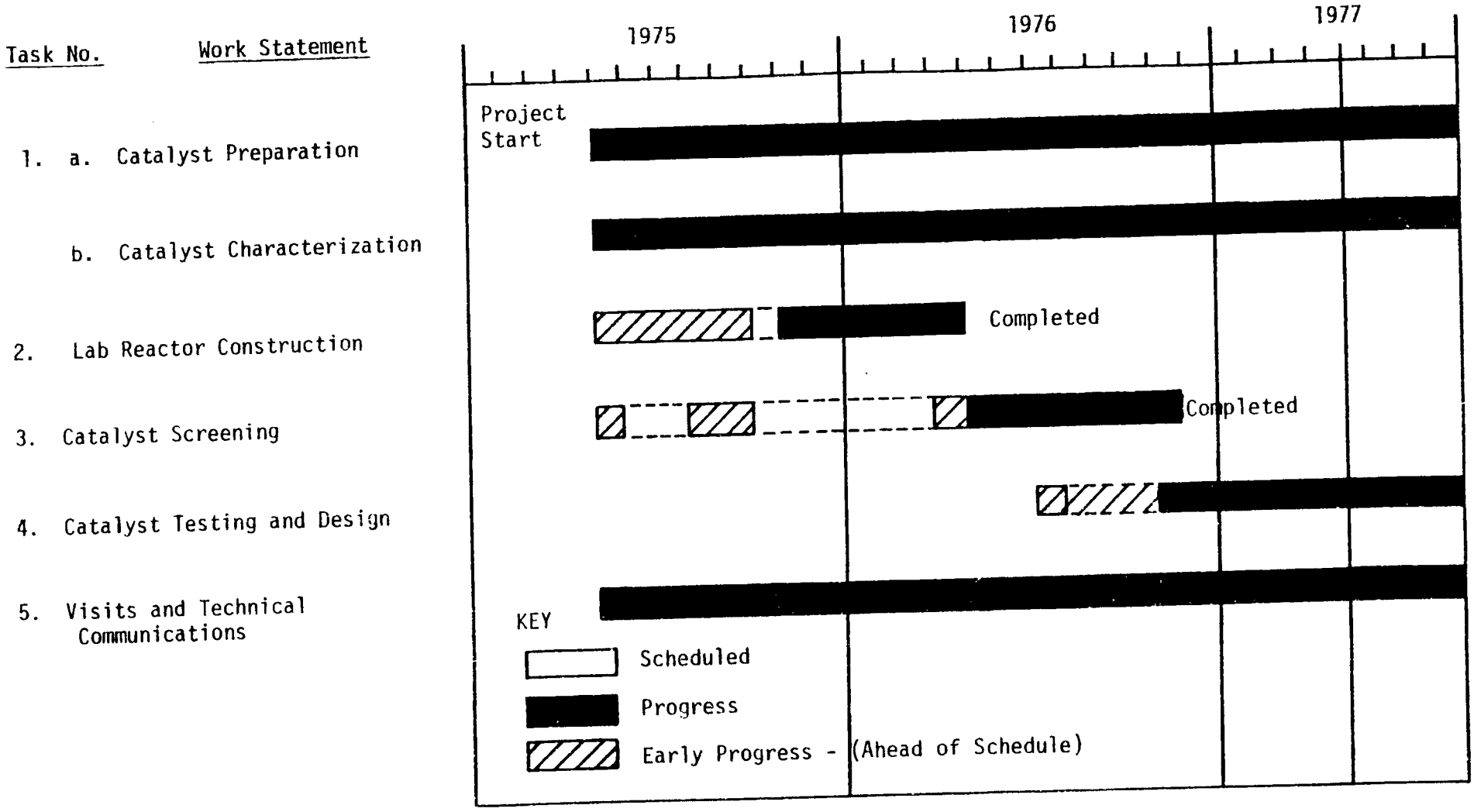

Figure 1. Project Progress Summary.

Task 3. Measurements of specific methanation activity were carried out before and after exposure to 10 ppm H_2S for 25 pellet-supported catalysts. The test conditions were 225 and 250°C, 20.5 psia and a space velocity of 30,000 hr^{-1}. The results show the order of specific activity at 250°C (based upon metal surface area measured by hydrogen adsorption) to be Co > Ni-Co > Ni > Ni-MoO_3 > Ni-Pt ≥ Ni-Ru; after 12-24 hours exposure to 10 ppm H_2S the order of specific activity (based upon remaining catalytic surface area) is Ni-Co > Co > Ni-MoO_3 > Ni > Ni-Pt > Ni-Ru. The activity of the remaining catalytic sites is actually increased in the case of Ni-Co, Ni-Ru, and Ni-MoO_3 catalysts suggesting these catalysts may be more resistant to short term exposure to H_2S than Ni. Several of the nickel and nickel bimetallic catalysts prepared in this study have intrinsic activities exceeding those of typical commercial methanation catalysts by factors of 100 to 200%.

Task 4. Conversion versus temperature (integral) tests were carried out at low pressure for 11 pellet-supported catalysts and at high pressure for 12 pellet-supported catalysts. Also, integral tests at low pressure with 1% reactant steam were carried out on 7 pelleted catalysts and steady state carbon deposition tests were performed for the same catalysts in powder form. Altogether 28 different temperature-conversion tests were conducted on monolithic-supported catalysts at low and high pressures and with 1% water vapor In the reactant mixture. Integral tests for 18 different nickel catalysts of varying monolithic and pellet geometries were also performed.

In the temperature-conversion tests at 1 atm and 15,000 hr^{-1}, 14% Ni/Al_2O_3 and 20% Ni-Co/Al_2O_3 achieved 99% conversion of carbon monoxide at 325°C with yields to methane of 89 and 84% respectively compared to 79% yield for a commercial nickel methanation catalyst. The rate of methane production on nickel is increased 2-3 fold at high conversions and 4-5 fold at low conversions by increasing the reaction pressure from 1 to 25 atm. Addition of 1% steam to the reactants dramatically increases the rate of carbon dioxide production while substantially decreasing methane production, presumably by increasing the rate of the water-gas-shift reaction.

In carbon deposition tests at 400-450°C (H_2/Co = 2), alumina-supported Ni, Ni-Co, Ni-Pt, Ni-Rh, and Ni-Ru lose 30-50% of their activity after 7-10 hours, while Ni-MoO_3/Al_2O_3 is completely deactivated under the same conditions. Temperature-conversion tests at both 15,000 and 30,000 hr^{-1} (1 atm) show that monolithic-supported nickel catalysts are significantly more active than pellet-supported nickel catalysts and commercial nickel catalysts (pellet form) on either a mass or volume basis. Thus, monolithic-supported catalysts are especially attractive

for achieving high conversions of CO to CH_4 in a high throughput recycle methanator.

Task 5. During the first year the principal investigator attended the Symposium on Catalytic Conversion of Coal, April, 1975; ERDA/EPRI/NSF-RANN Contractors Conference, October, 1975; California Catalysis Society Meeting, November, 1975; 68th Annual AIChE Meeting in Los Angeles, November, 1975; First Rocky Mountain Fuel Symposium, January, 1976 where Blaine Barton gave a paper; and the Spring Meeting of the California Catalysis Society in March, 1976 where Richard Pannell presented a paper. During the second year and the contract extension period Dr. Bartholomew also attended the Gordon Research Conference in June, 1976; the Centennial Meeting of the American Chemical Society where he presented two papers; the Second Rocky Mountain Fuel Symposium with six students where George Jarvi gave a paper; the Spring Meeting of the California Catalysis Society (1977) where he presented a paper; North American Catalysis Society Meeting where he and Mr. Richard Pannell each gave papers; and a special conference of Chemical Engineering Educators at Snowmass, Colorado. Recently Dr. Bartholomew attended the ERDA/EPRI Contractors Meeting in Pittsburgh and presented a paper at the National ACS meeting in Chicago.

During the contract period Dr. Bartholomew visited other catalysis laboratories at the National Bureau of Standards, Carnegie-Mellon University, Pittsburgh Energy Research Center, Institute of Gas Technology, Stanford Research Institute, Stanford University, University of Utah, Continental Oil Company, University of Idaho (Moscow), University of Wisconsin (Madison), and Ventron Corporation. Also, our laboratory was visited by Professor Michel Boudart of Stanford University, Mr. Tony Lee of IGT, Mr. Bill Boyer of Corning Glass Works, Mr. Robert Wade of Ventron Corporation, Dr. Gerald Krulik of Borg-Warner Chemicals, Drs. Ed Tucci and George McGuire of Matthey Bishop Inc., Mr. Fred Hoover and Dr. Larry Guibault of Ventron, and Professor Alex Bell of Berkeley.

Journal publications from this study include two that have been accepted, one that is submitted, and four that are in preparation. Eight graduate and seven undergraduate students have contributed to this research project. Three students have completed a masters thesis in connection with this work, three others students have master's research in progress, and two others have Ph.D. research underway.

III. DETAILED DESCRIPTION OF TECHNICAL PROGRESS

A. Task 1: Catalyst Preparation and Characterization

1. Catalyst Preparation

a. Pelleted Samples. Alumina pellet-supported nickel and ruthenium alloy catalysts were prepared by impregnation from aqueous solutions of nitrate salts of the base metals and chloride salts of the noble metals. Table 1 is a list of catalysts prepared with codes, amounts, and compositions. Kaiser SAS 5 x 8 mesh alumina (301 m^2/g) calcined at 600°C for 2 hours was used in all of the preparations. Further details of preparation for each catalyst can be found in earlier quarterly reports (3-10).

b. Monolith Catalysts. Over 80 monolithic catalysts involving five monometallic or bimetallic compositions have been prepared in this research. The various techniques employed have been detailed in the earlier quarterly reports (5-10).

The basic technique is as follows. Research size monoliths (1 inch O.D. by 3 inches long) were obtained from Corning Glass Works in three different geomtries: 200 and 300 squares per square inch and 236 triangles per square inch. In order to reduce the amount of gas needed to supply a space velocity of 30,000 hr^{-1}, the monolith length was cut down to 1/2 inch. These pieces were cleaned and rinsed in nitric acid to remove interfering ions. Several coats of Kaiser SA Medium alumina suspended in pH = 5 water were applied to the monoliths. Between each application, the monoliths were dried at 600°C to fix the previous coat before immersing it again. After a loading of 20% alumina was achieved, the coated monoliths were dipped in the appropriate metal salt solution. Often, the repeated dipping loosened the alumina substrate, hence calcining between dips at 200°C was found to be necessary. When a sufficient amount of metal salt had been impregnated upon the monoliths, they were carefully heated to 450°C in a hydrogen atmosphere. The temperature ramp was set in the range of 5°C/min with a hold at about 220°C for 1 hour to decompose the nitrate and thereby prevent highly exothermic ammonia formation. After reduction, the catalysts were slowly exposed to air (passivated) at 25°C to prevent sintering of the active metal upon exposure to the atmosphere.

Table 2 is a summary of monolithic catalysts prepared during the contract period; alumina and metal compositions are listed in weight percent along with references to the details of preparation. Several of the monolithic Ni, Ni-MoO_3, Ni-Pt and Ni-Ru catalysts were prepared during

TABLE 1

Preparation of Alumina-Supported
Nickel and Nickel-Alloy Catalysts

Catalyst	Code	Amount	Composition (wt.%)	Preparation
Ni/Al_2O_3	Ni-A-111	500g	3.0% Ni	2 impregnations
$Ni-Ru/Al_2O_3$	Ni-Ru-A-100	20g	2.5% Ni .5% Ru	acidic 1 impreg.
$Ni-Ru/Al_2O_3$	Ni-Ru-A-101	20g	2.5% Ni .5% Ru	ion exchange
$Ni-Ru/Al_2O_3$	Ni-Ru-A-102	20g	2.5% Ni .5% Ru	basic 2 impreg.
$Ni-Ru/Al_2O_3$	Ni-Ru-A-103	20g	2.5% Ni .5% Ru	Same as Ni-Ru-A-100
$Ni-Ru/Al_2O_3$	Ni-Ru-A-104	150g	2.5% Ni .5% Ru	acidic 1 impreg.
$Ni-Ru/Al_2O_3$	Ni-Ru-A-105	150g	2.5% Ni .5% Ru	basic 2 impreg.
$Ni-Ru/La/Al_2O_3$	Ni-Ru-La-A-100	20g	2.5% Ni .5% Ru 3.0% La	basic 2 impreg.
$Ni-Ru/La/Al_2O_3$	Ni-Ru-La-A-101	20g	2.5% Ni .5% Ru 3.0% La	acidic 1 impreg.
$Ni-Rh/Al_2O_3$	Ni-Rh-A-100	70g	2.5% Ni .5% Rh	acidic 2 impreg.
$Ni-MoO_3/Al_2O_3$	$Ni-MoO_3$-A-101	200g	2.5% Ni 3.0% MoO_3	basic 5 impreg.
$Ni-Fe/Al_2O_3$	Ni-Fe-A-100	100g	10% Ni 10% Fe	acidic 3 impreg.
$Ni-Co/Al_2O_3$	Ni-Co-A-100	100g	10% Ni 10% Co	neutral 2 impreg.

TABLE 1 continued

Catalyst	Code	Amount	Composition (wt.%)	Preparation
$Ni-Pt/Al_2O_3$	Ni-Pt-A-100	100g	15% Ni 0.5% Pt	slightly acidic 2 impreg.
$Ni-Pd/Al_2O_3$	Ni-Pd-A-100	100g	15% Ni 1% Pd	acidic 2 impreg.
$Ni-Cu/Al_2O_3$	Ni-Cu-A-100	100g	5% Ni 0.6% Cu	neutral solution of nitrates 2 impreg.
MoO_3/Al_2O_3	MoO_3-A-100	100g	3% MoO_3	$(NH_4)_6Mo_7O_{24}\cdot 4H_2O$ dissolved in ammonical solution
$Ru-Co/Al_2O_3$	Ru-Co-A-100	100g	0.52% Ru 15.0% Co	acidic
$Ru-Pd/Al_2O_3$	Ru-Pd-A-100	100g	0.49% Ru 0.51% Pd	acidic 2 impreg.
$Ru-Pt/Al_2O_3$	Ru-Pt-A-100	80g	0.5% Ru 0.5% Pt	$RuCl_3$ and $H_2PtCl_6\cdot 9H_2O$ 2 impreg.
Ni/Al_2O_3	Ni-A-112	500g	3% Ni	2 impregnations
Ni/Al_2O_3	Ni-A-116	500g	15% Ni	neutral 7 impreg.
Co/Al_2O_3	Co-A-100	100g	20% Co	neutral 3 impreg.
$Ni-MoO_3/Al_2O_3$	$Ni-MoO_3$-A-102	---	10% Ni 10% Mo	---
$Ni-Rh/Al_2O_3$	Ni-Rh-A-100	70g	2.5% Ni 0.5% Rh	acidic 2 impreg.
$Ni-Ru/Al_2O_3$	Ni-Ru-A-106	---	16.6% Ni 3.4% Ru	---
$Ni-Ru/Al_2O_3$	Ni-Ru-A-107	---	16.6% Ni 3.4% Ru	---

TABLE 2

Preparation of Monolithic Supported Nickel and Nickel Alloy Catalysts

Catalyst	Code	Composition (wt.%) Alumina	Ni	Other	Preparation Ref.
$Ni/Al_2O_3/M$ on 3" monolith	Ni-M-101	13.5	15.7		QPR-3, page 10 1" DIA x 3" CGW monoliths coated with powdered alumina and impregnated with nickel nitrate by various procedures.
	Ni-M-103	13.2	13.7		
	Ni-M-104	19.9	15.9		
	Ni-M-105	12.6	16		
	Ni-M-106	14.1	18.5		
$Ni/Al_2O_3/M$ on 1/2" monoliths	Ni-M-107	20	15		QPR-6, page 7 1" DIA x 1/2" monoliths alumina washcoat sintered at 600°C, nickel nitrate reduced in H_2 at 450° experienced over-temperature.
	Ni-M-108	21	15		
	Ni-M-109	19	14		
	Ni-M-110	20	15		
	Ni-M-111	21	16		
	Ni-M-112	18	15		
	Ni-M-113	19	20		QPR-7, page 7 experienced temperature excursion during reduction
	Ni-M-114	20	20		
	Ni-M-115	19	19		
	Ni-M-117	20	12		QPR-7, page 7 had higher H_2 uptakes than the previous group
	Ni-M-118	20	11		
	Ni-M-119	20	12		
	Ni-M-120	19.9	6.9		QPR-8, page 8
	Ni-M-121	20.0	5.9		
	Ni-M-122	20.0	7.4		
	Ni-M-123	19.9	11.2		
Ni/Al_2O_3 for different geometry comparison	Ni-M-204 thru -209	~20	6		QPR-8, page 8
	Ni-M-204 thru -209	~17	15		QPR-8, page 8
	Ni-M-303	~19	20		QPR-8, page 8
Ni/Al_2O_3 on 200□/in^2	Ni-M-151	19.4	19.1		Page 9 this report carefully controlled procedures to ensure representative loading were employed.
	Ni-M-152	19.1	19.4		
	Ni-M-154	19.5	18.6		
Ni/Al_2O_3 on 236△/in^2	Ni-M-250	20.6	22.2		
	Ni-M-252	19.8	21.8		
	Ni-M-254	21.9	21.7		
Ni/Al_2O_3 on 300□/in^2	Ni-M-350	19.0	18.0		
	Ni-M-351	19.6	19.8		

TABLE 2 continued

Catalyst	Code	Composition (wt.%) Alumina	Ni	Other	Preparation Ref.
$Ni/Co/Al_2O_3$	Ni-Co-M-100	18.8	4.4	4.4(Co)	QPR-7, page 7
	Ni-Co-M-101	20.4	4.0	4.0	May have sintered in
	Ni-Co-M-102	19.0	3.4	3.4	reduction.
	Ni-Co-M-103	17.3	4.5	4.5(Co)	QPR-8, page 8
	Ni-Co-M-104	18.3	5.1	5.1	
	Ni-Co-M-105	18.5	5.5	5.5	
	Ni-Co-M-106	19.6	4.8	4.8	
	Ni-Co-M-107	16.5	5.3	5.3	
	Ni-Co-M-108	17.1	6.4	6.4	
$Ni/MoO_3/Al_2O_3$	$Ni-MoO_3$-M-100	18	1.6	1.6(MoO_3)	QPR-8, page 8
	$Ni-MoO_3$-M-101	19	1.8	1.8	
	$Ni-MoO_3$-M-102	17	1.6	1.6	
	$Ni-MoO_3$-M-103	21	3.9	3.9(MoO_3)	Page 14 this report
	$Ni-MoO_3$-M-104	18	3.1	3.1	Numbers 103, 104 and 105
	$Ni-MoO_3$-M-105	18	3.0	3.0	actually were coated and reduced twice.
	$Ni-MoO_3$-M-106	20.4	4.2	4.2(MoO_3)	
	$Ni-MoO_3$-M-107	19.7	4.1	4.1	
	$Ni-MoO_3$-M-108	20.4	3.9	3.9	
$Ni/Pt/Al_2O_3$	Ni-Pt-M-100	20.7			Page 14 this report
	Ni-Pt-M-101	19.8			
	Ni-Pt-M-102	20.5			
	Ni-Pt-M-107	20.0	11.0	0.58	
	Ni-Pt-M-108	18.5	10.4	0.56	
	Ni-Pt-M-109	19.7	10.3	0.55	
	Ni-Pt-M-110	19.3	10.3	0.55	
$Ni/Ru/Al_2O_3$	Ni-Ru-M-100 thru -105	~20	~10	~2	Page 14 this report
	Ni-Ru-M-108	19.3	5.8	1.2	
	Ni-Ru-M-109	19.5	8.8	1.8	
	Ni-Ru-M-110	21.1	~ 3.3	~0.7	
	Ni-Ru-M-111	18.4	~10	~1	
	Ni-Ru-M-112	18.5	~10	~1	

the ninth quarter. Additional nickel catalysts were prepared for the geometry comparison tests. Five monoliths of each geometry were carefully prepared sinultaneously using identical preparation techniques and loadings in order to produce more uniform samples than before. Of these fifteen samples, the most apparently uniform (eight) were chosen for further testing.

Three of the six Ni-MoO_3 catalysts prepared during the previous quarter were re-impregnated and reduced along with three new samples. The percent metal loadings were increased from about 3% to around 7%, although in the process some of the alumina substrate was lost. These three new catalysts were estimated to contain 8% metal after reduction.

Seven Ni-Pt monoliths were prepared during the past quarter. The first three were ruined after the impregnation and drying steps by overnight exposure to air at room temperature. Apparently, the hydroscopic metal salts adsorbed water from the air causing the crystals to liquify. The alumina layers, in fact, were wet to the touch and sloughed off upon further dipping in the impregnating solution. After precautions were taken to prevent the monoliths from being exposed to air for significant periods of time, four more Ni-Pt monoliths were successfully prepared.

The first six Ni-Ru monoliths were prepared by dissolving the hydrated $RuCl_3$ salt with nickel nitrate in sufficient quantity to produce monoliths with 15% Ni and 3% Ru. Unfortunately, these catalysts were accidentally immersed in water overnight, and may have lost as much as half of their metal loading.

In the preparation of the bimetallic catalysts it was necessary to use chloride salts of the noble metals. Unfortunately, chlorine and/or chlorides are poisons for methanation. Hence, the six Ni-Ru catalysts were washed in Na_2CO_3 solution so as to remove Cl^- from the surface. The samples were then rinsed in distilled water until the rinse water showed no sign of CO_3 or Cl^- by testing with $AgNO_3$ and were then reduced in hydrogen. Because of the uncertainty in the metal loadings for the six Ni-Ru catalysts (100-105), seven more Ni-Ru monoliths were prepared for testing (106-112). Of these, only Ni-Ru-M-110 was washed in Na_2CO_3 solution. In the process an unknown amount of catalyst and alumina was lost. For future work it is recommended that the Na_2CO_3 wash be used only after high temperature reduction of the catalyst.

2. <u>Hydrogen and Carbon Monoxide Chemisorption on Nickel and Nickel Alloys and Effects of Hydrogen Sulfide on Adsorption</u>.

a. Equipment and materials. Gas adsorption measurements were carried out in a conventional Pyrex glass volumetric adsorption apparatus capable of evacuation to 10^{-6} Torr. Each catalyst sample was placed in a Pyrex flow-through cell to enable reduction of samples in flowing hydrogen prior to the chemisorption measurement. The amount of gas adsorbed by the catalyst was determined by using one of two available volumetric chemisorption systems. The details of design and construction of these systems and a large reduction apparatus were presented in an earlier report (3).

To avoid contamination of our chemisorption and metal reactor systems with H_2S a separate poisoning apparatus was constructed (3). The H_2S concentration was determined analytically using a technique described earlier (5).

b. Catalyst pretreatment and poisoning procedure. All catalyst samples were prepared by impregnation, dried at 100°C, and reduced in flowing hydrogen at 450°C for at least ten hours and usually overnight for 14-16 hours. The temperature schedule for reduction was reported earlier (3). Most of the samples used in adsorption measurements were reduced *in situ* using a glass cell of the design shown in Figure 2. Samples pre-reduced and passivated in a large quartz tube were again reduced in flowing hydrogen for a minimum of 2 hours at 450°C prior to adsorption measurements. Ni-Fe/Al_2O_3 samples were found to require at least 6 hours rereduction at 450°C after exposure to air.

Hydrogen adsorption measurements were performed at 25°C and pressures from 100 to 500 Torr. This procedure is based upon surveys of the literature (11) and upon adsorption studies (3-5,12,13) of nickel catalysts over the past three years. A similar procedure was used for ruthenium catalysts except that a longer equilibration time (about 2 hours) was necessary. In the case of Pd containing samples, the adsorption measurements were carried out at 130°C to prevent interfering absorption.

Catalyst surface areas and dispersions were calculated (3) using hydrogen uptake data and assuming (i) the number of hydrogen atom/surface metal atom = 1, (ii) complete reduction of nickel and nickel alloys to the metallic state (except for Ni-MoO_3), (iii) a surface metal composition identical to the bulk metal composition, and (iv) planar site densities (See Appendix of QPR 4) based upon the three lowest index crystallographic planes for each metal. Assumptions i-iii are currently under investigation as part of the NSF methanation study in this laboratory (13).

The measurement of carbon monoxide adsorption uptake for nickel and nickel alloy catalysts was carried out according to a procedure reported in our fourth quarterly progress

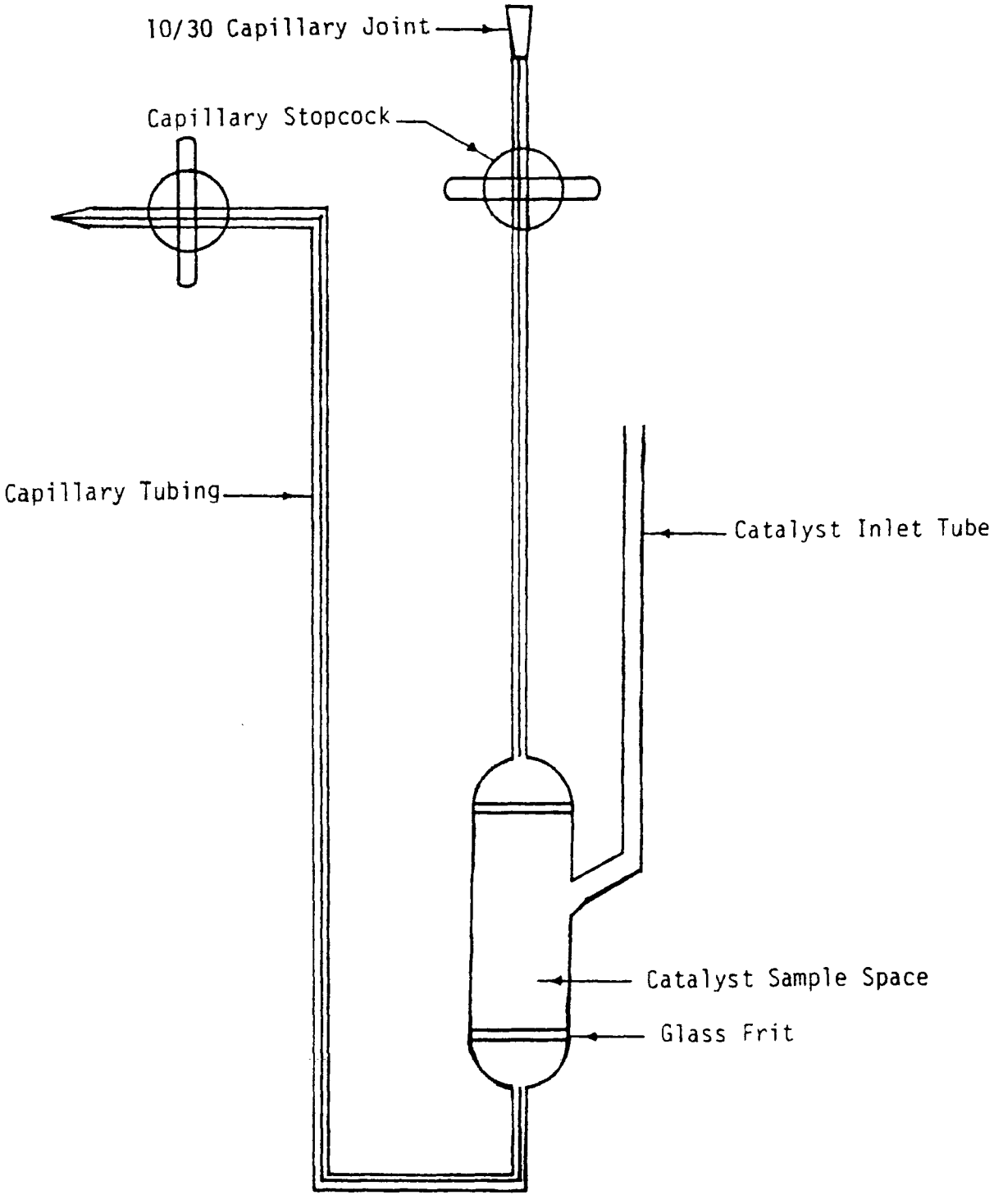

Figure 2. Chemisorption Sample Cell.

report, QPR-4 (at -83°C and relatively high equilibration pressure (400-500 Torr)). Unfortunately, under these conditions there is also considerable physical adsorption on the support. Hence, adsorption measurements were corrected for physical, as well as chemical adsorption on the support.

Controlled poisoning of catalysts with H_2S involved 6 or 12 hour exposure of small samples to a flowing stream of 10, 25 or 50 ppm H_2S in H_2 at 450°C using a separate poisoning apparatus. Details of calibration and operation have been described in QPR-3.

The basic steps in pretreatment and surface area measurement were as follows:

1. A large sample (50-100 g) consisting of Al_2O_3 pellets impregnated with metal salts was dried at 100°C and reduced at 450-500°C at a hydrogen space velocity of 1500 hr^{-1}.

2. H_2 chemisorption uptake was measured for a small sample (2-3 g) at 25°C(135°C for Pd or Ru samples) and CO uptake at -83°C.

3. The sample was exposed to 10 or 25 ppm H_2S at 450°C for 6 hours (GHSV = 2000 hr^{-1}).

4. H_2 and CO uptakes were again measured.

5. The sample was exposed to 10 ppm H_2S at 450°C for an additional 6 hours.

6. H_2 and CO uptake measurements were repeated.

Throughout the entire procedure the sample was contained in the same glass sample cell to prevent exposure to the atmosphere.

c. Adsorption Data. Hydrogen uptake, percent dispersion, and surface area data are listed in Table 3 for nickel, nickel alloy and ruthenium alloy catalysts prepared in this study. A typical hydrogen adsorption isotherm is shown in Figure 3 for 3% Ni/Al_2O_3. Hydrogen adsorption uptakes were determined by extrapolating to zero the straightline portion of each isotherm above the saturation pressure (about 100 Torr). The relatively small values for the slopes of these isotherms indicate that physical adsorption on the support is a small effect at 25°C.

One of the objectives of this study is to find catalysts for methanation which are more efficient, active, and stable than nickel. One measure of efficiency is the active catalyst surface area per unit mass or volume. The

TABLE 3

a. Hydrogen Chemisorptive Uptake Data for Alumina Pellet-Supported Nickel Nickel Alloy and Ruthenium Alloy Catalysts

Catalyst	Nominal Composition (wt%)	H_2 Uptake (μmoles/gram)	Metal Particle Size (A)	Percent Dispersion	Surface Area (m^2/g)
Ni-A-111	3% Ni	21.4	116	8.35	1.75
Ni-A-112	3% Ni	39.4	63	15.4	3.23
Ni-A-116	14% Ni	187.8	62	15.7	15.39
G-87 (Girdler)	32% Ni	161.6	163	5.93	13.24
Ni-MoO_3-A-101	2.5% Ni - 3% MoO_3	22.5	92*	10.6*	1.84*
MoO_3-A-101	3% MoO_3	1.0	--	--	--
Ni-Ru-A-105	2.5% Ni - 0.5 wt% Ru	44.6	52	18.76	3.71
Ni-Rh-A-100	2.5% Ni - 0.5% Rh	38.3	62	16.1	3.16
Ni-Co-A-100	10% Ni - 10% Co	114.9	142	6.76	9.54
Ni-Fe-A-100	10% Ni - 10% Fe	80.6	278	4.60	5.14
Ni-Pt-A-100	15.7% Ni - 0.5% Pt	106	119	8.22	8.66
Ni-Pd-A-100	15% Ni - 1.0% Pd	107.4	115	8.13	8.82
Ru-Pd-A-100	0.49% Ru - 0.51% Pd	21.0	24	43.6	2.08
Ru-Co-A-100	0.52% Ru - 15% Co	48.3	253	3.72	4.11
Ni-Rh-101	16.6% Ni - 3.4% Rh	168.8	91.6	10.7	14.0
Ni-Ru-106	16.6% Ni - 3.4% Ru	171.7	89.9	10.9	14.3
Ni-MoO_3-102	10 % Ni- 10% MoO_3	136.5	60.6*	16.0*	11.1*
Ni-MoO_3-103	10% Ni - 10% MoO_3	92.3	89.5*	10.8*	7.53*

*Based upon nickel only

TABLE 3 continued

b. Nominal Composition and Hydrogen Chemisorptive Uptake Data for Monolithic-Supported Nickel Catalysts

Catalyst	Nominal Composition	Preparation*	H_2 Uptake (μmoles/g-catalyst)	% Dispersion	Surface Area (m^2/g-cat.)
Ni-M-101	15.7 wt% Ni 13.5 wt% Al_2O_3	Nickel nitrate melt (6) Washcoat - Dispal Al_2O_3 slurry (8)	45.2	3.38	3.69
Ni-M-103	13.7 wt% Ni	Nickel - Aqueous nickel soln., ppt. with NH_3 (11)	96.5	8.27	7.87
	13.2 wt% Al_2O_3	Washcoat - SA Medium Al_2O_3 slurry (3)			
Ni-M-104	15.9 wt% Ni	Nickel nitrate melt (3)	97.6	7.21	7.96
	19.9 wt% $NiAl_2O_3$	Washcoat - SA Medium Al_2O_3 slurry plus Ni Nitrate to form $NiAl_2O_4$ (6)			
Ni-M-105	16 wt% Ni	Nickel - Aqueous nickel soln. (15)	70.2	5.15	5.72
	12.6 wt% $NiAl_2O_4$	Washcoat - Ni & Al Nitrate slurry to give $NiAl_2O_4$ (8)			
Ni-M-106	18.5 wt% Ni 14.1 wt% Al_2O_3	Nickel - Aqueous nickel soln. (5) Washcoat - SA Medium Al_2O_3 slurry (3)	83.3	5.29	6.79
Ni-A-116	15 wt% Ni	Alumina Pellets	187.8	14.7	15.39

* the number of metal applications or support washcoats is given in parentheses

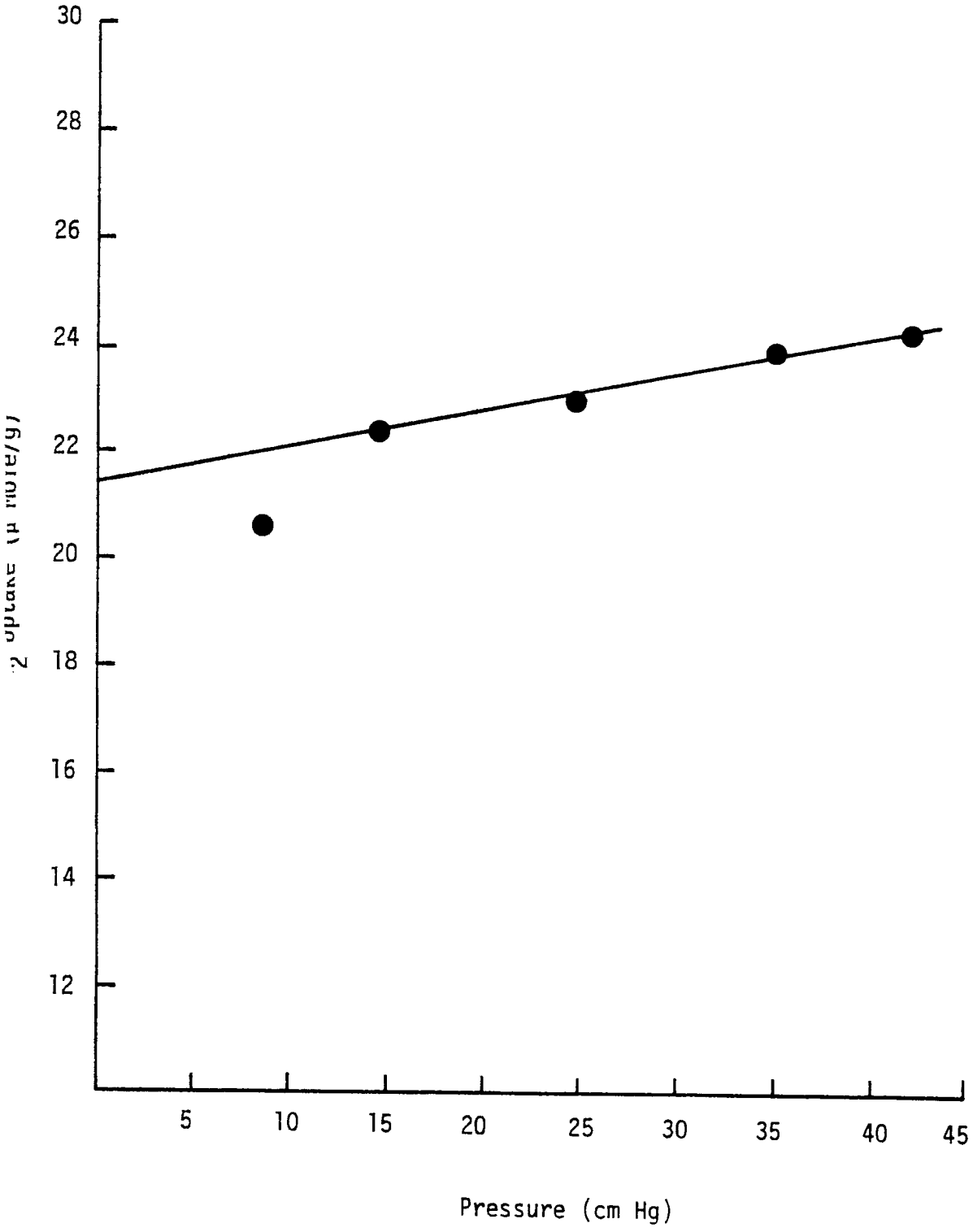

Figure 3. H_2 Chemisorption on Ni-A-111 at 25°C.

magnitude of the hydrogen uptake in moles/gram of catalyst depends upon (1) the amount of active metal(s) in the sample and (2) the dispersion (or particle size) of the active component(s). Previous work (12) in this laboratory has established that metal dispersion decreases with increased nickel loading in the nickel-alumina system. This same effect is also apparent in the data for 3, 14 and 32 wt. % Ni in Table 3; in fact, the 14 wt. % Ni catalyst prepared in this laboratory has a higher surface area and significantly higher dispersion than the 32 wt. % commercial nickel (Girdler G-87). This can be explained in terms of differences in preparation and pretreatment. Commercial catalysts are normally prepared by calcination of the impregnated or precipitated supported metal salt followed by reduction in hydrogen. This high temperature calcination ultimately prevents complete reduction of nickel to the metallic state; in fact, a typical commercial nickel probably contains 30-50% NiO and/or $NiAl_2O_4$ even after reduction in flowing hydrogen at 500°C (12). Our catalysts on the other hand are prepared by direct reduction of the supported metal salt in hydrogen to produce samples containing 80-90% of the metal in the metallic state and in a significantly higher state of dispersion compared to calcined samples (12).

Comparison of surface areas and dispersions from Table 3 for nickel alloys compared to nickel catalysts show approximately the same surface areas for 3% Ni-Rh and 3% Ni-Ru compared to the 3% Ni catalyst. The 5.5% Ni-Mo catalyst, however, has approximately half the surface area of the 3% Ni, possibly because of interaction of part of the nickel with MoO_3 to form a complex which does not adsorb hydrogen. Moreover, the data for the 3% MoO_3/Al_2O_3 indicate that hydrogen adsorption on the molybdenum oxide is negligibly small. These observations suggest that the nickel sites do and the MoO_3 sites do not chemisorb hydrogen. All of the alloys in the 15-20% range have 40-50% lower surface areas compared to the 15% Ni/Al_2O_3. The dispersion of Ru-Co is the lowest, Ru-Pd the highest. In regard to the effects of alloy composition on H_2 chemisorption, since most of metals chemisorb hydrogen dissociatively with $H/M_s = 1$, the relative abundance of metals at the surface of a crystallite should have little effect on adsorption stiochiometry even though the surface compositions may not be the same as the bulk compositions for many of these alloy catalysts (14). The stoichiometry of CO adsorption, on the other hand, may well depend upon surface composition.

Hydrogen adsorption uptakes, nickel dispersions and surface areas are also shown for selected monolithic supported nickel catalysts in Table 3. A comparison of the hydrogen uptake data shows Ni-M-103 and Ni-M-104 to have the highest uptakes, Ni-M-103 has the highest dispersion, while the Ni-M-104 catalyst, by virtue of its higher loading,

has the highest surface area. Though these two catalysts are nearly equal in terms of uptake data, the Ni-M-104 catalyst requires far fewer impregnations to reach a reasonable nickel loading. This may be considered a significant advantage, as each impregnation requires several hours of additional preparation time. Ni-M-106 also requires few impregnations and has an uptake nearly as great as that of Ni-M-104. Therefore, the techniques used to prepare Ni-M-104 and Ni-M-106 (or some combination of these techniques) appear to be the most promising. A comparison of the dispersion of the monolithic-supported catalysts with that of Ni-A-116 shows that the monoliths have roughly one-half the dispersion. This is to be expected as the monolithic catalysts have approximately a 50% loading of nickel on the alumina coating, as compared to 14% for Ni-A-116 (5).

Table 4 summarizes data for chemisorption of CO on nickel, nickel alloys and ruthenium alloys. Figures 4 and 5 are representative isotherms for unsupported and supported nickel. The data in Table 4 show the ratios of adsorbed carbon monoxide molecules to hydrogen atoms on nickel and ruthenium catalysts ranging from 0.61 to as high as 3.54. The higher ratios indicate the possibility of multiple adsorption of CO molecules on metal atoms (i.e. formation of surface metal carbonyls), and the results are generally in agreement with previous studies of nickel, ruthenium, and rhodium catalysts. Any large discrepancies between our CO adsorption data and those reported by others are very likely due to differences in equilibration pressure and corrections for physical and chemical adsorption on the support. Data from an earlier report (3), for a nickel catalyst show that CO uptake can vary significantly as a function of equilibration pressure; in other words the monolayer coverage of CO is not well defined. Moreover, there is evidence from the literature and from our data which suggests that metal carbonyl formation occurs at the surface during exposure to CO for many catalyst systems. A detailed discussion of most of the results and comparison with the literature was presented in an earlier report (4), the most important aspects of which will be summarized here.

Data from Table 4 for Kaiser SAS Al_2O_3 show that CO uptake is significant at 25 and -83°C. These support uptake data were used to correct for chemisorption on the support in determining CO uptake for the alumina-supported catalysts listed in Table 4.

Isotherms for CO adsorption on an Inco nickel powder (a high purity nickel having particles in the 1-3 micron range) are shown in Figure 4. The first isotherm at 25°C corresponds to the CO uptake of sample obtained after evacuation at 400°C; the CO adsorption extrapolated to zero pressure is 12.1 micromoles/g of nickel and corresponds to a value

TABLE 4

CO Chemisorption Uptakes for Alumina-Supported Nickel and Ruthenium Catalysts

Catalyst	Nominal (wt%) Composition	H_2 Uptake (μmole/g)	CO Uptake (μmoles/g)	CO/H
Kaiser Al_2O_3	Pure Al_2O_3	0.5	26.3	26.3
Inco Ni Powder	Pure Ni	3.47	5.3	0.76
Ni-A-111	3% Ni/Al_2O_3	21.4	80.0	1.87
Ni-MoO_3-A-101	2.5% Ni 3% MoO_3	24.0	107.3	2.23
MoO_3-A-101	3% MoO_3	1.0	8.0	4.0
Engelhard Ru	0.5% Ru	7.62	54.0	3.54
Ni-Ru-A-105	2.5% Ni 0.5% Ru	47.6	148.2	1.56
Ni-Rh-A-100	2.5% Ni 0.5% Rh	43.5	145.6	1.67
Ni-Fe-A-100	10% Ni 10% Fe	80.6 118.0	259.0 274.8	1.61 1.16
Ni-Co-A-100	10% Ni 10% Co	114.9 116.0	173.8 190.8	0.76 0.82
Ni-Pd-A-100	15% Ni 1% Pd	107.4 75	145.5 175.5	0.68 1.17
Ni-Pt-A-100	15.7% Ni 0.5% Pt	106.0 107.5	206.0 363	0.97 0.66
Ru-Pd-A-100	0.49% Ru 0.51% Pd	21.0	70.0	1.67
Ru-Co-A-100	0.52% Ru 15% Co	48.3 40.4	58.5 69	0.61 1.30
Ni-Rh-A-101	16.6% Ni 3.4% Rh	168.8	307.1	0.91
Ni-Ru-A-106	16.6% Ni 3.4% Ru	171.7	461.3	1.34
Ni-MoO_3-102	10% Ni 10% MoO_3	136.5	242.9	0.89

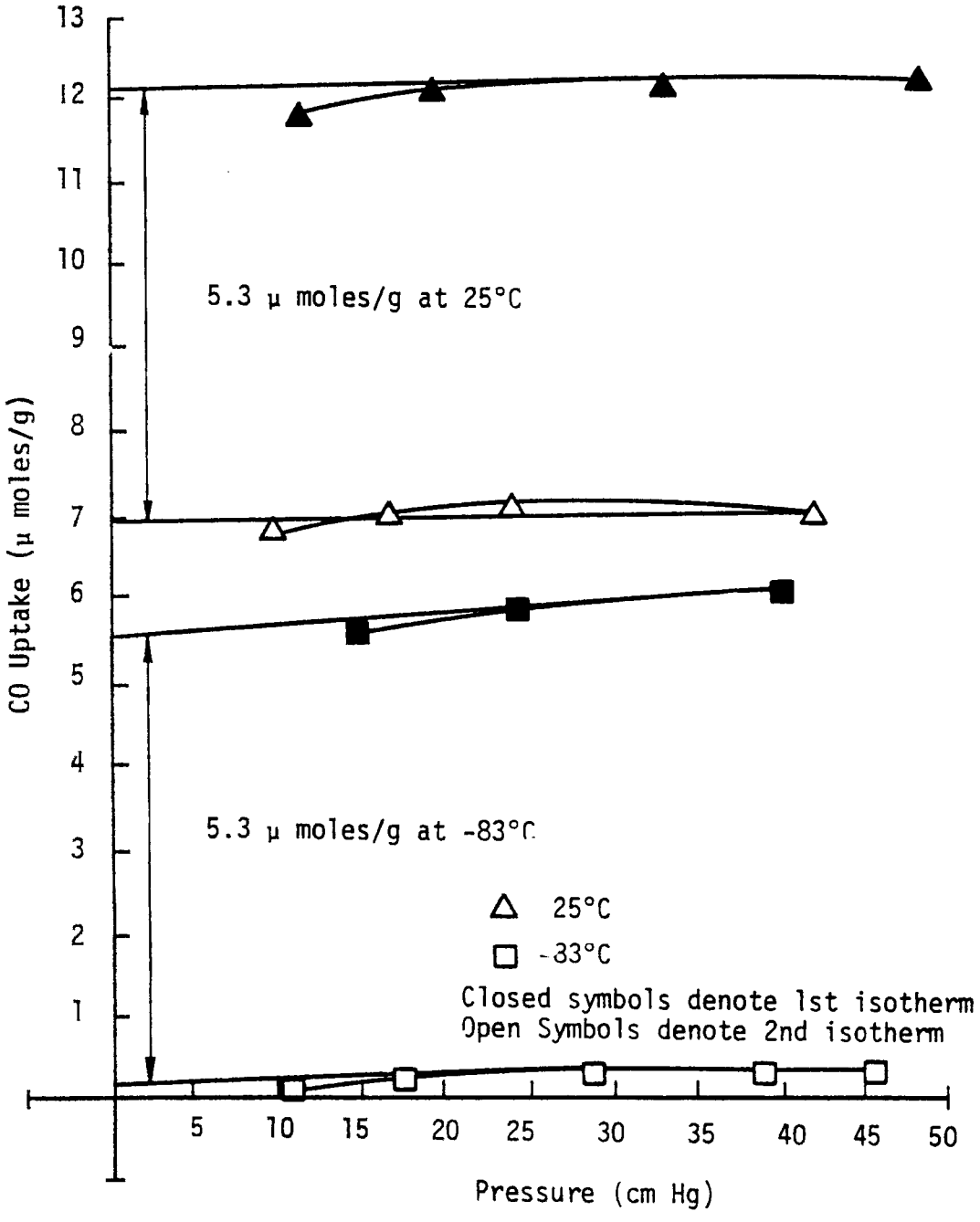

Figure 4. CO Adsorption on Inco Nickel Powder at 25° and -83°C.

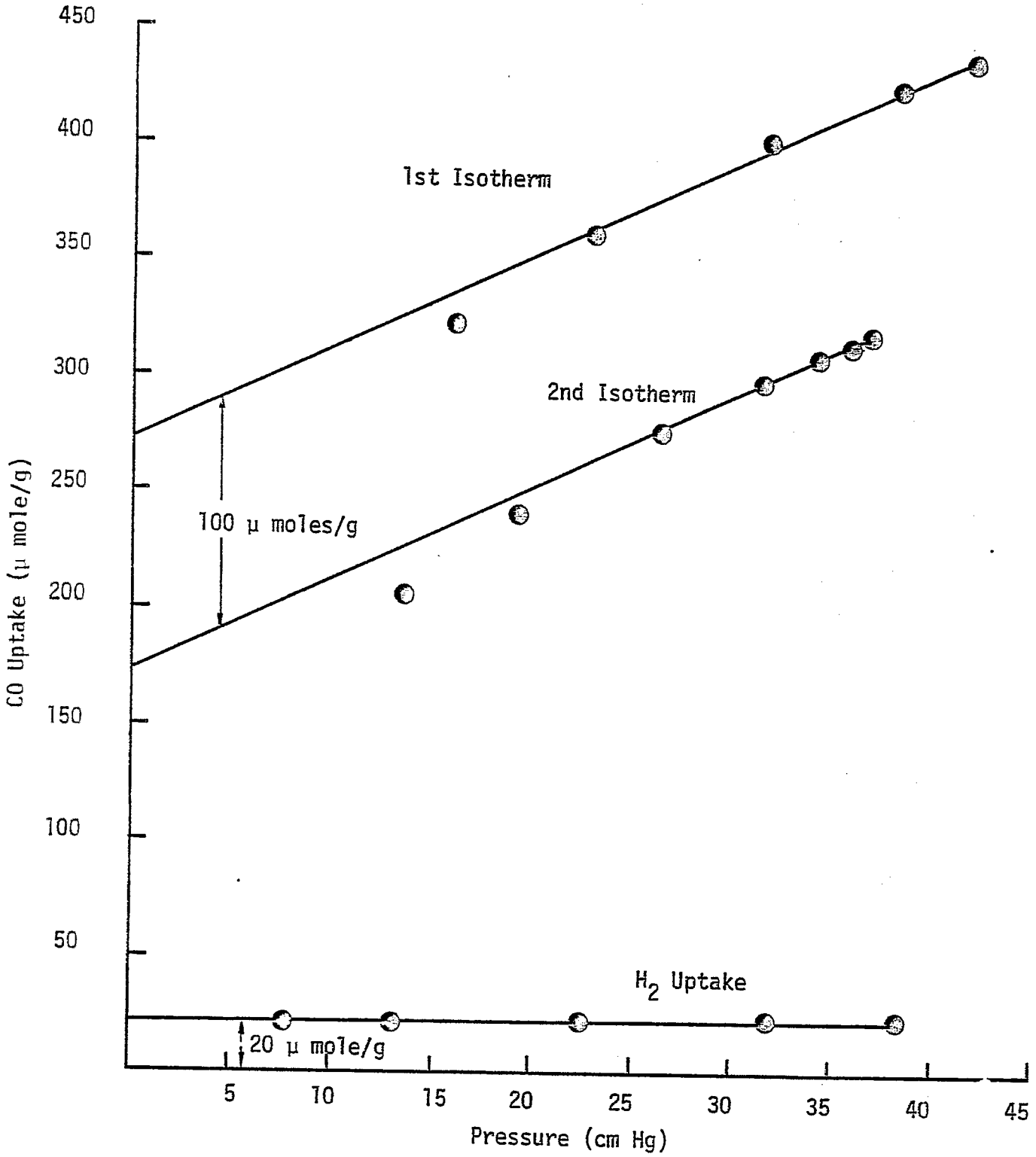

Figure 5. CO Chemisorption on Ni-A-111 at -83°C

of CO/H of 1.74. Recent nitrogen and argon BET and H_2 chemisorption measurements (13,15) obtained in this laboratory for the same nickel powder show that hydrogen chemisorbs dissociatively on nickel with a surface stoichiometry of $H/Ni_s = 1$. Together, the H_2 and CO chemisorption data provide strong evidence for the existence at room temperature of surface complexes such as $Ni(CO)_2$ and $Ni(CO)_3$.

After evacuation of the CO covered nickel powder at 25°C, the second isotherm (at 25°C) was obtained--the amount corresponding to carbon monoxide (or possibly nickel carbonyl) removed by evacuation at room temperature. The difference between the first and second isotherm, 5.3 moles/g corresponds to irreversibly held CO, and the corresponding CO/H value is 0.76. CO uptake data for the Inco nickel powder at -83°C show the small amount of irreversibly adsorbed CO as compared to 25°C but a negligible uptake for the second isotherm. In other words, at -83°C the initial CO/H value is 0.76 and there is no reversibly adsorbed CO (or nickel carbonyl) which can be pumped off at -83°C.

In summary, our data for the nickel powder combined with earlier observations (3) of nickel loss for Ni/Al_2O_3 samples strongly suggest nickel carbonyl formation at 25°C whereas at -83°C no easily evacuated carbonyl is formed. Hence, our procedure involving CO adsorption at -83°C avoids the problem of carbonyl formation and loss of nickel metal or alternatively loss of reversibly adsorbed CO.

The data in Table 4 for 3% Ni/Al_2O_3 show a value of CO/H of 1.87 suggesting that twice as many CO molecules are adsorbed on the nickel catalyst as hydrogen atoms. Recent studies in our laboratory (13) have shown the nickel in this 3% catalysts to be 70% reduced to the metallic state. Ni/Al_2O_3 catayst with higher metal loadings (15-25%) and states of reduction of 90-95% were found to have CO/H adsorption ratios close to 1. Thus, the metal loading and extent of support metal interaction affect the stoichiometry of CO adsorption.

The data in Table 4 show that nickel in combination with ruthenium or rhodium adsorbs about twice as many CO molecules as hydrogen atoms. This is not unexpected since the separate metals behave very similarly and are also observed to form carbonyls. On the other hand, cobalt combined with either nickel or ruthenium adsorbs less carbon monoxide molecules per site than do nickel or ruthenium. The CO/H ratio for Ni-Pd and Ni-Pt catalysts was found to vary with dispersion and catalyst pretreatment as shown by the data for two different measurements. These effects are significant considering that these metals are only present in the samples in the amounts of 1 and 3.6 at.% respectively. Aldag, et al. (11) and Scholten (12) have reported that CO/H ratios for Pd vary from about 0.39 to

1.1 depending upon temperature and crystallite size. For Pt, several authors (18-20) report CO/H values varying from 0.3 to 1. Our data also show effects of crystallite size. For example, in the case of Ni-Pd-A-100 the ratio increased from 0.68 to 1.17 as the particle size increased from 115 to 164 Å. The increase in CO/H with increasing crystallite size observed in our experiments, however, shows a trend which is opposite to that observed in other studies. Nevertheless, the low CO/H values for Ni-Pd and Ni-Pt suggest the possibility that Pd and Pt may be concentrated at the alloy surface.

Hydrogen chemisorption uptakes, measured during the contract extension period for 28 different catalysts, are reported in Table 5. The bulk of the work performed during the first two months of the contract extension was with 17 monolith and 6 Climax Molybdenum powder samples. The rest of the catalysts characterized were pellet samples except for one extruded nickel catalyst provided by Haldor-Topsoe.

Using a procedure from Borg-Warner Chemical for electroless plating, several samples of nickel plated pellets and monoliths were prepared. A H_2 chemisorptive measurement made on an unwashed pellet sample showed a negligible H_2 uptake, suggesting that the surface area is either very small or highly poisoned by some species present in the preparation solution.

d. Effects on H_2S on CO and H_2 Adsorption. Tables 6 and 7 summarize data obtained for several catalysts during the past two years showing changes in H_2 and CO adsorption after exposure to 10 and 25 ppm H_2S for 6 and 12 hours. Figures 6 and 7 are representative isotherms illustrating the effects of H_2S on H_2 and CO adsorption for two of the samples described in Tables 6 and 7. Two very significant trends are apparent from the data in Table 6. First the effect of H_2S exposure is to decrease the H_2 uptake of the sample; second CO chemisorption is generally increased (except for the ruthenium catalysts). The increase in CO adsorption after H_2S exposure is a most surprising result. A detailed discussion of these results was presented in QPR 2 and QPR 3. The decrease in hydrogen adsorption after H_2S exposure is believed to be due to blocking of adsorption sites by adsorbed sulfur. The number in parenthesis listed just after each H_2 uptake value in Table 7a is the percent decrease in surface area for a given 6 or 12 hr. poisoning period, based on initial uptake. The data show that in most instances the fractional decrease in surface area due to H_2S poisoning is fairly linear in time. Obvious exceptions are the data for Ni-A-111 (3% Ni) and Ni-MoO_3-A-100 (5.5% Ni-MoO_3) which show a sharp decrease in the first 6 hours followed by a small decrease in the next 6 hours. The increase in CO adsorption may be due to formation

TABLE 5

Hydrogen Chemisorptive Uptake Date
During the Contract Extension Period

Catalyst	Nominal Composition	H_2 Uptakes (μmoles/gram)
Monoliths		
Ni-M-120	6.9% Ni	61.2[b,h]
Ni-M-121	5.9% Ni	65.8[b,h]
Ni-M-122	7.4% Ni	62.7[e]
Ni-M-123	11.2% Ni	48.5[d]
Ni-M-151	19.1% Ni	72.8[a,b]
Ni-M-154	18.6% Ni	78.0[b]
Ni-M-200	6.4% Ni	82.5[a,b]
Ni-M-201	6.5% Ni	57.4[a,b,]
Ni-M-202	6% Ni	97.1
Ni-M-203	6% Ni	94.1[b]
Ni-M-204	6.3 Ni	86.7
Ni-M-205	5.8 Ni	81.8[b]
Ni-M-250	22.2% Ni	154.8
Ni-M-252	21.8% Ni	126.2[b]
Ni-M-254	21.7% Ni	125.9[a,b]
Ni-M-303	20% Ni	100.3[a,e]
Ni-M-350	18.0% Ni	65.4[a,b]
Ni-M-351	19.8% Ni	111.2[a,b]
Ni-Co-M-103	4.5% Ni, 4.4% Co	57.0[d]
Ni-Co-M-104	5.1% Ni, 5.1% Co	68.0[d]
Ni-Co-M-105	5.5% Ni, 5.4% Co	54.6[d]
Ni-Co-M-106	4.8% Ni, 4.8% Co	67.2[d]
Ni-Co-M-107	5.3% Ni, 5.3% Co	50.3[d]
Ni-Co-M-108	6.4% Ni, 6.4% Co	69.0[d]
Ni-MoO_3-M-100	1.6% Ni, 1.5% MoO_3	17.4[d]
Ni-MoO_3-M-101	1.5% Ni, 1.5% MoO_3	6.0[d]
Ni-MoO_3-M-102	1.6% Ni, 1.5% MoO_3	14.3[d]
Ni-MoO_3-M-103	2.5% Ni, 2.5% MoO_3	23.1[d]
Ni-MoO_3-M-104	2.5% Ni, 2.5% MoO_3	18.2[d]

TABLE 5 continued

Catalyst	Nominal Composition	H_2 Uptakes (μmoles/gram)
$Ni-MoO_3$-M-105	2.5% Ni, 2.5% MoO_3	23.6[d]
$Ni-MoO_3$-M-106	1.5% Ni, 2.5% MoO_3	24.8[d]
Ni-Pt-M-107	10.9% Ni, 0.6% Pt	72.7[b]
Ni-Ru-M-108	5.2% Ni, 1.7% Ru	32.0[b]
Ni-Ru-M-109	7.9% Ni. 2.6% Ru	31.2[e]
Powders		
$La_4Mo_9O_{24}$		0.4[c]
$Co_2Mo_3O_8$		4.4[d]
Ni_2MoO_3		8.5[d]
$FeMoO_3$		9.3[c]
$NiMoAl_2O_3$-SiO_2		15.2[d]
$NiCoMo$-Al_2O_3-SiO_2		46.3[c]
Pellets		
Ni-Co-A-101	1.5% Ni, 1.5% Co	12.9[d]
Ni-Pt-A-101	2.9% Ni, 0.1% Pt	15.9[d]
Ni-Ru-A-105	2.5% Ni, 0.5% Ru	49.4[d,f] 52.4[d,i]
Ni-Ep-100	Electroless Plated	negligible[g]
Girdler T-310	10% Ni	39.4[d] 47.0[b]
$Ni-MoO_3$-A-103		92.3[d] 57.2[b,h]
Extrudates		
Haldor-Topsoe	11-12% Ni	123.9[a,b]

---

[a] Geometry Tested

[b] Integral Reactor Tested

[c] Differential Reactor Tested

[d] Reduced Only

[e] Reactor Water Run

[f] Washed

[g] Unwashed

[h] High Pressure Reactor Tested

[i] Reported in Previous Quarter

TABLE 6

Effects of H_2S on H_2 and CO Chemisorption
for Alumina-Supported Nickel and Nickel Alloys
(10 ppm H_2S at 450°C)

CATALYST	NOMINAL COMPOSITION	H_2 Uptake (μmoles/g) H_2S Exposure			CO Uptake (μmoles/g) H_2S Exposure		
		INITIAL	6 HOURS	12 HOURS	INITIAL	6 HOURS	12 HOURS
Kaiser Al_2O_3	Pure Al_2O_3	0.5	--	--	26.3	31.1	38.9
Inco Ni Powder	Pure Ni	3.47	--	--	5.3[c]	--	--
Ni-A-111	3% Ni	21.4[d]	16.8	14.0	80.0	243.9	373.6
Ni-MoO_3-A-101	2.5% Ni -	24.0[a]	--	--	107.3	260.8	257.6
	3% MoO_3	21.1[b]	13.57	12.45*	--	--	--
MoO_3-A-101	3% MoO_3	1.0	--	--	8.0	8.0	--
Engelhard Ru	0.5% Ru	7.62	5.33	3.45	54.0	45.2	42.5
Ni-Ru-A-105	2.5% Ni -	47.6[a]	--	--	148.2	283.1	295.6
	0.5% Ru	39.4[b]	32.0	25.8	--	--	--
Ni-Rh-A-100	2.5% Ni -	43.5[a]	--	--	145.6	225.8	256.4
	0.5% Rh	38.3[b]	33.5	28.3	--	--	--

*After 24 hours H_2S

[a&b]Refer to different measurements for the same catalyst batch

[b]Data reported in QPR-1

[c]Irreversibly chemisorbed at 25 and -83°C

[d]Reduced in small glass sample cell

TABLE 7

a. Effect of 10 ppm H_2S (GHSV = 2000 hr^{-1}) on H_2 and CO chemisorption

Catalyst	Initial H_2 Uptake	H_2 uptake after 6 hrs poisoning	H_2 uptake after 12 hrs. poisoning	Initial CO Uptake	CO Uptake after 6 hrs poisoning	CO uptake after 12 hrs poisoning
Ni-Fe-A-100	80.6	49.6 (38)	42.7 (47)	259	302.9	390.7
Ni-Co-A-100	114.9	109.6 (4.6)	102.0 (11)	173.8	228.6	223.7
Ni-Pd-A-100	107.4	107.8 (-0.37)	103.0 (4.1)	145.5	240.0	328.4
Ni-Pt-A-100	152	144.0 (5.3)	138.0 (9.2)	139.0	356.0	352.5
Pd-Ru-A-100	21.0	18.0 (14)	6.5 (69)	70.0	57	21.0
Co-Ru-A-100	48.3	35.0 (27)	34.1 (29)	58.5	59	81.0
$Y\text{-}Al_2O_3$	0.5	———	———	48.8	48.8	48.8

H_2 uptakes are not corrected for H_2 chemisorption on support (∿.5 μmoles/g catalyst for these conditions) Numbers in parentheses indicate the % decrease in uptake for 6 (or 12) hour exposure based on initial uptake.

TABLE 7 continued

b. Effect of 25ppm H_2S (GHSV = 2000 hr^{-1}) on H_2 and CO chemisorption

Catalyst	Initial H_2 Uptake	H_2 uptake after 6 hrs. poisoning	H_2 uptake after 12 hrs. poisoning	Initial CO Uptake	CO uptake after 6 hrs. poisoning	CO uptake after 12 hrs. poisoning
Ni-Fe-A-100	118	79.5(33)	73.0(38.1)	274.8	328	372
Ni-Co-A-100+	116	114.4(1.3)	100(13.8)	190.8	243	—
Ni-Pd-A-100++	75	50(33)	66.3(11.6)	142.1	175.5	300.5
Ni-Pt-A-100+	121.0	107.5(11)	100(21.0)	160.8	363	909
Co-Ru-A-100+	40.4	18.9(53)	29.0(28.2)	104.8	69	56
γ-Al_2O_3	0.42	0.92	0.5	29	42	60

+ May be in bulk sulfide forming region - H_2 chemisorption run at 25°C.

++ H_2 adsorption run at 25°C - H_2 chemisorption results are only approximate

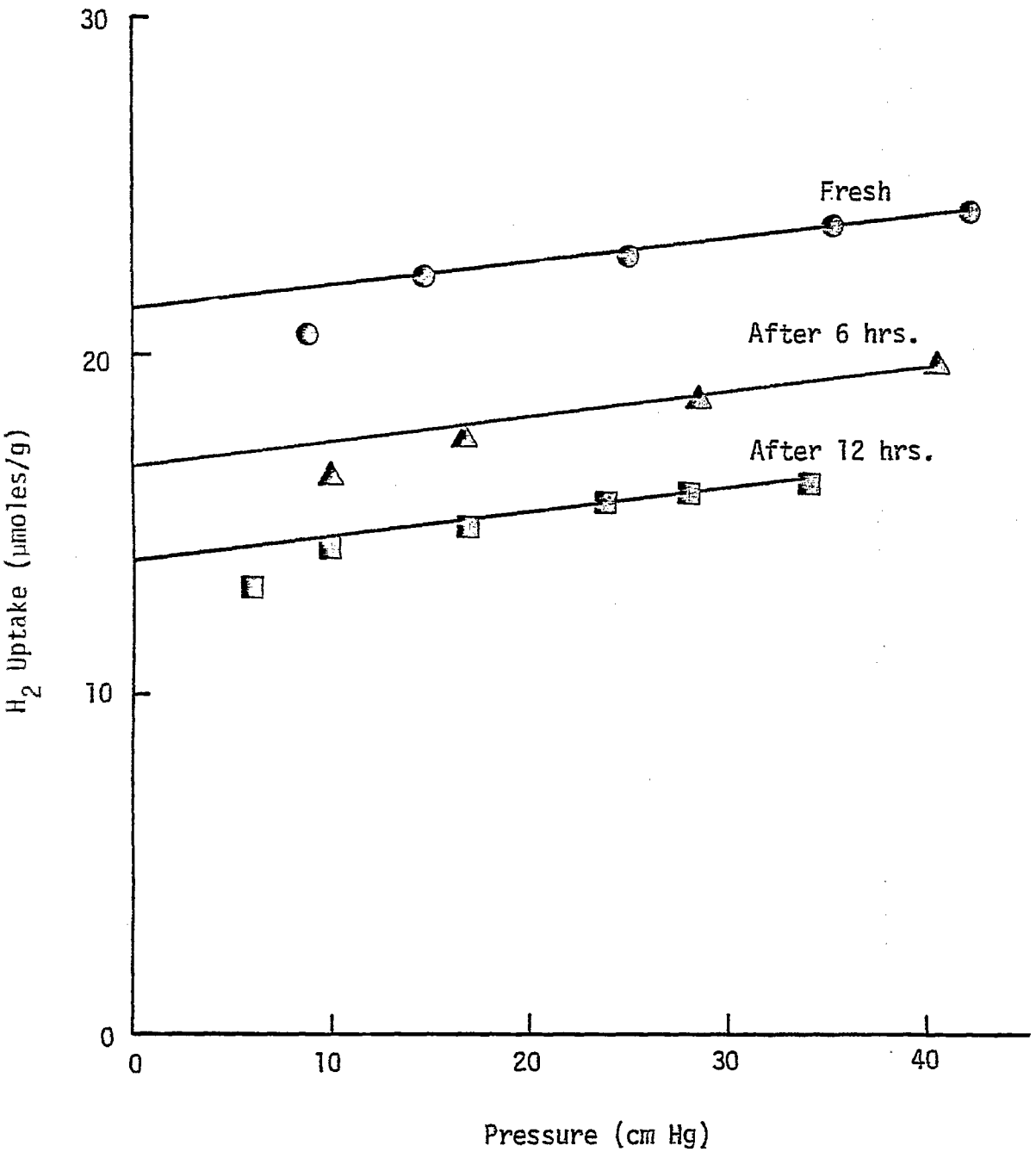

Figure 6. Effect of 10 ppm H_2S (450°C) on H_2 Chemisorption for Ni-A-111 at 25°C.

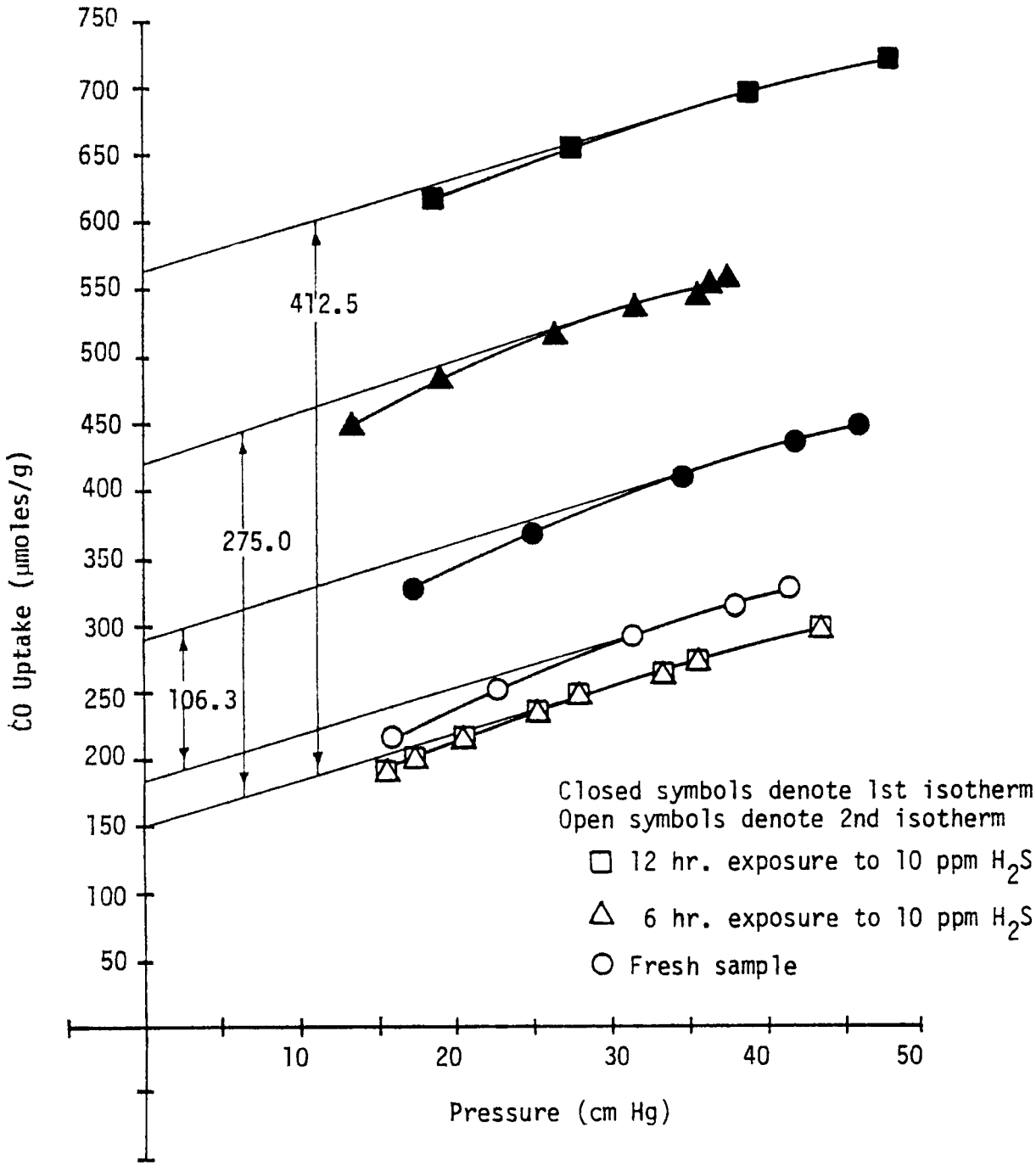

Figure 7. Effects of 10 ppm H_2S on CO Adsorption (-83°C) on Ni-A-111.

of nickel carbonyl or a surface complex such as $(CO)_xS$. An alternative or contributing mechanism may be that of carbon monoxide or COS spillover from the metal surface to the support.

3. X-ray Diffraction and Chemical Analysis.

During the first year, X-ray diffraction measurements were completed for a number of pelletized nickel and alloy catalysts. The measurements were complicated considerably by the presence in each catalyst of small Al_2O_3 crystallites or pores (about 50 A in diameter) causing several intense peaks. In many cases, the line broadening due to the Al_2O_3 support made identification difficult or impossible for a number of metal peaks, e.g. the (111) peak for Ni.

The crystallite diameters calculated from x-ray line broadening are shown in Table 8 and compared with crystallite diameters calculated from hydrogen chemisorption and electron microscopy. Apparently fair to good agreement is obtained between the values determined for the 25% Ni sample from x-ray diffraction (200 peak) and from chemisorption. The particle size from x-ray for the 13.5% sample is also lower than determined from chemisorption. Normally it is expected that particle diameter calculated from x-ray line broadening will be larger than for those calculated from chemisorption since the former is a volume averaged property and the latter a surface area averaged property. This discrepancy might be explained by unreduced nickel which is known to occur in Ni/Al_2O_3 catalysts (12). It has been observed that the percent reduction to nickel metal increases and that percent dispersion decreases with increased metal loading. If we suppose that this unreduced nickel occupies a portion of the surface of each crystallite or is even situated separately from the reduced metal crystallites, then the particle diameter calculated from hydrogen chemisorption will be higher than the true diameter since hydrogen does not adsorb on the nickel oxide sites and since our calculation assumes that hydrogen adsorbs on every available metal surface site. This model predicts an increasing discrepancy between x-ray and chemisorption calculations as the metal loading and percent reduction to nickel metal are decreased. Indeed the data are consistent with this view. It is also expected that better agreement will be found for Ni-Pd and Ni-Pt catalysts where nickel is believed to be more completely metallic. In fact, data in Table 8 for Ni-Pt do show slightly better agreement between the two methods. Exceptionally good agreement is obtained in the case of Ni-Co-A-100.

A detailed discussion of the x-ray diffraction data is presented in QPR-4. In summary, evidence for alloy formation is not conclusive for any of the alloy samples

TABLE 8

Comparison of Particle Sizes Calculated from X-ray Line Broadening Hydrogen Adsorption, and Electron Microscopy

Catalyst	X-ray plane	d particle (Å) X-ray	d particle (Å) H_2 Adsorption	d particle (Å) electron* microscopy
Ni-A-115 (25%Ni/Al_2O_3)	(200)	53.2	65.3	68
	(220)	36.4		
Ni-A-114 (13.5% Ni/Al_2O_3)	(200)	32.3	46.4	53
Ni-Fe-A-100	no easily distinguishable peaks			
Ni-Co-A-100	(200)	95.3	99.1	
	(102)	77.7		
	(225) or (110)	88.8		
Ni-Pt-A-100	(111)	75.3	86.6	
	(200)	67.9		
	(220)	78.8		
Ni-Pd-A-100	(200)	75.4	115	
	(220)	89.2		
Ru-Co-A-100	(002) or (100)	121.6	253	
	(110)	108.6		

*Particle size distribution from electron microscopy

Size (Å)	<39	39-49	50-61	62-72	73-83	>83
Ni-A-115	2	9	11	3	1	2
Size (Å)	**<33**	**33-42**	**43-52**	**53-62**	**63-72**	**>73**
Ni-A-114	3	20	7	1	9	0

(data are relative numbers of particles in each size range)

although it provides support for this conclusion; on the other hand, there is very little evidence suggesting that alloys were not formed in any of the alloy catalysts examined. In the case of Ni-Co and Ru-Co several weak Co peaks were identified, however, generally these peaks were very low in intensity. Separation and identification of alloy peaks is complicated by several factors: (1) some alloy peaks occur very close to peaks for one of the constituent metals, and differentiation of the metal from the alloy in this case is not possible, (2) some of the alloys are characterized by only a small amount of one of the metal constituents; hence, the alloy behaves similar to the metal in predominant concentration, and (3) broad interfering alumina peaks obscure some of the important metal peaks. From the data it is inferred that alloy crystallites are probably the predominant metallic structure in the alloy catalysts; however, the presence of small amounts of pure metals cannot be ruled out.

As part of our chemical analysis work two alumina-supported nickel catalysts, Ni-A-113 and Ni-A-114, having nominal compositions of 9 and 15 wt. % respectively, were submitted to Gulf Research for chemical analysis. The analysis revealed 7.55 and 13.53 wt. % nickel. Thus, these nickel catalysts actually contain 10-15% less nickel than expected by assuming that all of the nickel nitrate originally present in the impregnation solution had been transferred to the alumina pellets. This assumption is clearly approximate since in each preparation a small portion of the nickel nitrate is left on the bottom and walls of the breaker after impregnation and drying; indeed, this small portion might account for the 10-15% nickel lost in the preparation.

4. Electron Microscopy

During the contract extension period, transmission electron microscopy measurements for nickel-alumina catalysts were initiated to determine metal crystallite size and characterize sample composition.

Samples of Ni-A-115 (25% Ni) were studied using a Hitachi H.S. electron microscope. Elemental analysis was performed using a Phillips 400 microscope with EDAX.

Procedure. Two preparative techniques were used. Both involved crushing the catalyst to a powder with a mortar and pestle.

The first method involved placing the ground powder in an epoxy resin (Mollenhauer - a mixture of Shell Epoxy 812 and araldite resins). Small particles approximately 0.25 mm in diameter were then trimmed and sectioned on a Porter-Blum ultramicrotome using glass knives.

Figure 8. Transmission Electron Micrograph of 13.5% Ni/Al_2O_3 (297,000 X).

Figure 9. Transmission Electron Micrograph of 25% Ni/Al_2O_3 (265,000 X).

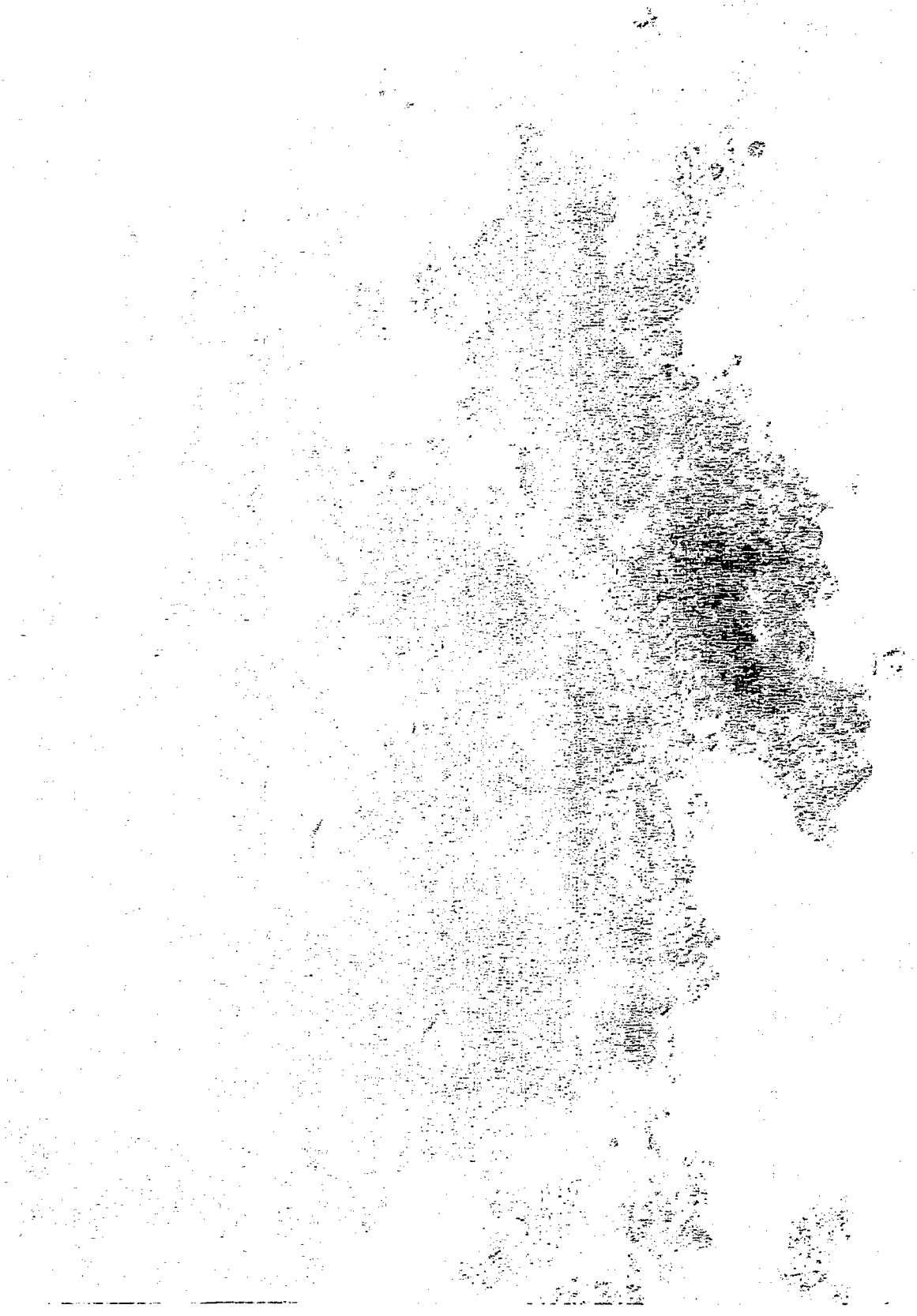

In the second method the powder was placed in n-butyl alcohol and more finely ground in a 7 ml tissue grinder. The sample was then ultrasonicated to suspend the fine particles. A drop of the suspension was transferred to a Formovar-coated, copper grid. The alcohol was then evaporated leaving fine particles ready for observation.

Results. Electron micrographs were taken of catalysts prepared by the first method. However, the particle images were too light to give an accurate size distribution of nickel crystallites.

The second method proved more successful and two micrographs are shown in Figures 8 and 9. Figure 8 is a micrograph of Ni-A-115 (25% Ni) at 265,000X. This catalyst was analyzed with EDAX, and showed very definite aluminum and nickel K adsorption peaks. Figure 9 is a micrograph of Ni-A-114 (13.5% Ni) at 297,000X. Size distributions were made from both micrographs. The average particle diameters and particle size distributions are shown in Table 8. Very good agreement is obtained between the values calculated from H_2 chemisorption and those determined from electron microscopy.

5. Auger and and ESCA

During the last quarter, two catalyst samples were analyzed by Auger spectroscopy and by ESCA (electron spectroscopy for chemical analysis).

Samples of Ni-Co-A-100 and of Ni-MoO_3-A-102 were sent to Dr. Bernard J. Wood of Stanford Research Institute to be analyzed by Auger spectroscopy. The data in Table 9 shows that the relative surface concentrations of Ni and Co on the Ni-Co-A-100 catalyst are about the same. This is in agreement with our predictions of surface composition (QPR 8). However, the results for the Ni-MoO_3 catalyst show approximately 10 times as many Mo atoms as Ni at the surface.

In addition, two samples were sent to the University of Utah for ESCA analysis. The results are also given in Table 9. There is evidence for nickel metal, nickel oxide, and cobalt metal at the surface of the Ni-Co-A-100 catalyst. In the Ni-MoO_3-A-102 catalyst there is evidence for nickel metal, nickel oxide, and molybdenum oxide at the surface. The presence of nickel oxide at the surface is expected as the reduced samples were unavoidably exposed to air. The ESCA measurements suggest a ratio of 2:1 for molybdenum and nickel atoms at the surface, compare to 10:1 from the Auger measurements. However, both results should be considered to be more qualitative than quantitative in nature, since the relative peak heights were not converted to molar ratios by comparison wth standard materials.

TABLE 9

Auger and ESCA Information

Relative Auger Peak Heights[1] (at constant gain)

Catalyst	Minutes of Ar^+ etching	Mo	C	Ca	O	Co	Ni	Al
Ni-Co-A-100	0	0	3.5	6	504	0.88	1.0	79
	5	0	6	6	523	0.73	1.0	87
	10	0	0	4	489	0.63	1.0	87
$Ni-MoO_3$-A-102	0	10.5	0	0	186	0	1.0	26
	10	6.8	2	3	181	0	1.0	27

Relative ESCA Peak Areas[1] (at constant gain)

Catalyst	Ni	Co	Mo	
Ni-Co-A-100	1.0	0.95	---	There is evidence for nickel metal, nickel oxide and cobalt metal on the surface.
$Ni-MoO_3$-A-102	1.0	---	1.9	There is evidence for nickel metal, nickel oxide, and molybdenum oxide on the surface.

[1] Ni peak height or area = 1.0

B. Task 2: Laboratory Reactor Construction

1. Reactor Design and Construction. At the beginning of the contract period we had operational in our laboratory a continuous flow reactor system for catalyst screening and measurement of methanation catalyst activity at either high (integral) or low (differential) conversions over a pressure range of 0-60 psig. As part of this study the system was redesigned to (1) allow for operation to 400 psig, (2) significantly upgrade the system with the addition of mass flow meters, a new furnace with temperature programming, and a continuous temperature recorder, and (3) improve the analysis of gaseous products with the addition of a continuous CO-detector, a gas concentration calibration system, and chromatograph accessories to allow accurate measurement of all reactants and products. A schematic of the completed reactor system is presented in Figure 10.

The reactor system is designed such that various concentrations of desired reactant gases can be mixed with or without steam in the pressure range of 0-400 psig and at any temperature from 25-1000°C. The catalyst sample may be of either pellet or monolithic form, of any sample size from 2 ml to 100 ml. Small sample sizes are used in differential testing and large sizes are used for integral testing.

Reaction conditions are monitored in the following ways. Pressure is controlled by high pressure cylinder regulators and a back pressure regulator. Temperature is sensed by a type K (chromel-alumel) thermocouple inserted in the reactor bed. The signal is continuously recorded by means of a Hewlett-Packard 7132 2-pen laboratory strip chart recorder. Flow rates are read with a Matheson mass flowmeter system incorporating five stainless steel transducers with digital readout. The reactor furnace temperature is programmed and controlled using electronics designed and constructed by the BYU Chemistry Instrument Shop. This instrument coupled with a Lindberg 24-inch zone furnace allows 2% control of catalyst sample temperature from 25°C to 1000°C, incorporating programmable temperature-time ramps and constant temperature holds.

The reactant and/or product streams are continuously analyzed for CO using a Beckman model 864-12 NDIR analyzer and then routed to a Hewlett-Packard gas chromatograph model 5830 for periodic sampling and analysis for H_2, CO, CH_4, CO_2, H_2S, and hydrocarbons. The chromatograph with the addition of new accessories features digital control for automatic operation, sub-ambient temperature programming, column switching, and internal or external standard methods of calibration.

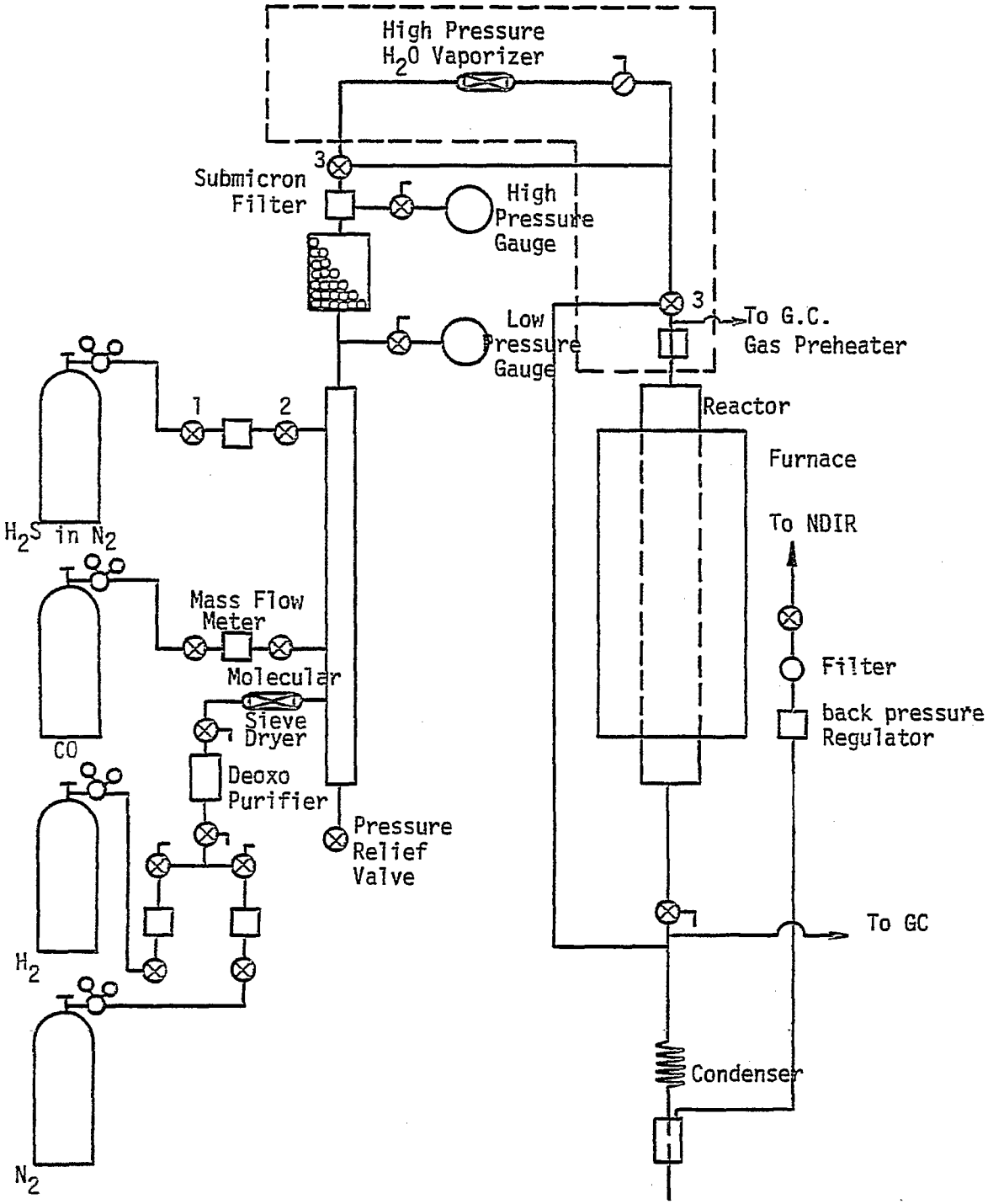

1 S.S. Micro Valve
2 Toggle Valves
3 3-way Valves

The area enclosed in dotted lines will be wrapped with heating tape and asbestos cloth.

Figure 10. High Pressure Laboratory Reactor

To facilitate investigation of the effects of steam on catalyst activity and surface area, a water vaporizer was designed and fabricated. The vaporizer consists of an eight-inch length of three-quarter inch schedule 40 stainless steel pipe into which has been inserted a six-inch length of perforated 1/4" stainless steel tubing which is stuffed with a glass wool wick. Reactant gases enter at the wick end of the pipe and leave after picking up water vapor. The vaporizer and all downstream components of the reactor are wrapped with heating tape and insulation. The vaporizer is maintained at a temperature of 400°C and the downstream components and tubing at 100°C. The water is metered by a Milton-Roy mini pump into the perforated tube where it is carried the length of the tube by capillary action, vaporized, and mixed with other reactant gases before entering the reactor.

The reactor is a stainless steel tube (see Figure 11) with an inside diamter of one-inch and a length of 26 inches. Centered at the outlet end of the reactor is a thermocouple well through which a thermocouple may be extended up into the sample zone of the reactor. This thermocouple may be placed at any desired position along the central axis of the bed. The reactor inlet is flanged so the reactor may be opened for charging or removal of samples. To insure a uniform gas temperature entering the catalyst bed, the gases entering the reactor are preheated by passing through tubing coiled around a portion of the reactor which contacts the furnace. Two such reactors have been fabricated with a shut off valve at each end so that catalyst pretreatment and reduction can be carried out for a sample using our separate reduction system while running simultaneously on the reactor system an already pretreated and reduced sample.

During the contract extension period two new Pyrex reactors and one new quartz reactor were constructed (see Figures 12 and 13). One of the Pyrex reactors was constructed for testing powdered pellet samples in the carbon deposition tests (a smaller reactor in which higher space velocities could be obtained was needed). A very similar quartz reactor was constructed for sintering and *in situ* H_2S studies. The other Pyrex reactor was constructed to accommodate monolithic supported catalysts for reactor tests where the feed gas contains 10 ppm H_2S (the stainless steel reactor would be unsuitable for these tests because it would be corroded by the H_2S). All three reactors are designed with a gas preheater and a sliding thermocouple which is placed in the sample bed.

To accommodate these new reactors, the reactor system was modified so that the new glass reactors could be run in parallel with the stainless steel reactors.

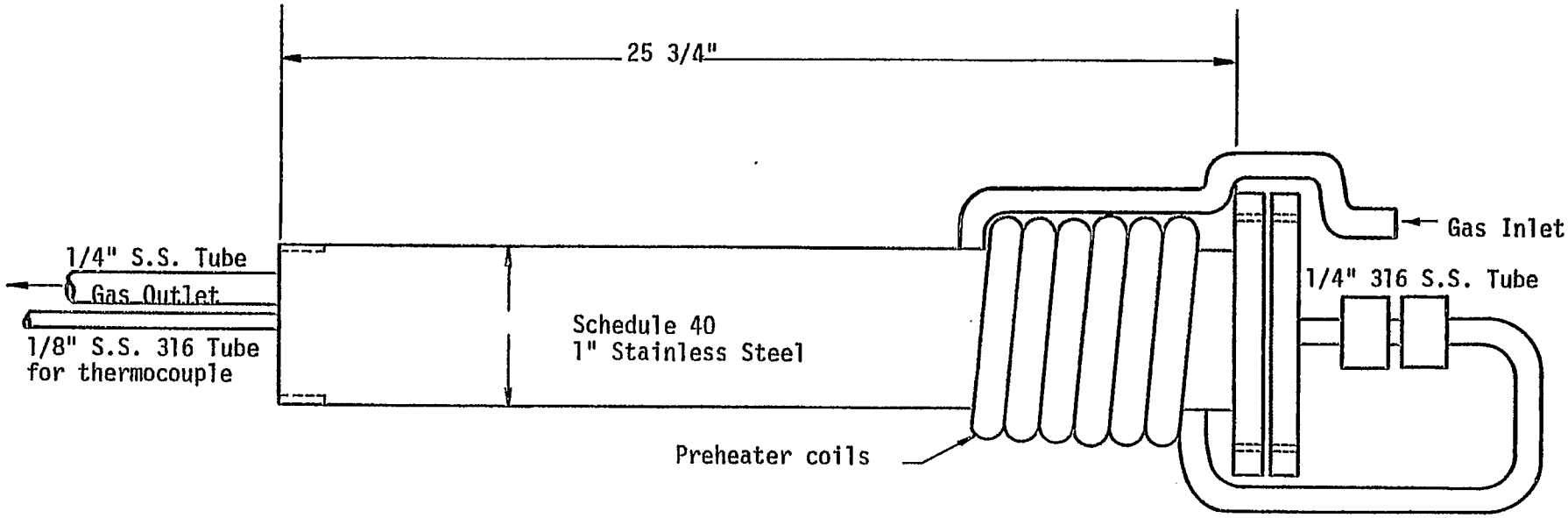

Figure 11. High Pressure Stainless Steel Reactor for Catalyst Testing.

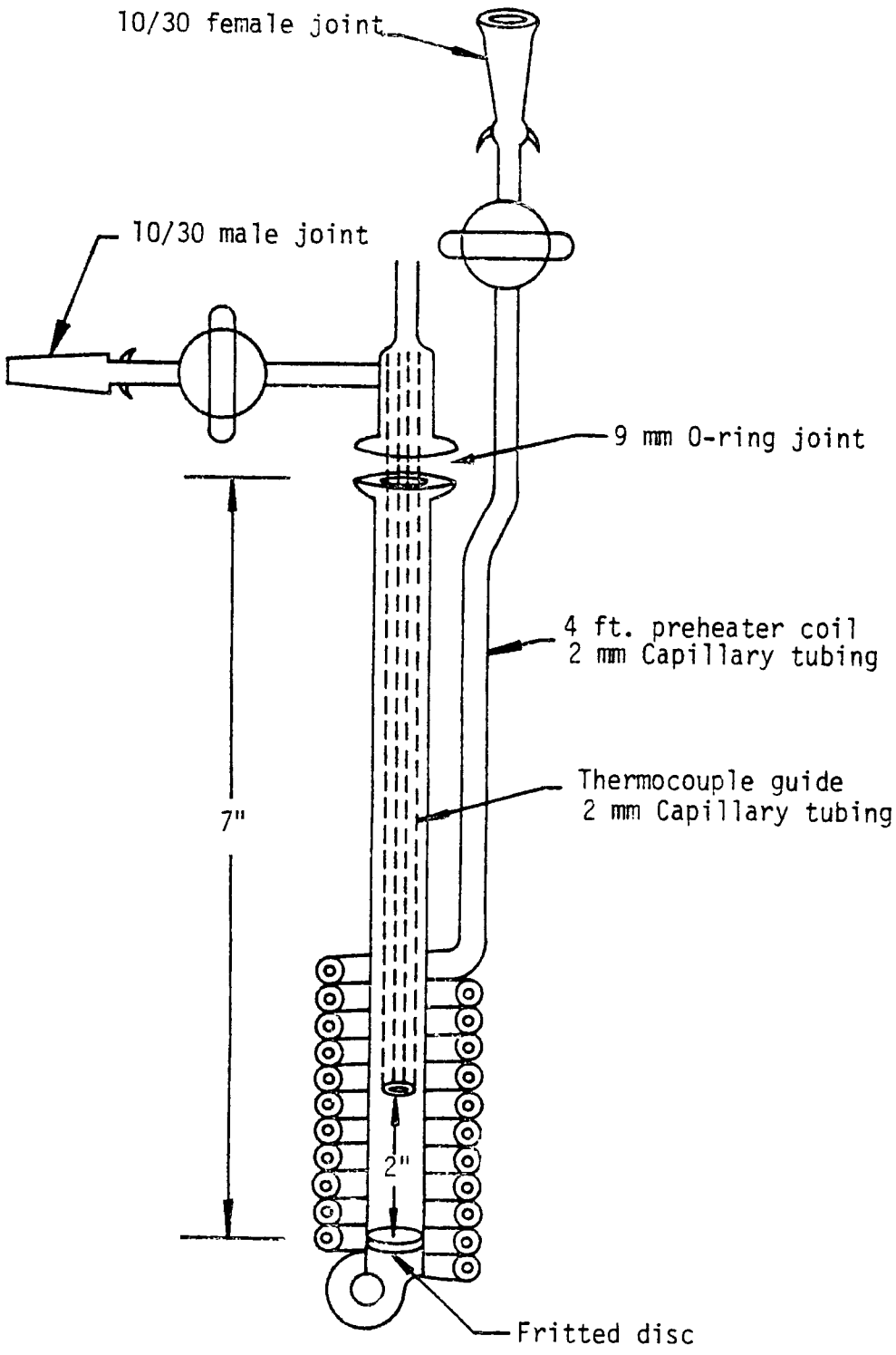

Figure 12. Laboratory Pyrex Reactor.

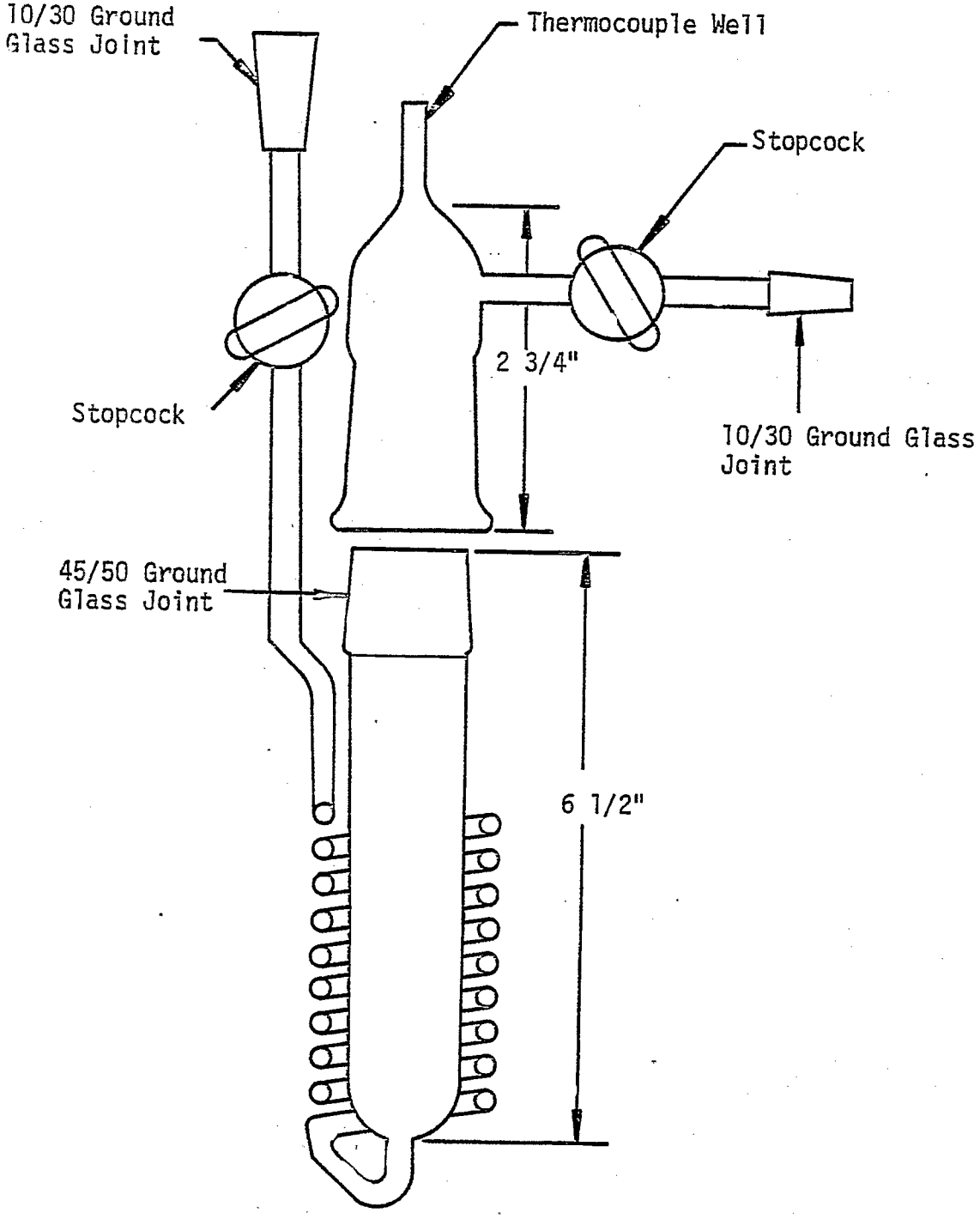

Figure 13. Pyrex Reactor for Monolith Catalysts.

2. Design and Construction of a Dilution Calibration Apparatus. A dilution apparatus was designed and constructed for the calibration of the gas chromatograph (G.C.). The dilution technique allows calibration gas mixtures to be prepared in various concentrations by dilution with a high degree of accuracy. By injecting known dilutions into the G.C. for analysis, the chromatographic areas of reactant and product mixtures can be related to concentrations on a daily basis. Using this technique, very low concentrations can be accurately achieved. The plexiglass dilution chamber with magnetic stirrer was described in considerable detail in QPR 1.

C. Task 3: Reactor Screening of Alloy Catalysts

1. Design of Screening Activity Tests

a. Introduction. During the first quarter a screening test was designed to provide a quick, useful comparisons of catalyst methanation activity under steady-state, reaction-limited conditions using a continuous flow system at atmospheric pressure.

b. Differential test (low conversion screening test) conditions and procedures. Most catalysts are initially reduced and passivated in our catalyst reduction system. A previously reduced sample of catalyst (usually one to four grams) is loaded into the stainless steel reactor. The sample is heated in flowing H_2 (approximately 500 cm^3/min) to 450°C and held for two hours at that temperature. The sample is then allowed to cool in flowing H_2 to about 225°C. Reactant gases (1% CO, 4% H_2 and 95% N_2) are next allowed to flow through the reactor at a space velocity of 30,000 or 60,000 hr^{-1} for 30 minutes during which time the reactor temperature is stabilized at 225, 250, or 275°C. Reactor pressure is usually about 5-8 psig for screening tests. From five to six chromatographic samples each of reactant and product gases are taken and at the same time all important experimental conditions such as temperature and pressure are recorded.

The data are next computer-reduced and the following quantites are calculated: a) conversion of CO to products, b) production of CH_4, c) production of other species such as CO_2 and other hydrocarbons, d) selectivity, the ratio of b to a, e) rate of CH_4 production and CO conversion per unit weight, f) turnover number, the number of product molecules produced per atomic catalytic site per second based on both CO conversion and CH_4 production.

c. Testing of poisoned catalysts. The catalysts are reduced in H_2 and exposed to a stream containing various H_2S concentrations from 1-50 ppm (usually 10 ppm) in a

special pyrex system for a period of 6-24 hours. A sample of the poisoned catalyst is charged to the stainless steel reactor and tests are carried out under either differential or integral conditions as previously outlined. Catalysts can also be exposed to H_2S *in situ* using special Pyrex and quartz reactors constructed for poisoning and sintering studies.

d. Data collection and reduction. Reactor test data for each run are recorded on reactor test data sheets (3). Similar data sheets are used for recording adsorption data and summary data (composition, physical properties, and test results) for each catalyst.

During the first year of investigation interacting calculator programs to calculate kinetic data (conversions, rates, and turnover numbers) were written for use on a Hewlett-Parkard 9810 calculator equipped with a Plotter/Alpha ROM and a printer option. Similar programs were also written for calculation of gas uptakes from adsorption data. During the second year the programs to calculate kinetic data were adapted to our DEC-10 computer to enable us to handle our large volume of data more efficiently.

2. Results - Differential Screening Tests

Preliminary screening tests were made during the first year (see QPR-4). However, the reactor was heated by a small 6-inch zone furnace with no preheating section. Thus, the gas entering the catalyst bed was cooler than the bed, and the temperature gradients (probably on the order of 10°C) were a significant source of error. Also, the thermocouple used to measure the bed temperature was placed in the center (radially) of the leading edge of the bed, thus sensing the lowest bed temperature. Hence, the present reactor system with a more than adequately designed gas preheater and 22 inch heating zone was built and used during the second year. This system is not subject to such large thermal gradients and deviates from isothermal operation only a small amount due to the heat of reaction. This effect was minimized by using shallow bed depths and operating at low conversions.

Catalyst activity data obtained using the present system are presented in Tables 10-13 for fresh and poisoned catalysts at temperatures of 225 and 250°C respectively, a pressure of 20.5 psia, and a space velocity of 30,000 hr^{-1}. Apparent activation energies calculated from the activities at 225 and 250°C for each catalyst are shown in Table 14. Engelhard Ru and Ru-Pd-A-100 which showed no measurable activity at 225°C were tested at 250 and 275°C.

TABLE 10

Reactor Screening Data - Conversions and Selectivities
225°C, GHSV = 30,000 hr^{-1}; 20.5 PSIA

Catalyst	% Conversion CO	% Production CH_4	% Production CO_2	% Selectivity CH_4	% Selectivity CO_2
Pelleted Catalysts					
Greater than 13% active metal					
Co-A-100	5.17	4.32	0.12	84.3	2.3
Co-A-100-Poisoned	4.28	3.18	0.22	75.9	5.4
G-87	13.7	10.9	0.3	79	2.2
G-87-Poisoned*	14.2	11.8	0.5	83	3.4
Ni-A-116	19.6	14.1	0.3	72	1.3
Ni-A-116-Poisoned	18.2	14.2	0.3	78	1.5
Ni-Co-A-100+	14.8	12.3	3.6	84	2.4
Ni-Co-A-100-Poisoned+	16.7	14.3	4.8	86	2.8
Ni-Co-A-100-Poisoned‡	14.8	12.25	0.29	82.8	2.0
Ni-MoO_3-A-102	15.0	11.2	1.05	74.2	7.0
Ni-MoO_3-A-102-Poisoned	13.38	9.63	0.94	72.1	7.1
Ni-Pt-A-100+	12.3	9.6	0.1	79	0.0
Ni-Pt-A-100-Poisoned+	10.0	8.3	0.1	83	1.0
Ni-Pt-A-100-Poisoned‡	11.3	8.9	0.1	79.1	0.7
Ni-Pd-A-100+	5.5	4.4	0.0	80	0.0
Ni-Pd-A-100-Poisoned+	2.5	2.7	0.0	136	0.9
Ni-Rh-A-101	6.33	4.49	0.0	71.1	0.0
Ni-Rh-A-101-Poisoned	2.21	1.95	0.0	89.7	0.0
Ni-Ru-A-106	4.9	3.5	0.0	72	0.0
Ni-Ru-A-106	7.12	5.07	0.02	74.0	0.5
Ni-Ru-A-106-Poisoned	5.99	4.81	0.0	80.7	0.0
Ru-Co-A-100	4.34	3.31	0.02	76	0.5
Ru-Co-A-100-Poisoned	2.83	2.17	0.02	81	0.6
Ru-Co-A-100+	4.56	3.66	0.06	80	1.3
Ru-Co-A-100-Poisoned+	4.94	3.19	0.04	65	0.8
Less Than 6 wt.% active metal					
Ni-A-112	2.43	1.70	0.06	70	0.2

TABLE 10 continued

Catalyst	% Conversion CO	% Production CH_4	% Production CO_2	% Selectivity CH_4	% Selectivity CO_2
Ni-A-112-Poisoned	1.32	0.70	0.0	61	0.0
Ni-MoO_3-A-101	1.36	0.80	0.0	59	0.0
Ni-MoO_3-A-101-Poisoned	0.58	0.32	0.0	56	0.0
Ni-Rh-A-100	2.55	1.72	0.0	68	0.0
Ni-Rh-A-100-Poisoned	1.13	0.82	0.0	75	0.0
Ni-Ru-A-105	2.34	1.62	0.0	70	0.0
Ni-Ru-A-105-Poisoned	1.26	0.94	0.0	77	0.0
Engelhard Ru**	0.78	0.29	0.0	37	0.0
Ru-Pd-A-100**	4.71	2.85	0.0	61	0.0
Ru-Pd-A-100-Poisoned**	1.41	0.13	0.0	20	0.0
Monolithic catalysts					
Ni-M-107	6.61	4.98	0.0	75.6	0.0
Ni-M-113	11.57	8.72	0.05	75.4	0.4
Ni-M-114	13.52	10.2	0.14	75.4	1.1
Ni-Co-M-100	14.8	12.3	3.6	84.0	2.4
Ni-Co-M-100-Poisoned	14.8	12.25	0.29	82.8	2.0
Ni-Pt-M-100	12.3	9.6	0.1	79.0	0.0
Ni-Pt-M-100-Poisoned	11.3	8.89	0.08	79.1	0.7

* Data after exposure of the catalyst to 10 ppm (molar basis) H_2S for 12 hours at a temperature of 450°C.

+ These catalysts were reduced for 10 hours at 450°C before the reactor test. All other catalysts were reduced for 2 hours at 450°C.

** Run at 275°C, GHSV = 5,000

‡ Data after exposure of the catalyst to 10 ppm H_2S for 18-24 hours at a temperature of 450°C.

Table 11

Reactor Screening Data - Rates
225°C, GHSV = 30,000 hr^{-1}; 20.5 psia

Catalyst	Rate x 10^7 gmoles/gcat-sec		Turnover Number x 10^3 Based on Fresh H_2 Uptake		Turnover Number x 10^3 Based on Poisoned H_2 Uptake	
	CO	CH_4	CO	CH_4	CO	CH_4
Pelleted Catalysts						
Greater than 13 wt. % active metal						
Co-A-100	3.2	2.7	3.7	3.1	--	--
Co-A-100-Poisoned	2.7	2.0	3.1	2.3	3.9	2.9
G-87	6.8	5.4	2.3	1.8		
G-87-Poisoned*	6.9	5.7	2.3	1.9	2.3	1.9
Ni-A-116	12.2	8.8	3.9	2.8		
Ni-A-116-Poisoned	11.4	8.9	3.6	2.8	3.2	2.5
Ni-Co-A-100+	8.4	7.0	3.6	3.0		
Ni-Co-A-100-Poisoned+	9.5	8.1	4.0	3.4	4.2	3.6
Ni-Co-A-100-Poisoned‡	8.5	7.0	3.7	3.0	6.5	5.4
Ni-MoO_3-A-102	9.3	6.9	2.9	2.1	--	--
Ni-MoO_4-A-102-Poisoned	7.9	5.7	2.9	2.1	4.1	2.9
Ni-Pt-A-100+	7.4	5.8	2.9	2.3		
Ni-Pt-A-100-Poisoned+	6.0	5.0	2.4	2.0	2.4	2.0
Ni-Pt-A-100-Poisoned‡	6.6	5.2	2.2	1.7	3.2	2.5
Ni-Pd-A-100+	3.4	2.7	2.0	1.6		
Ni-Pd-A-100-Poisoned+	1.3	1.7	0.74	0.97	0.74	0.97
Ni-Ru-A-106	3.2	2.3	1.0	0.73		
Ni-Ru-A-106	4.6	3.3	1.2	0.87	--	--
Ni-Ru-A-106-Poisoned	3.8	3.1	1.0	0.83	1.75	1.4
Ru-Co-A-100+	2.8	2.2	2.6	2.1		
Ru-Co-A-100-Poisoned+	3.0	2.0	2.9	1.9	2.7	1.8
Ru-Co-A-100	2.6	2.0	2.9	2.2		
Ru-Co-A-100-Poisoned	1.7	1.3	1.9	1.5		

TABLE 11 continued

Catalyst	Rate x 10^7 gMoles/gcat-sec		Turnover Number x 10^3 Based on Fresh H_2 Uptake		Turnover Number x 10^3 Based on Poisoned H_2 Uptake	
	CO	CH_4	CO	CH_4	CO	CH_4
Less than 6 wt.% active metal						
Ni-A-112	1.8	1.3	2.3	1.6		
Ni-A-112-Poisoned	0.97	0.52	1.2	0.65	1.7	0.88
Ni-MoO_3-A-101	1.0	0.60	2.8	1.6		
Ni-MoO_3-A-101-Poisoned	0.44	0.24	1.2	0.65	1.2	0.67
Ni-Rh-A-100	1.8	1.2	2.4	1.6		
Ni-Rh-A-100-Poisoned	0.8	0.6	1.1	0.8	1.7	1.2
Ni-Ru-A-105	1.7	1.2	2.2	1.5		
Ni-Ru-A-105-Poisoned	0.91	0.68	1.2	0.88	1.5	1.1
Engelhard Ru**	0.27	0.10	1.5	0.58		
Ru-Pd-A-100 **	0.69	0.42	3.4	2.0		
Ru-Pd-A-100-Poisoned **	0.22	0.02	1.0	0.10		
Monolithic Catalysts						
Ni-M-107	3.8	2.9	7.4	5.5		
Ni-M-113	6.3	4.8	4.2	3.2		
Ni-M-114	7.5	5.7	4.7	3.5		
Ni-Co-M-100	8.4	7.0	3.6	3.0	--	--
Ni-Co-M-100-Poisoned	8.5	7.0	3.7	3.0	6.5	5.4
Ni-Pt-M-100	7.4	5.8	2.9	2.3	--	--
Ni-Pt-M-100-Poisoned	6.6	5.2	2.2	1.7	3.2	2.5

* Data after exposure of the catalyst to 10 ppm (molar basis) H_2S for 12 hours at a temperature of 450°C.

\+ These catalysts were reduced for 10 hours at 450°C before the reactor test. All other catalysts were reduced for 2 hours at 450°C.

** GHSV = 5,000; 275°C.

‡ Data after exposure of the catalyst to 10 ppm H_2S for 18-24 hours at a temperature of 450°C.

TABLE 12

Reactor Screening Data
Conversions and Selectivities
250°C, GHSV = 30,000 hr^{-1}; 20.5 PSIA

Catalyst	%Conversion	%Production		%Selectivity	
	CO	CH_4	CO_2	CH_4	CO_2
Pelleted Catalysts					
Greater than 13% active metal					
Co-A-100	19.84	15.11	3.13	76.3	15.8
Co-A-100-Poisoned	12.59	9.3	1.0	73.9	8.1
G-87	30.4	27.2	0.85	89	2.8
G-87-Poisoned*	29.1	26.4	1.95	91	6.7
Ni-A-116	40.3	32.8	1.55	82	3.8
Ni-A-116-Poisoned	37.3	31.7	1.31	85	3.5
Ni-Co-A-100+	35.5	28.5	2.27	80	6.4
Ni-Co-A-100-Poisoned+	38.4	30.9	3.69	81	9.6
Ni-Co-A-100-Poisoned‡	35.4	29.3	4.15	82.7	11.7
Ni-MoO_3-A-102	34.38	27.64	3.01	80.4	8.8
Ni-MoO -A-102-Poisoned	34.0	28.23	2.99	83.1	8.8
Ni-Pt-A-100+	25.9	22.2	0.17	89	1.4
Ni-Pt-A-100-Poisoned+	21.8	19.5	0.30	88	0.9
Ni-Pt-A-100-Poisoned‡	21.2	18.4	0.21	86.7	1.0
Ni-Pd-A-100+	13.4	11.4	0.00	87	0.0
Ni-Pd-A-100-Poisoned+	8.3	8.2	0.13	98	1.5
Ni-Rh-A-101	11.28	8.31	0.00	73.7	0.0
Ni-Rh-A-101-Poisoned	4.06	3.14	0.00	78.0	0.0
Ni-Ru-A-106	10.3	8.9	0.00	87	0.0
Ni-Ru-A-106	12.95	9.90	0.02	76.5	0.2
Ni-Ru-A-106-Poisoned	11.58	1.52	0.03	82.3	0.3
Ru-Co-A-100	10.9	9.29	0.28	86	2.6
Ru-Co-A-100-Poisoned	10.9	8.78	0.24	81	2.2
Ru-Co-A-100+	11.1	9.52	0.37	86	3.3
Ru-Co-A-100-Poisoned+	8.67	6.60	0.16	76	1.9
Less than 6 wt.% active metal					
Ni-A-112	6.77	6.07	0.07	90	0.0
Ni-A-112-Poisoned	2.91	2.56	0.00	89	0.0
Ni-MoO_3-A-101	3.71	2.94	0.00	79	0.0
Ni-MoO_3-A-101-Poisoned	1.67	1.36	0.03	81	1.6

TABLE 12 continued

Catalyst	%Conversion CO	%Production CH_4	%Production CO_2	%Selectivity CH_4	%Selectivity CO_2
Ni-Rh-A-100	6.32	5.27	0.00	83	0.0
Ni-Rh-A-100-Poisoned	3.07	2.67	0.00	88	0.0
Ni-Ru-A-105	6.06	5.49	0.04	91	0.7
Ni-Ru-A-105-Poisoned	3.64	3.08	0.00	89	0.0
Engelhard 0.5 wt.% Ru **	0.15	0.03	0.00	25	0.0
Ru-Pd-A-100 **	2.35	1.08	0.00	47	0.0
Ru-Pd-A-100-Poisoned**	0.48	0.04	0.00	10	0.0
Monolithic Catalysts					
Ni-M-107	14.62	11.38	0.17	77.9	1.2
Ni-M-113	27.95	24.60	0.49	88.0	1.8
Ni-M-114	31.7	27.82	0.55	87.8	1.7
Ni-Co-M-100	35.5	28.5	2.27	80.0	6.4
Ni-Co-M-100-Poisoned	35.4	29.3	4.15	82.7	11.7
Ni-Pt-M-100	25.9	22.2	0.17	89.0	1.4
Ni-Pt-M-100-Poisoned	21.2	18.4	0.21	86.7	1.0

* Data after exposure of the catalyst to 10 ppm H_2S in H_2 for 12 hours at a temperature of 450°C.

+ These catalysts were reduced for 10 hours at 450°C before the reactor test. All other catalysts were reduced for 2 hours at 450°C.

** GHSV = 5,000.

‡ Data after exposure of the catalyst to 10 ppm H_2S in H_2 for 18-24 hours at 450°C

Reactor Screening Data - Rates
250°C, GHSV = 30,000 hr^{-1}; 20.5 PSIA

Catalyst	Rate x 10^7 (Moles/gcal-sec)		Turnover Number x 10^3 Based on Fresh H_2 Uptake		Turnover Number x 10^3 Based on Posioned H_2 Uptake	
	CO	CH_4	CO	CH_4	CO	CH_4
Pelleted Catalysts						
Greater than 13 wt.% active metal						
Co-A-100	12.4	9.4	14.3	10.9	--	--
Co-A-100-Poisoned	8.0	5.9	9.2	6.8	11.6	8.6
G-87	15.1	13.5	5.1	4.5	--	--
G-87-Poisoned	14.2	12.9	4.8	4.3	4.8	4.4
Ni-A-116	25.1	20.5	8.0	6.5	--	--
Ni-A-116-Poisoned	23.4	19.8	7.4	6.3	6.6	5.6
Ni-Co-A-100+	20.3	16.3	8.5	6.9	--	--
Ni-Co-A-100-Poisoned+	21.7	17.5	9.2	7.4	9.6	7.7
Ni-Co-A-100-Poisoned‡	20.3	16.8	8.7	7.2	15.6	12.9
Ni-MoO_3-A-102	21.3	17.1	7.8	6.3	--	--
Ni-MoO_3-A-102-Poisoned	20.2	16.8	7.4	6.1	10.3	8.5
Ni-Pt-A-100+	15.6	13.3	6.2	5.3	--	--
Ni-Pt-A-100-Poisoned+	13.1	11.7	5.2	4.6	5.2	4.6
Ni-Pt-A-100-Poisoned‡	12.3	10.7	4.1	3.5	6.0	5.2
Ni-Pd-A-100+	8.2	6.9	4.8	4.1	--	--
Ni-Pd-A-100-Poisoned+	5.2	5.1	3.1	3.0	3.04	2.98
Ni-Rh-A-101	7.1	5.3	2.3	1.7	--	--
Ni-Rh-A-101-Poisoned	2.75	2.10	0.81	0.63	1.2	0.93
Ni-Ru-A-106	6.7	5.8	2.1	1.8	--	--
Ni-Ru-A-106	8.3	6.3	2.25	1.70	--	--
Ni-Ru-A-106-Poisoned	7.2	6.4	1.95	1.70	3.3	2.9
Ru-Co-A-100	6.7	5.7	7.3	6.3	--	--
Ru-CO-A-100-Poisoned	5.3	4.0	5.9	4.4	--	--
Ru-Co-A-100+	6.6	5.6	6.3	5.4	--	--
Ru-Co-A-100-Poisoned+	6.7	5.4	6.3	5.1	6.0	4.8
Less than 6 wt.% active metal						
Ni-A-112	5.0	4.5	6.3	5.7	--	--
Ni-A-112-Poisoned	2.2	1.9	2.7	2.4	3.6	3.2

TABLE 13 continued

Reactor Screening Data
250°C, GHSV = 30,000 hr^{-1}; 20.5 PSIA

Catalyst	Rate x 10^7 (Moles/gcal-sec)		Turnover Number x 10^3 Based on Fresh H_2 Uptake		Turnover Number x 10^3 Based on Poisoned H_2 Uptake	
	CO	CH_4	CO	CH_4	CO	CH_4
Ni-MoO_3-A-101	2.9	2.2	7.5	6.0	--	--
Ni-MoO_3-A-101-Poisoned	1.3	1.0	3.4	2.8	3.5	2.9
Ni-Rh-A-100	4.5	3.8	6.0	5.0		
Ni-Rh-A-100-Poisoned	2.3	2.0	3.0	2.7	4.5	3.9
Ni-Ru-A-105	4.4	4.0	5.6	5.1	--	--
Ni-Ru-A-105-Poisoned	2.6	2.3	3.4	3.0	4.3	3.8
Engelhard Ru**	0.051	0.012	0.29	0.068	--	--
Ru-Pd-A-100 **	0.35	0.16	1.7	0.77	--	--
Ru-Pd-A-100-Poisoned**	0.071	0.006	0.34	0.03	--	--
Monolithic Catalysts						
Ni-M-107	8.4	6.5	16.3	12.7	--	--
Ni-M-113	15.4	13.5	10.2	9.0	--	--
Ni-M-114	17.6	15.5	11.0	9.6	--	--
Ni-Co-M-100	20.3	16.3	8.5	6.9	--	--
Ni-Co-M-100-Poisoned	20.3	16.8	8.7	7.2	15.6	12.9
Ni-Pt-M-100	15.6	13.3	6.2	5.3	--	--
Ni-Pt-M-100-Poisoned	12.3	10.7	4.1	3.5	6.0	5.2

* Data after exposure of the catalyst to 10 ppm (molar basis) H_2S for 12 hours at a temperature of 450°C.

+ These catalysts were reduced for 10 hours at 450°C before the reactor test. All other catalysts were reduced for 2 hours at 450°C.

** GHSV = 5,000

‡ Data after exposure of the catalyst to 10 ppm H_2S for 18-24 hours at 450°C.

TABLE 14

Apparent Activation Energies for Methanation Catalysts
Based on measurements at 225-250°C and a space velocity of 30,000 hr^{-1}

Catalyst	CO Conversion (kcal/mole)	CH_4 Production (kcal/mole)
Pelleted Catalysts		
Co-A-100	28.0	26.0
Co-A-100-Poisoned	22.5	22.5
G-87	16.5	19.0
G-87-Poisoned	14.9	16.8
Ni-A-116	15.0	17.5
Ni-A-116-Poisoned	14.9	16.7
Ni-Co-A-100	18.2	17.3
Ni-Co-A-100-Poisoned	17.2	16.0
Ni-MoO_3-A-102	20.5	22.8
Ni-MoO_3-A-102-Poisoned	19.4	22.1
Ni-Pt-A-100	20.5	12.3
Ni-Pt-A-100-Poisoned	16.1	17.7
Ni-Pd-A-100	18.1	19.4
Ni-Pd-A-100-Poisoned	29.5	23.2
Ni-Rh-A-101	11.8	12.5
Ni-Rh-A-101-Poisoned	12.5	9.9
Ni-Ru-A-106	20.6	23.7
Ni-Ru-A-106	12.2	13.4
Ni-Ru-A-106-Poisoned	13.2	15.0
Ni-A-112	22.2	26.8
Ni-A-112-Poisoned	21.8	27.8
Ni-MoO_3-A-101	20.8	27.0
Ni-MoO_3-A-101-Poisoned	21.9	30.0
Ni-Rh-A-100	18.8	20.7
Ni-Rh-A-100-Poisoned	23.2	24.6
Ni-Ru-A-105	19.7	25.3
Ni-Ru-A-105-Poisoned	22.0	25.5
Engelhard Ru*	37.7	48.8

TABLE 14 continued

Catalyst	CO Conversion (kcal/mole)	CH_4 Production (kcal/mole)
Ru-Pd-A-100*	15.8	22.3
Ru-Pd-A-100-Poisoned*	25.5	27.0
Ru-Co-A-100	19.4	21.9
Ru-Co-A-100-Poisoned	23.2	23.0
Monolithic Catalysts		
Ni-M-107	16.4	17.1
Ni-M-113	18.3	21.5
Ni-M-114	17.6	20.8
Ni-Co-A-100	18.3	17.3
Ni-Co-A-100-Poisoned	18.0	18.0
Ni-Pt-A-100	20.5	17.2
Ni-Pt-A-100-Poisoned	13.0	15.0

*Based on 250-275°C

All catalysts were tested using a reactant mixture of 1% CO and 4% H_2 in N_2 diluent. The catalyst samples of 1/8 inch beads were approximately 4 to 6 ml in volume, giving a maximum bed depth of one centimeter. Under these conditions CO conversions ranging from 1 to 40% were obtained. The higher values, obtained on the more heavy metal loading catalysts are admittedly much too high to realize differential kinetic data. However, these catalysts also gave the most consistent and reproducible results. The catalysts containing 13-20 wt.% active metal had confidence limits of + 7% or better while the 0.5-6 wt.% catalysts showed variations in the data up to + 15%. The data for Ni-MoO_3-A-101 in particular showed wide variations in its selectivity. This may be an effect of either a competing reaction which is very temperature sensitive, i.e., Fischer-Tropsch, or a change in the state of reduction from run to run.

The selectivities to CH_4 for nickel containing catalysts as shown in Tables 10 and 12 are higher at 250°C than at 225°C. This is consistent with the well-known observation that Fischer-Tropsch Synthesis favors the lower temperature. The ruthenium containing catalysts have lower selectivities to methanation than the nickel catalysts. Moreover, they do not show appreciable CO_2 formation except in alloy with cobalt, suggesting the formation of higher hydrocarbons on the ruthenium surface. As the percentage of ruthenium increases the selectivity to methane decreases, the lowest selectivity evidenced by the pure ruthenium catalyst. However, for the conditions studied the selectivity for methane of the Ru and Ru-Pd catalysts unexpectedly decreases with increasing temperature.

Selectivity for carbon dioxide formation is exhibited to a significant extent only by the pure nickel and cobalt containing catalysts. The cobalt and nickel-cobalt catalysts in particular exhibit CO_2 formation at least double that of other catalysts. As nickel is alloyed with other metals the CO_2 production is significantly reduced. However, it should be noted that with the lower metal loading catalysts the CO_2 detection capacity of the chromatograph is pushed to the limit because of the very small CO conversions. Additional information regarding selectivities over a wider temperature range for several of these catalysts has been obtained in the integral catalyst tests as part of Task 4.

Methanation rates per gram of catalyst are shown in Tables 11 and 13 for 225 and 250°C and in Figures 14 and 15 for 250°C. Figure 14 shows specific rate data for the catalysts with metal loading of 13 wt.% and higher. Of these catalysts Ni-A-116 has the highest activity (per gram catalyst) followed closely by Ni-MoO_3-A-102 and Ni-Co-A-100 while the Ni-Ru-A-106 has the lowest activity. Co and Ni-Pt catalysts have activities which compare favorably

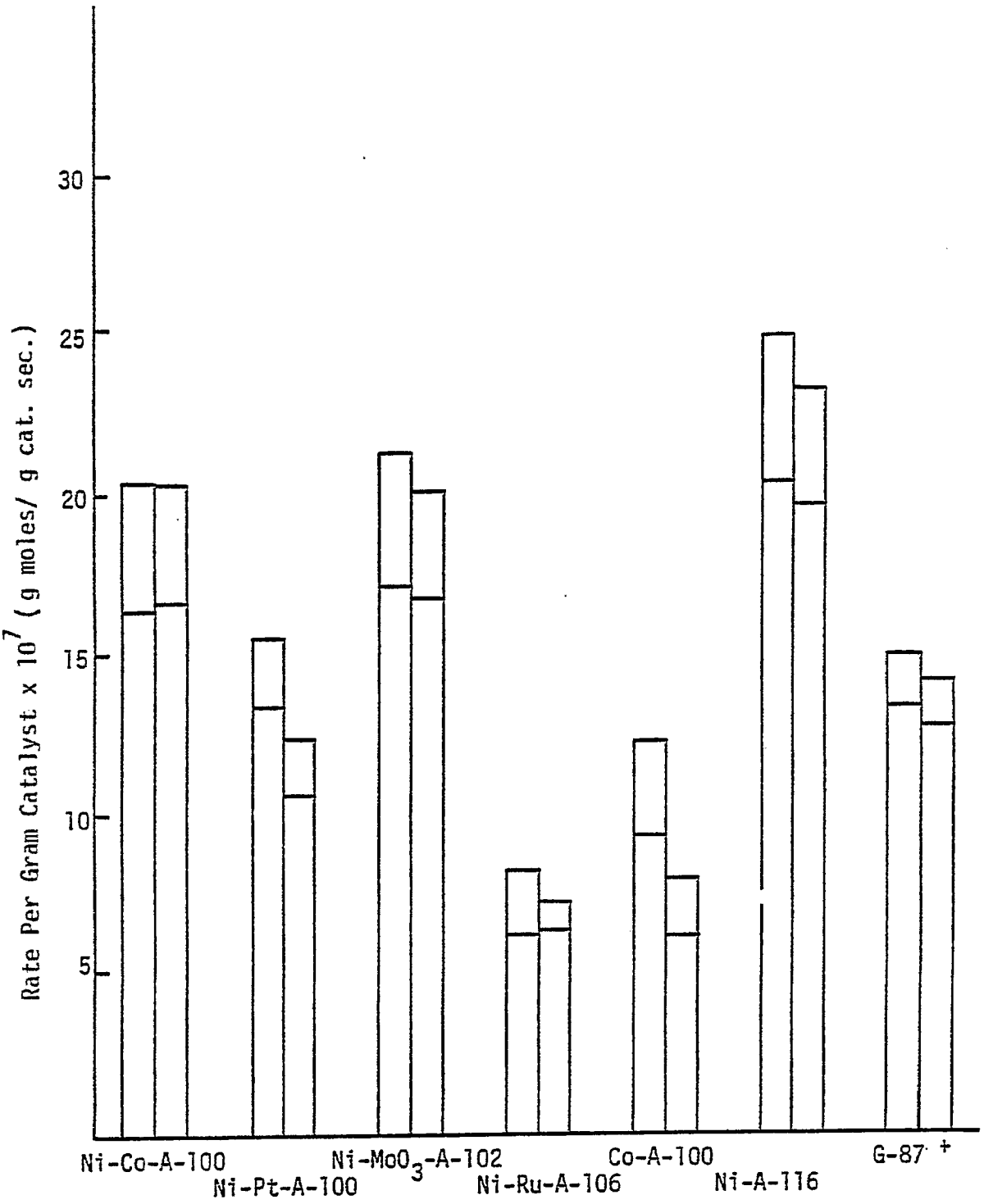

Figure 14. The effect of H_2S on Methanation Activity at 250°C (GHSV = 30,000 hr^{-1}). The first bar of each pair represents the activity of the fresh catalyst; the second indicates the activity after exposure to 10 ppm (molar basis) H_2S in H_2 until 30 to 40% of the metal sites were poisoned at a space velocity of 2,000 hr^{-1} and 450°C. The upper bar represents CO conversion while the lower bar represents methane production. The catalysts were reduced for 2 hours in flowing H_2 at 450°C.

+Exposed to 10 ppm H_2S in H_2 for 12 hours at a space velocity of 2,000 hr^{-1} and 450°C.

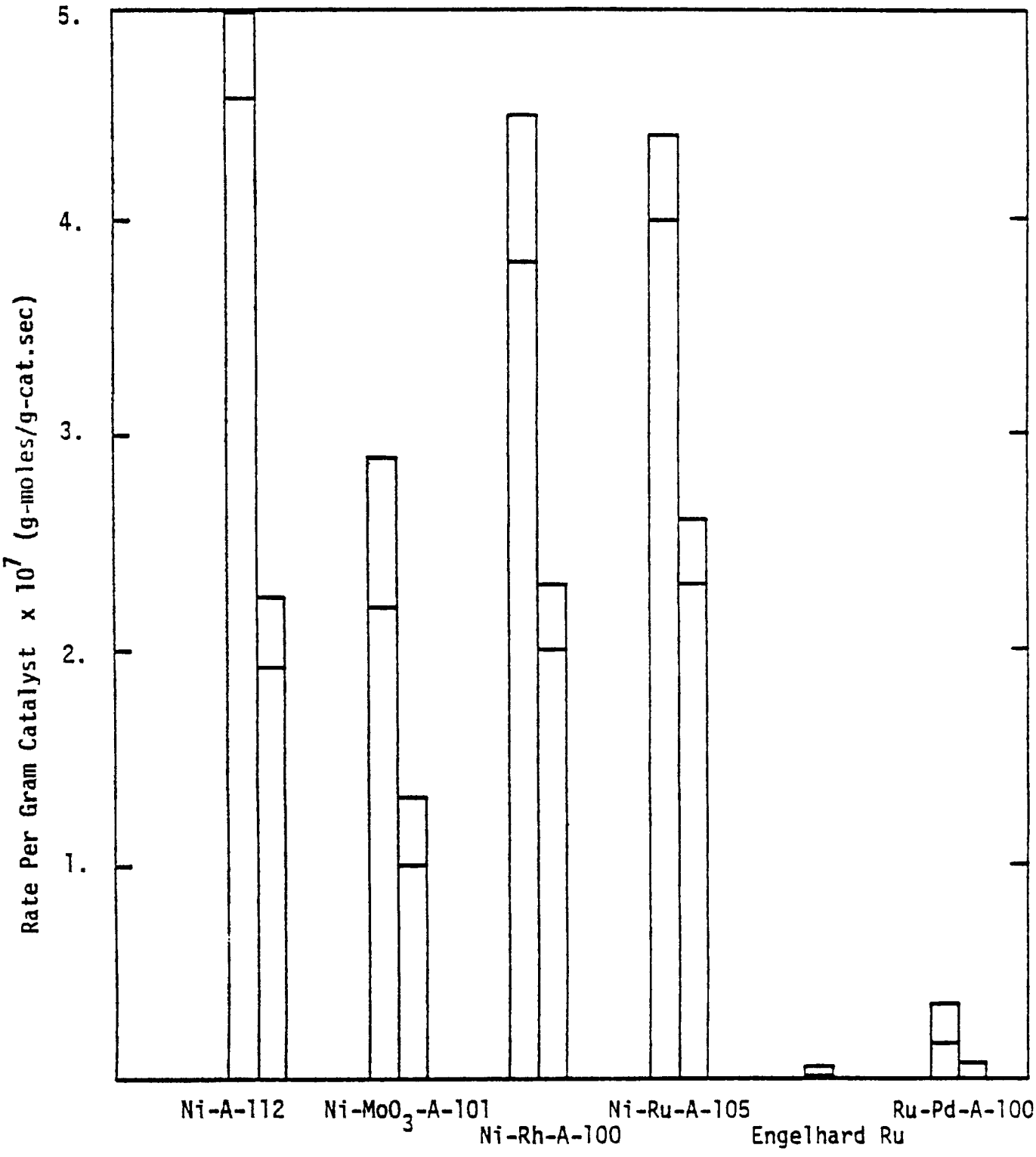

Figure 15. The Effect of H_2S on Methanation Activity at 250°C (GHSV = 30,000). For explanation of figure see Figure 2. The catalysts were reduced for 2 hours at 450°C in flowing H_2. Ru-Pd-A-100 was tested at a space velocity at 5,000 hr^{-1} because it had no detectable activity at 30,000 hr^{-1}.

with G-87 (Girdler), the commercial nickel catalyst. The effect of exposure to H_2S is to lower the rate/g catalyst in all cases except Ni-Co.

Activity data for the 0.5-6 wt.% metal catalysts, shown in Figure 15, indicate a much lower activity on a per mass basis than those with higher metal contents. Ni, Ni-Rh and Ni-Ru catalysts show about the same activity while the Ni-MoO_3 catalyst shows the lowest activity (per gram) of the Ni containing catalysts. The Engelhard Ru and Ru-Pd catalysts have by far the lowest activities of those tested. The lower activity per gram for catalyts having lower metal loadings simply reflects the lower amount of catalytic surface area (per gram) available to catalyze the reaction. This result emphasizes the advantage of comparing activities on a surface area basis rather than a weight or volume basis.

The turnover numbers, activity per H chemisorption site, for the catalysts having high metal contents are shown in Figure 16. The Co catalyst has the highest initial activity followed by Ni-Co, Ni, and Ni-MoO_3, while the Ni-Ru catalyst has the lowest activity; after partial exposure to H_2S, however, the activity per remaining site actually increases for Ni-Co, Ni-MoO_3, and Ni-Ru, whereas it decreases for Co, Ni, and Ni-Pt. The order of activity after poisoning is Ni-Co > Co > Ni-MoO_3 > Ni > Ni-Pt > Ni-Ru. Calculations (22) made during the third quarter show that even at high conversions (10-30%) the kinetic data for these particular catalysts are not affected by heat transfer effects. These calculations, however, do show that the data are influenced to a small degree by pore diffusion. Nevertheless, the comparisons of specific activity are valid because the same support was used for all samples except the commercial catalyst (G-87).

Figure 17 shows the turnover numbers for the catalysts having low metal contents. These data show no effects of heat or mass transfer and negligible pore resistance effects. The turnover numbers obtained for the fresh nickel catalysts are slightly lower then for those having a heavy metal loading, suggesting metal-support interactions may lower the rate. The role of metal-support interactions and crystallite size effects in methanation on nickel are currently under investigation in a separate study in this laboratory supported by NSF.

The order or activity/site for the fresh catalysts is Ni-MoO_3 > Ni > Ni-Rh > Ni-Ru > Ru-Pd > Ru; after partial poisoning with H_2S the order is Ni-MoO_3 = Ni-Ru > Ni > Ni-Rh > Ru-Pd. Again, the ruthenium catalysts show much lower turnover numbers than the nickel catalysts; this result is in disagreement with the work of Vannice (23). We believe this lower activity observed for our ruthenium

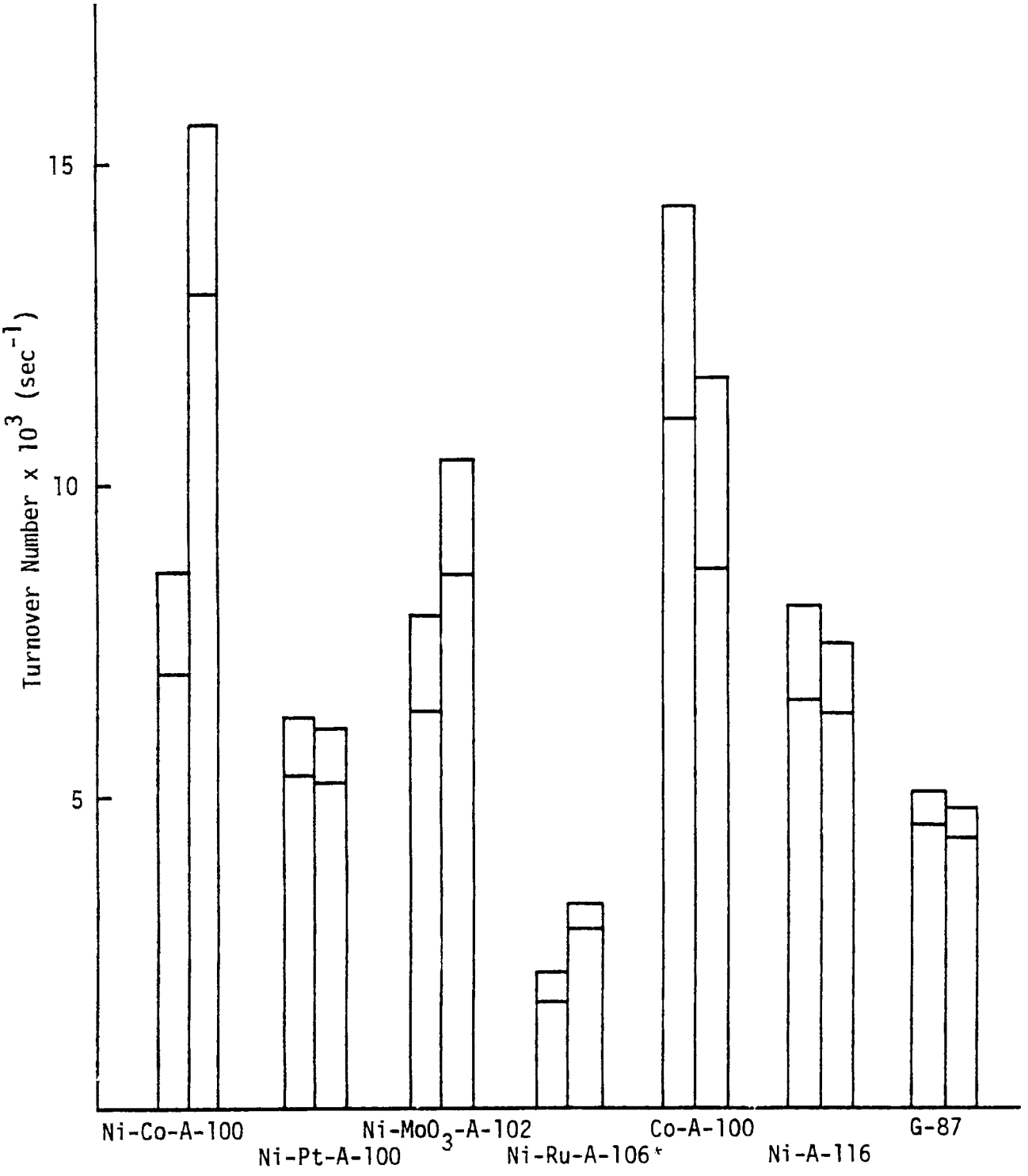

Figure 16. The effect of H_2S on Turnover Number at 250°C (GHSV = 30,000 hr^{-1}). For explanation of the bars see Figure 2. The catalysts were reduced for 2 hours in flowing H_2 at 450°C. Fresh catalyst turnover number based on fresh H_2 uptake; poisoned catalyst turnover number based on poisoned H_2 uptake.

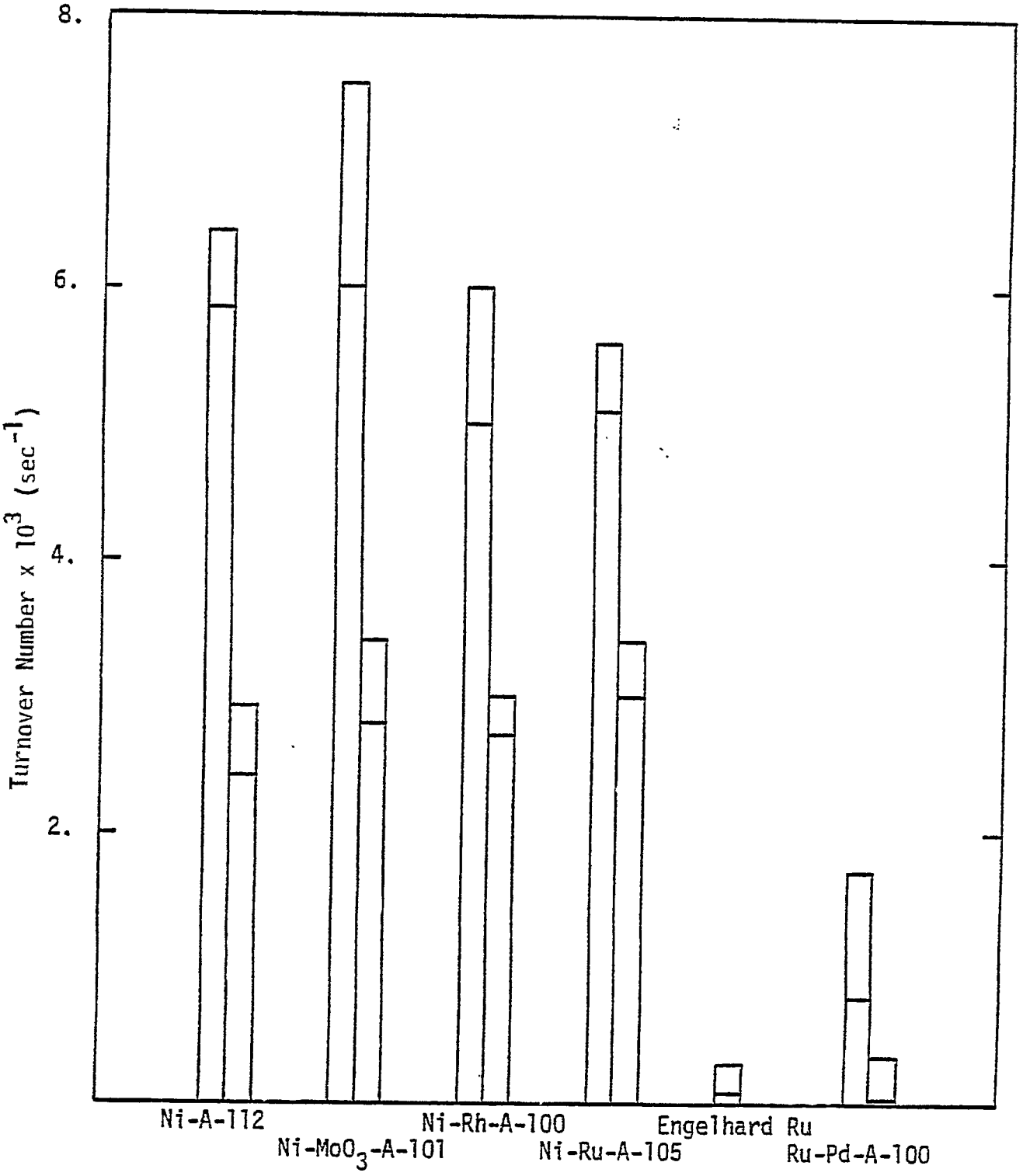

Figure 17 The Effect of H_2S on Turnover Number at 250°C. (GHSV = 30,000). The catalysts were reduced for 2 hours at 450°C in flowing H_2. Ru-Pd-A-100 was tested at a space velocity of 5,000 hr^{-1} because it had no detectable activity at 30,000 hr^{-1}. Both turnover numbers for each catalyst before and after poisoning are based upon the initial surface area (before poisoning).

catalysts might be an effect of poisoning by chloride salts used in the impregnation or of some other form of surface contamination. In the continuation of this work we intend to prepare ruthenium catalysts using chloride-free salts and to pursue techniques for removing impurities from the surface.

The H_2S poisoning experiments in this study were purposely designed such that less sulfur would pass over the catalyst than necessary to completely saturate the surface. This, it was reasoned, would provide experimental leverage to compare residual metal areas and methanation activity for alloy catalysts exposed to just a "little bit" of H_2S. Recent experiments in this laboratory, however, have shown that poisoning of nickel catalysts by H_2S, even at 10 ppm and lower concentrations, is effectively irreversible, exhibiting a very steep breakthrough curve. Thus, the catalyst beads on the leading edge of the bed are heavily poisoned while those on the trailing edge "see" very little if any H_2S. Because of the nonuniform nature of the poisoned sample, it would not be meaningful to divide the sample and test only a portion for methanation activity or surface area. Hence the effects of poisoning on surface area and methanation activity reported here are the average values taken over non-uniform samples.

The fractional changes in hydrogen uptake and turnover number with poisoning of the catalyst (the latter which is called the poisoned site activity ratio (PSAR)) are shown in Table 15. The PSAR is a measure of the change in activity of the methanation sites as a result of partial poisoning. A value less than 1.0 indicates that either the most active sites are poisoned first or that the H_2S interacts strongly with the remaining sites to decrease their activity. Conversely, a PSAR value greater than 1.0 indicates either the least active sites are poisoned first or that the H_2S interacts with the remaining sites to enhance their activity. Thus, Ni-Co-A-100, Ni-Ru-A-106, and Ni-MoO_3-A-102 (of the high loading catalysts) with PSAR values of 1.87, 1.695, and 1.35 respectively are less susceptible to the effects of low concentrations of H_2S since the least active sites are presumably poisoned first. Ni-A-112 (3% Ni/Al_2O_3) and Ni-MoO_3-A-101 of the low metal loading catalysts appear to be least resistant to sulfur. Ni-Ru-A-105 and Ni-Rh-A-100 appear to have slightly greater resistance to H_2S than Ni-A-112.

These results model behavior of a catalyst in response to a plant upset where the bed is inadvertantly exposed to 10 ppm H_2S over a 12 to 24 hour period. For instance, this situation might arise in a large scale methanator as a result of a purification plant upset. Of course these results for partial poisoning of the catalyst should be

TABLE 15

Changes in H_2 Uptake and Turnover Number Due to Poisoning
250°C; CHSV = 30,000

Catalyst	H_2 Uptake^f/H_2 Uptake^I	Poisoned Site Activity Ratio*
Ni-A-112	0.757	0.555
Ni-MoO_3-A-101	0.967	0.481
Ni-Rh-A-100	0.676	0.784
Ni-Ru-A-105	0.785	0.746
Co-A-100	0.795	0.785
Ni-A-116	0.347	0.944
G-87	0.989	0.965
Ni-Co-A-100	0.560	1.87
Ni-MoO_3-A-102	0.719	1.350
Ni-Rh-A-101	0.670	0.554
Ni-Ru-A-106	0.590	1.695
Ni-Pt-A-100	0.678	0.980
Ru-Co-A-100	1.06	1.00

^{I}before poisoning

^{f}after poisoning

* PSAR value = $\frac{CH_4 \text{ turnover number of poisoned catalyst based on poisoned } H_2 \text{ Uptake}}{CH_4 \text{ turnover number of fresh catalyst based on fresh } H_2 \text{ Uptake}}$

and will be followed up with steady state activity tests with dilute H_2S in the reactants.

The data in Tables 10 and 12 show that exposure to H_2S effected increases in selectivity for Ni, Ni-Pd, Ni-Rh and Ni-Ru catalysts, whereas decreases in selectivity were observed for Co and Ru-Pd catalysts. The effects were most dramatic for the Ni-Pd and Ru-Pd catalysts. In a kinetic study of nickel, ruthenium, and rhenium methanation catalysts, Dalla Betta et al. (24) showed that exposure to H_2S effects an increase in selectivity to hydrocarbons (C_{2+}) and a decrease in selectivity for methane. Our results for Co and Ru-Pd catalysts agree with their observations; however, our results for nickel and noble metals promoted nickel catalysts do not.

Data are listed in Tables 11 and 13 for two samples of the Ru-Co catalyst. These two samples received identical treatment except for the length of reduction prior to the activity tests. The first sample was reduced 2 hours while the second was reduced 10 hours. The length of reduction seems to have a significant effect on the catalyst's response to partial poisoning by H_2S; that is, the sample which was reduced longer appeared unaffected by the H_2S. The Ni-Pt catalyst also exhibited variations in selectivity to methane depending upon the reduction time; for example, 99% selectivity to methane was measured after 2 hours reduction (QPR-4, p.59) as compared to 85-90% for 10 hours reduction (see Tables 10 and 12). These effects are probably due to: (i) an increase in the state of reduction of the surface with increasing reduction time, and/or (ii) changing surface metal composition of the catalyst due to induced surface reconstruction by the reducing hydrogen environment. The latter might come about because the Ni-H bond is stronger than the Pt-H bond, causing Ni enrichment on the surface. Since Ni has a lower selectivity for methane than Pt (23), the increased nickel content of the surface would bring about a decrease in selectivity.

Table 14 shows the apparent activation energies calculated from the data in Tables 10-13. The high metal loading catalysts exhibit values 2-5 kcal/mole lower then the low metal loading catalysts. This effect is due likely to the presence of pore diffusional resistance in the case of the former catalysts simply because they operated at higher conversions and rates/gram catalyst. The value of 26.8 kcal/mole for Ni-A-112 (3% Ni/Al_2O_3) is in excellent agreement with the value of 25 ± 2 kcal/mole reported by Vannice for Ni/Al_2O_3 (23). It is informative to compare the values for the pure nickel catalysts with the alloys. The variations from catalyst to catalyst are strong evidence of alloy formation in the bi-metallic catalysts. Especially interesting is Ni-Pt which before poisoning shows a very

low activation energy for methane production. After poisoning the activation energy more closely approaches that of pure nickel, suggesting that the most active methanation sites on this catalyst are the first sites to be poisoned, or that the surface concentration of nickel is increased by a further exposure to the H_2S/H_2 reducing environment. The Ni-MoO_3 catalysts apparently evidence larger values for the activation energy than the nickel catalysts; hence at higher temperatures (e.g. 300-400°C) the Ni-MoO_3 catalysts should be by far the most active.

D. Task 4: Catalyst Life and Geometry: Testing and Design.

1. Planning of Experiments.

Task 4 involves a series of laboratory reactor tests of pellet and monolithic-supported Ni, Ni-Co, Ni-Ru, Ni-Rh, Ni-Pt, and Ni-MoO_3 catalysts as a function of temperature, pressure, H_2S concentration and geometry using the newly constructed reactor described previously. These particular catalysts were chosen for further testing on the basis of promising results obtained in the screening tests (Task 3). This extensive program of testing was begun ahead of schedule during late Summer 1976 and is scheduled for completion by December 1977.

During the first six quarters preliminary experiments, discussions and planning efforts by the principal investigator and students associated with the project resulted in the development of a detailed experimental program for the testing of the methanation catalysts listed above. Altogether there are five different kinds of tests: (1) conversion versus temperature measurements at low pressure with and without steam in the feed gas, (2) conversion versus temperature measurements at high pressure, (3) 24 hour runs at 400°C and different H_2/CO ratios to determine resistance to carbon deposition, (4) measurement of activity at 250°C during *in situ* exposure to 1 and 10 ppm H_2S, and (5) high conversion measurements at low pressure for the same nickel catalyst supported on monoliths of varying geometry. The detailed experimental conditions and basic procedures used in each of these tests are listed in Table 16.

The conversion versus temperature (integral) tests (Test 1 and 2) at high and low pressures provide rate data over the range of conversion from 0 to 100% and conversion and selectivity data over the range of temperature most appliable to industrial methanation. From these data, turnover numbers, selectivities, conversion versus temperature curves, and the effects of water on these parameters can be obtained. In order to determine turnover numbers, the metal surface area is measured after each set of integral runs. From the steady state, 24-hr. runs (Test 3) the

TABLE 16

Description of Reactor Tests for Task 4

Test Procedures	Experimental Conditions
1. Temperature-Conversion Test: Measure CO conversion and methane production as a function of temperature, with and without 1% (by vol.) of steam present in the reactant mixture.	200-400°C 8 psig 30,000 hr^{-1} 1% CO, 4% H_2, 95% N_2 (dry basis)
2. Temperature-Conversion Test (high pressure): Measure CO conversion and methane production as a function of temperature at 350 psig.	200-400°C 350 psig 30,000 hr^{-1} 1% CO, 4% H_2, 95% N_2
3. Steady State (24 Hr.) Carbon Deposition Test: Measure CO conversion and methane production at 225 and 250°C (30,000 hr^{-1}) before and after an exposure of 24 hours at 400°C.	400°C (24 hrs.) 8 psig 200,000-250,000 hr^{-1} 25% CO, 50% H_2 $H_2/CO = 2$
4. In situ H_2S Tolerance Test: Measure intermittently the production of methane and hydrocarbons (by FID) during 24 hours exposure to feed containing 1 or 10 ppm H_2S using a glass reactor.	250°C 8 psig 30,000 hr^{-1} 1% CO, 4% H_2, 95% N_2 1 or 10 ppm H_2S
5. Support Geometry Tests: Measure CO conversion and methane production as a function of temperature for the same Ni/Al_2O_3 catalyst supported on monoliths and pellets of varying geometries.	300-400°C 8 psig 30,000 hr^{-1} 1% CO, 4% H_2, 95% N_2

effect of carbon deposition on rate is determined. Following these runs selected catalysts are analyzed for carbon content to determine the extent of deposition. Test 4 provides data regarding the relative resistances to H_2S of nickel and nickel alloy catalysts (monolith and pellet supports), the rates of poisoning and the effects of H_2S concentration on the rate of poisoning. From the support geometry tests (Test 5) the effects of monolith and pellet geometry on CO conversion and selectivity to methane are determined. Since the methanation reaction is limited by mass transfer to the catalyst exterior at high conversions, the effects of different exterior surface areas should be moderately important in affecting conversion. It will also be important to measure metal surface areas for selected samples before and after Test 4.

2. Accomplishments - Pellet-Supported Catalysts.

a. Conversion vs. Temperature (Integral) Tests. During the first two years, low pressure conversion versus temperature tests were conducted on nickel, cobalt and nickel-bimetallic catalysts at space velocities of 15,000 hr^{-1} and 30,000 hr^{-1}. A representative plot of conversion versus temperature for 14% Ni/Al_2O_3 is shown in Figure 18. Conversion-temperature plots for each of the catalysts can be found in QPR-4,5,6,7. Important conversion parameters for these catalysts are listed in Table 17. Generally, the high metal loading catalysts perform better than the low metal loading catalysts. The high metal loading Ni, Ni-Co, and Co catalysts have the highest conversions of the catalysts tested. The 14% Ni catalyst has the highest methane production (89%) and reaches its maximum at the lowest temperature. CO conversion for the Ni-Co catalyst is approximately the same as the Ni catalyst but reaches its maximum at a slightly higher temperature. Conversion of CO to methane for the Co catalyst is not quite as high as the Ni or Ni-Co catalysts but does reach its maximum at the same temperature as the Ni catalyst. The Co catalyst has the highest CO_2 production of any of the high loading catalysts tested, followed by the Ni-Co catalyst. The Ni-Pt catalyst has a surprisingly low maximum conversion and methane yield considering its high metal loading and very low Pt content.

Table 18 shows rates per gram catalyst at high conversion. Surprisingly, the low metal content catalysts show approximately the same activities on this basis as the high loading catalysts. However, since the high metal loading catalysts have a higher density, their rates of methane production on a reactor volume basis would be significantly larger.

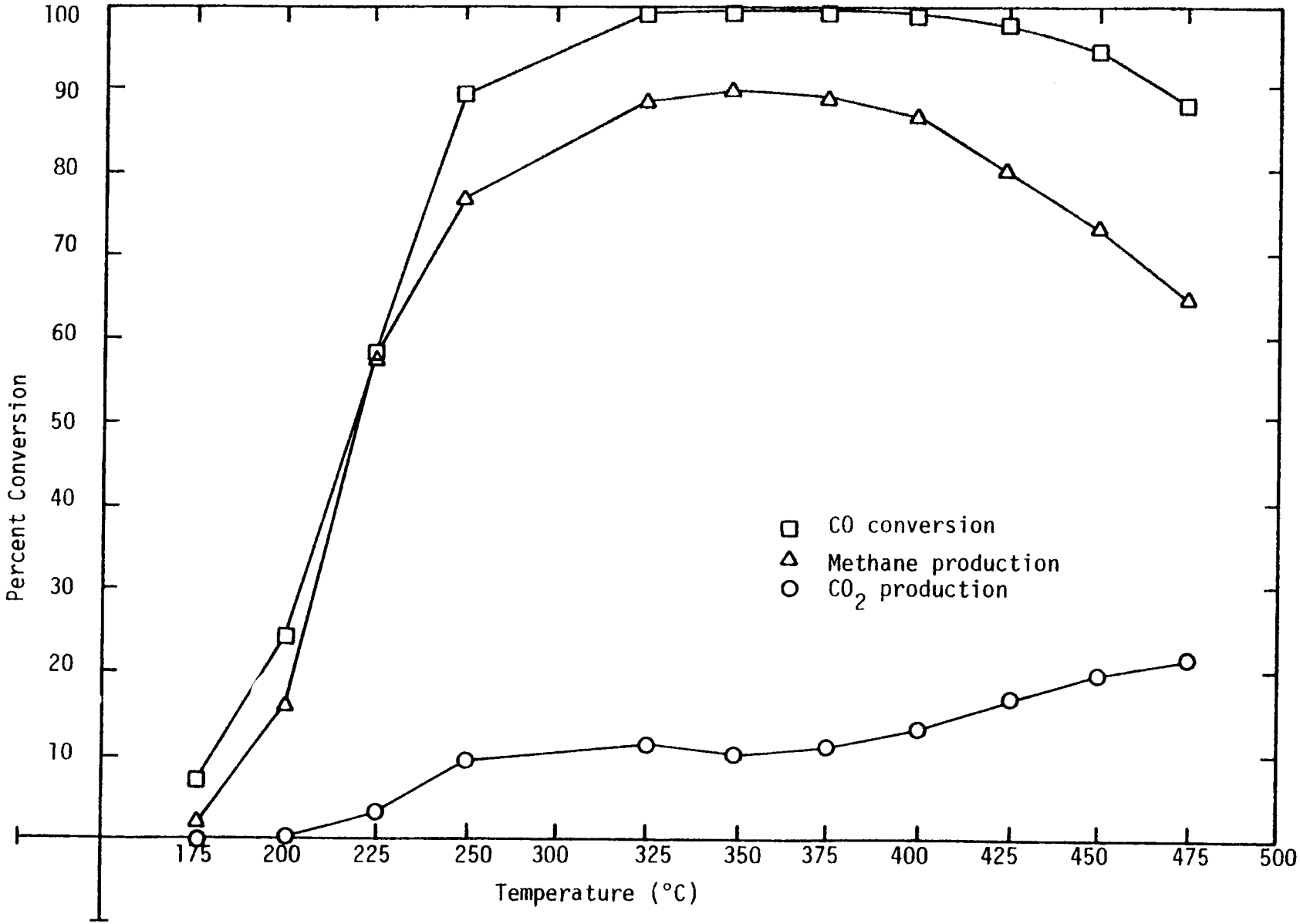

Figure 18. Conversion versus Temperature for Ni-A-116 (14.0 wt.% Ni/Al_2O_3) (20.5 psia; GHSV = 15,000 hr^{-1}).

TABLE 17

Summary of Integral Test Results
(20.5 psia; GHSV = 15,000 hr^{-1})

Catalyst	Temperature of CO Conversion 50% (°C)	Maximum (°C)	Maximum CO Conversion	At Maximum CO Conversion CH_4 Produc.	CO_2 Produc.
Low Loading Catalysts					
Ni-A-112	265	350	93%	74%	20%
Ni-MoO_3-A-101	270	375	86%	70%	17%
Ni-Rh-A-100	310	400	81%	64%	16%
Ni-Ru-A-105	312	414	73%	56%	16%
High Loading Catalysts					
Ni-A-116	220	325	99%	89%	10%
Ni-Co-A-100	210	329	99%	84%	16%
Ni-Pt-A-100	237	375	84%	70%	13%
Co-A-100	235	325	96%	71%	23%
Integral Tests with Steam Injection					
Ni-A-112	285	400	96%	3%	86%
Ni-A-116	245	350	99%	19%	75%
Monolithic Catalysts					
Ni-M-113	255	325	100%	96%	4%

TABLE 18

Rates* from Integral Tests
(20.5 psia, 15,000 hr^{-1})

Catalyst	325°C		At Maximum Conversion	
	R_{CO}	R_{CH_4}	R_{CO}	R_{CH_4}
Low Loading Catalysts				
Ni-A-112	35.4	27.6	36.2	28.8
Ni-MoO_3-A-101	31.4	27.3	32.9	26.8
Ni-Rh-A-100	18.3	17.0	25.9	20.6
Ni-Ru-A-105	21.5	19.0	28.2	22.2
High Loading Catalysts				
Ni-A-116	31.7	28.6	31.7	28.6
Ni-Co-A-100	29.9	25.6	29.9	25.6
Ni-Pt-A-100	25.5	23.4	26.9	22.4
Co-A-100	31.0	22.9	31.0	22.9

*All rates are reported in gmoles/gcat-sec x 10^7

Thus far, our efforts have been directed mainly at the hydrogenation of CO to methane. However, in using an activated charcoal trap to purify our reactant gases of iron carbonyl, H_2S and organics, we discovered that it produced small amounts of CO_2 (0.1%). During attempts to eliminate this CO_2 contamination it was noticed that at approximately 400°C and 20 psia the CO_2 was converted almost completely to CH_4 by Ni and Ni-Co catalysts. The N_2 concentration was 96% and the H_2 concentration was 4% (no CO or H_2O was initially present). The space velocity was varied from about 3,000 hr^{-1} to 15,000 hr^{-1} with the same results. No further quantitative measurements were attempted. At present we have removed the carbon trap and are using only Molecular Sieve 5A for purification.

b. Water injection integral runs. During the sixth quarter activity versus temperature tests with steam injection in the feed were performed for the same group of catalysts. Representative results for one Ni catalyst (Figure 19) show that water vapor has a large, detrimental effect on methane production. The overall conversion of CO is increased significantly at a given temperature by the presence of the water vapor. However, the methane production is reduced from 70-90% (no water) to 5-20% (with 15 vol.% water vapor); CO_2 is correspondingly increased by water. This undoubtedly results from an increase in the rate of the water gas shift reaction. The conversion to methane (in the presence of steam) is also found to decrease significantly with increases in temperature, as can be seen clearly in Figure 20. Consideration of the large observed effects of 15 vol.% water and the fact that industrial methanators involve much lower values of H_2O/CO suggests that realistically a lower concentration of steam should be used. Subsequent tests were carried out using 1% water vapor.

During the seventh quarter activity vs. temperature tests with 1% water injected in the feed were completed. A typical plot of percent conversion of CO and the percent productions of CH_4 and CO_2 versus temperature is shown in Figure 21. Each of the runs were conducted at a GHSV of 30,000 hr^{-1} with a reactant gas mixture containing 95% N_2, 4% H_2, and 1% CO on a dry mole basis with 1% (by vol) water vapor injected in the feed. Again the presence of water in the feed causes total conversion of CO to be increased at any given temperature; CH_4 production is significantly decreased and CO_2 production correspondingly increased, although, the effect of 1% water is significantly less than with 15% water.

The presence of water vapor changes the general trend of the conversion vs. temperature graph as well as increasing total conversion of CO. With no water present the conversion of CO usually reaches a maximum between

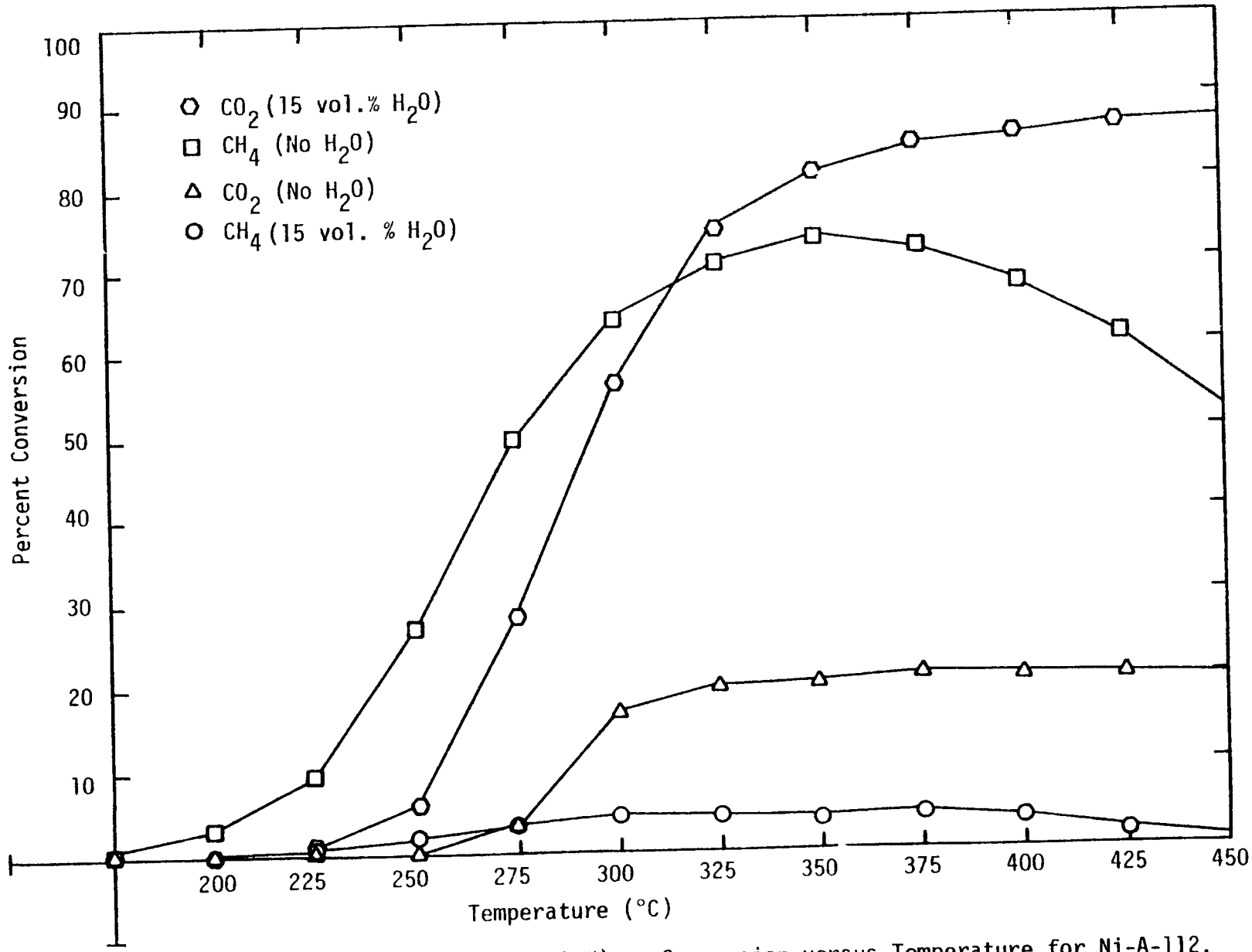

Figure 19. Effects of Steam (15 vol.%) on Conversion versus Temperature for Ni-A-112. (3% Ni/Al_2O_3) (20.5 psia; GHSV = 15,000 hr^{-1}).

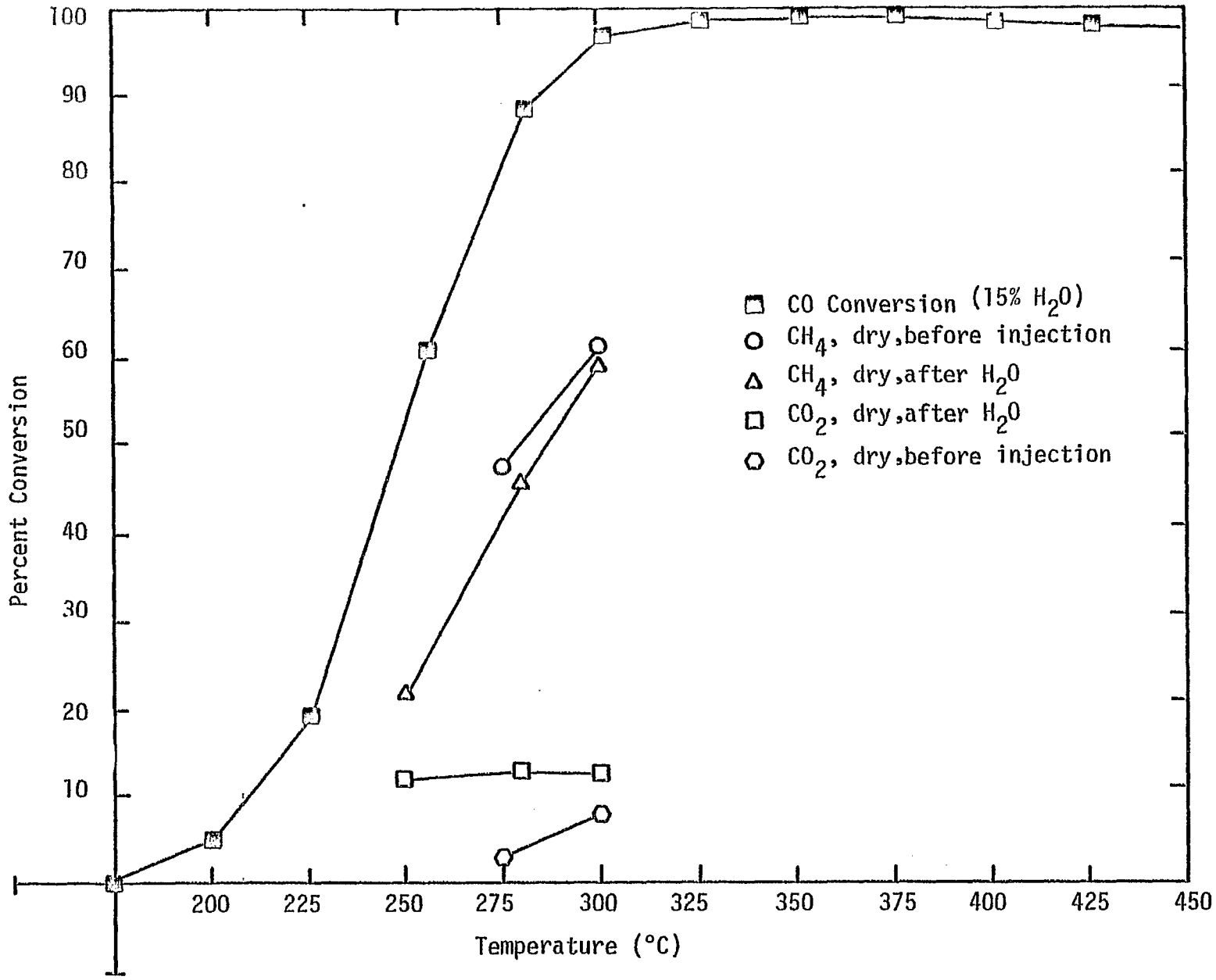

Figure 20. Methane Production Before and After Steam Injection for Ni-A-116 (14.0% Ni/Al_2O_3) (20.5 psia; GHSV = 15,000 hr^{-1}).

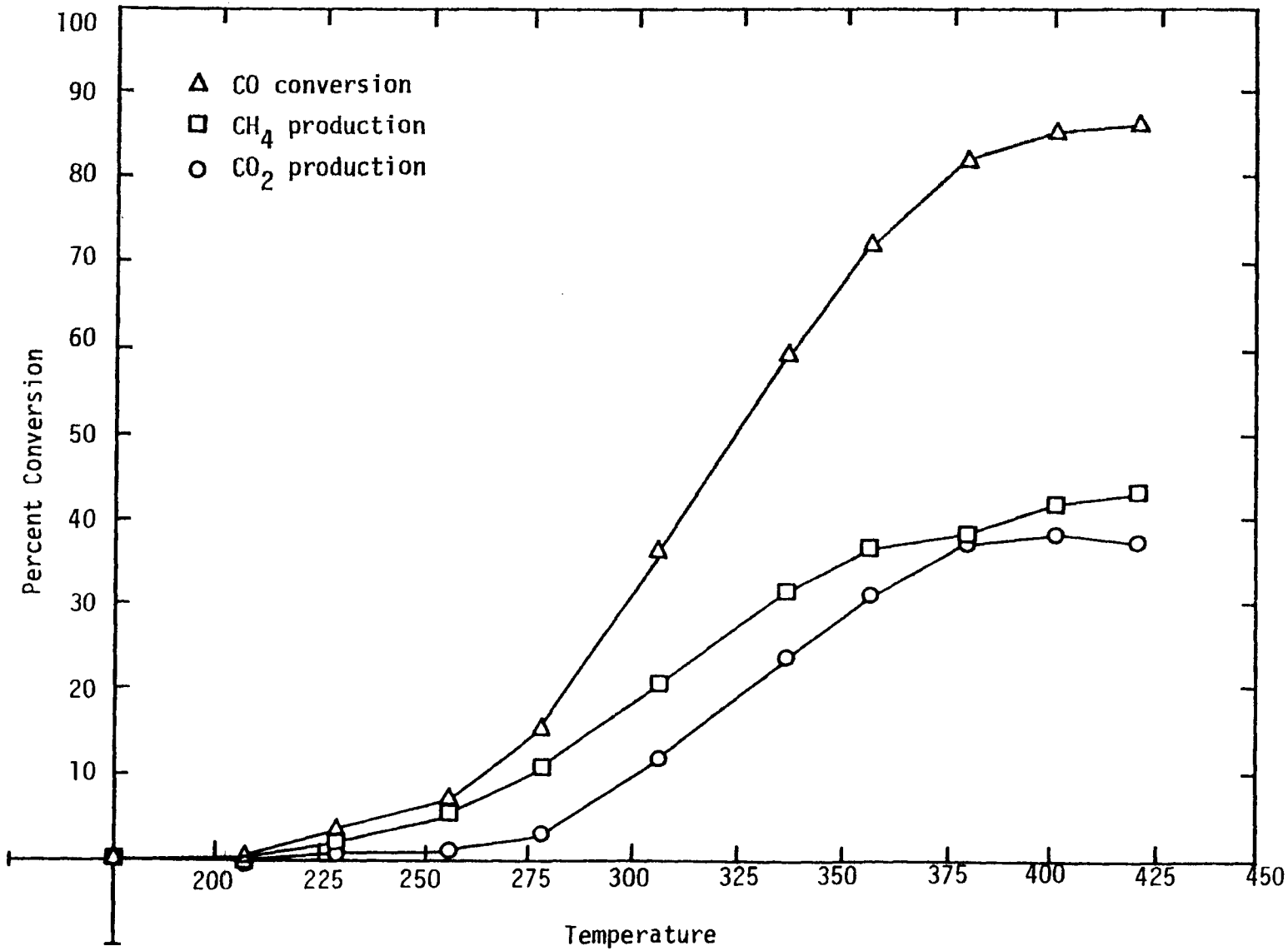

Figure 21. Conversion vs. temperature Ni-A-112 (3% Ni/Al_2O_3), 20.5 psia, GHSV = 30,000 hr^{-1}, 1% water vapor in feed.

325 and 400°C and then declines. With water present, however, the maximum does not occur but CO conversion continues to increase with temperature. However, conversion to CH_4 does reach a maximum at about 350 to 400°C and then declines. The maximum CH_4 production for each catalyst as well as its corresponding CO_2 production and selectivity to CH_4 (defined as the percent of converted CO which is converted to CH_4) are listed in Table 19. The behavior for conversion to CO_2 as a function of temperature generally falls into two categories: (i) CO_2 production rises quickly with increasing temperature and then levels off (Ni and Ni-Co catalysts) and (ii) CO_2 production increases steadily (Ni-MoO_3, Ni-Ru, Ni-Rh, and Ni-Pt).

From Table 19 it can be seen that Ni-A-116 (14% Ni) has the highest CH_4 production, highest selectivity, and reaches its maximum CH_4 production at the lowest temperature. The Ni-Co catalyst also has a high CH_4 production and high selectivity. Ni-Pt has the second highest selectivity but has a much lower CH_4 production than the Ni or Ni-Co catalysts. In comparison to the 14% Ni, the 3% Ni catalyst has lower selectivity and reaches its maximum CH_4 production at a higher temperature.

Since thermodynamics favors the water gas shift reaction and CO_2 production at high temperatures, it is interesting that the catalysts which have high CH_4 productions and selectivities in the presence of water vapor are the ones that achieve high conversions at low temperature.

The maximum selectivity for each catalyst is listed in Table 19; the maximum occurs at a low temperature where CH_4 production is low (5-20%). Ni-Pt has the highest selectivity on this basis, and the Ni catalysts have the worst. When a comparison is made at 350,C (Table 19b) Ni-Pt and Ni-Rh are found to have the highest CH_4 selectivities, 3% Ni the lowest. The Ni and Ni-Co catalysts have the highest values of percent CH_4 production at 350°C but their selectivity is not quite as good as the Ni-Pt.

Activity vs. temperature tests (at 225, 250°C - no H_2O) were conducted before and after the water injection tests to see what effect water vapor had on the catalyst surface area and degree of reduction. Generally there was no significant decrease in activity or in the levels of CH_4 and CO_2 production as observed in the tests with 15% water vapor (see Figure 20). There was, however, a loss of catalyst surface area as seen from Table 5. We are presently investigating sintering of Ni/Al_2O_3 and nickel alloy catalysts in H_2 and H_2/H_2O atmospheres as part of our NSF study. Thus far, we have determined that steam accelerates the loss of both support and metal surface area in high temperature reducing atmospheres.

Table 19

Summary of Water Injection Integral Runs
(GHSV = 30,000 hr^{-1}, 20.5 psia, 1% water vapor in feed)

a. At Maximum CH_4 Production

Catalyst	% CH_4 Prod.	Temp.°C	%CO_2 Prod.	% Sel. CH_4
Ni-A-112	43	421	37	50
Ni-A-116	66	353	25	69
Ni-Co-A-100	57	386	31	60
Ni-MoO_3-A-101	42	399	21	61
Ni-Ru-A-105	26	395	19	53
Ni-Rh-A-100	32	451	30	50
Ni-Pt-A-100	48	394	26	62
b. At Approximately 350°C				
Ni-A-112	37	357	31	51
Ni-A-116	66	353	25	69
Ni-Co-A-100	57	386	31	60
Ni-MoO_3-A-101	40	353	11	71
Ni-Ru-A-105	25	350	9.4	68
Ni-Rh-A-100	19	351	3.6	78
Ni-Pt-A-100	47	350	14	75
c. Maximum Selectivity for CH_4				
Ni-A-112	5.3	256	2.9	75
Ni-A-116	13.2	230	1.2	74
Ni-Co-A-100	16.9	234	1.5	79
Ni-MoO_3-A-101	10.5	275	1.7	80
Ni-Ru-A-105	9.0	280	1.3	84
Ni-Rh-A-100	10.5	302	1.0	82
Ni-Pt-A-100	19.0	259	1.2	95

c. High pressure integral runs. During the 7th and 8th quarters high pressure conversion vs. temperature tests for pellet supported catalysts were completed. Maximum conversions for the catalysts tested were 98% or greater for all except the 3% Ni-Ru and the 20% Ni-Co (GHSV = 50,000 hr^{-1}) for which maximums of 94 and 96 percent were observed. A typical conversion vs. temperature plot is shown in Figure 22. Since maximum CO conversions were all about the same (98%) over a wide range of temperature, comparison of temperatures for maximum conversion is not meaningful. Thus, the temperatures for 50 and 95 percent conversion of CO are listed in Table 20 along with the CH_4 production and selectivity. The Ni and Ni-Co catalysts reach the 95% conversion level at the lowest temperature (280°C). The other catalysts evidence more gradual increases in conversion as temperature is increased.

Selectivities to CH_4 production are much greater at high pressure than at low pressure. All the catalysts tested at high pressures have selectivities of 90% or greater and in some cases approach 100%. For example, Figures 23 and 24 show that 3% and 14% Ni evidence significantly higher selectivities in the high pressure test compared to the the low pressure tests (except at 225-250°C). At high pressure selectivity increases with increasing temperature, whereas at low pressure it decreases with increasing temperature. Comparison of the rates of methane production (Tables 18 and 20) reveals the rate based upon mass is approximately 2 to 2 1/2 times larger at 365 psia than at 20 psia. Thus a factor of 20 increase in pressure essentially doubles or triples the rate of reaction at high conversions.

CH_4 and CO turnover numbers at 225°C and 365 psia for four low metal loading catalysts are listed in Table 21 along with the corresponding turnover numbers for low pressure. The turnover numbers at 365 psia are 4-5 times higher than those reported previously for 20.5 psia, except for Ni-Ru. The CO turnover number for this catalyst is about the same as at low pressure and the methane turnover number a factor of 3-4 smaller suggesting that selectivity to higher molecular weight hydrocarbons is increased at the higher pressure. Hence, the conditions for using Ni-Ru in Fischer-Tropsch synthesis are defined: namely low temperature (225-250°C) and high pressure (20-25 atm).

d. Thermodynamic Calculations. In planning our steady state reactor tests we searched the literature and performed thermodynamic calculations to determine both conditions which might promote and those which might prevent carbon deposition. We are also concerned about minimizing ammonia and carbon dioxide formation in our test reactor. Ammonia is a reaction poison, carbon deactivates the catalyst, and carbon dioxide is an undesirable by-product. Accordingly, we performed thermodynamic calculations of our reaction

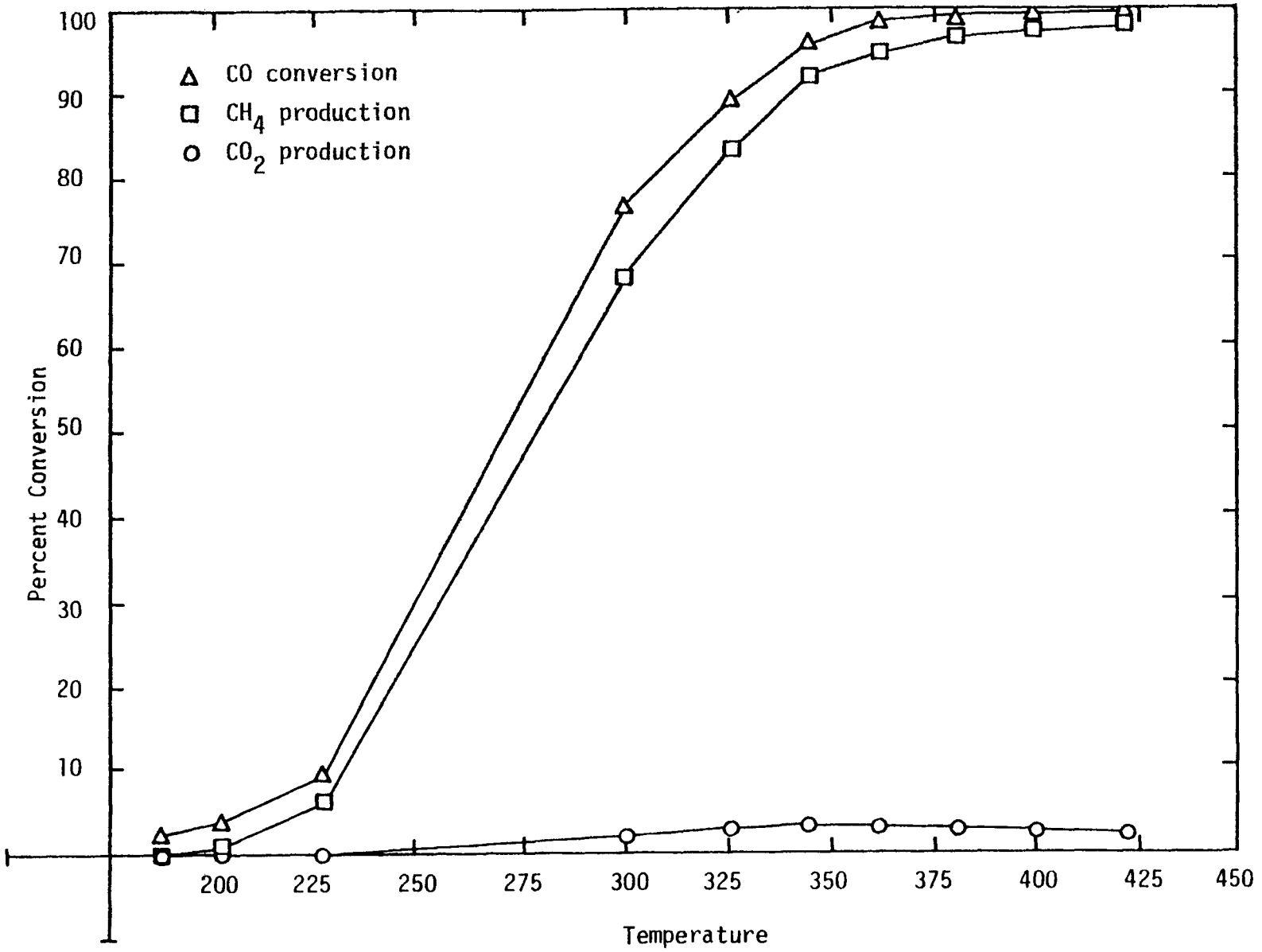

Figure 22. Conversion vs. temperature Ni-A-112 (3% Ni/Al_2O_3), 365 psia, GHSV = 30,000 hr^{-1}.

TABLE 20

Summary High Pressure Tests
(365 psia, GHSV = 30,000 hr^{-1})

a. At 50% CO Conversion

Catalyst	Temp.	$\%CH_4$ Prod.	% Sel. CH_4	$R^+_{CH_4}$ (x 10^3)	R^+_{CO}
Low Loading Catalysts					
Ni-A-112	270	43	98	33.1	37.9
Ni-MoO_3-A-101	275	43	84	28.9	40.2
Ni-Ru-A-105	330	43	86	26.7	31.1
Ni-Rh-A-100	280	38	76	27.9	36.7
High Loading Catalysts					
Ni-A-116	225	38	69	22.9	30.0
Ni-Co-A-100	215	26	47	15.7	30.4
Ni-Co-A-100*	240	30	59	29.0	47.1
Ni-MoO_3-A-103	241	31	60	19.8	31.5
Ni-Pt-A-100	220	24	46	14.3	30.1
Ni-Ru-A-106	280	37	75	15.8	20.8
Ni-Rh-A-101	245	35	68	20.0	28.6
Co-A-100	240	23	45	12.8	27.3

b. At 95% CO Conversion

Low Loading Catalysts					
Ni-A-112	342	91	96	69.4	72.5
Ni-MoO_3-A-101	340	89	94	62.8	66.9
Ni-Ru-A-105	437‡	85	90	54.0	60.0
Ni-Rh-A-100	350	89	93	64.7	69.2
High Loading Catalysts					
Ni-A-116	275	92	97	57.7	59.6
Ni-Co-A-100	280	90	94	53.8	56.9
Ni-Co-A-100*	325	89	94	84.9	90.2
Ni-MoO_3-A-103	340	93	98	70.2	71.9

TABLE 20 continued

Catalyst	Temp.	$\%CH_4$ Prod.	% Sel. CH_4	$R^+_{CH_4}$	R^+_{CO}
Ni-Pt-A-100	295	91	96	53.1	55.5
Ni-Ru-A-106	365	93	98	37.5	38.2
Ni-Rh-A-101	310	94	99	53.4	53.7
Co-A-100	292	85	90	46.5	52.1

*Run at a GHSV - 50,000 hr^{-1}

‡Max conversion was 94% at 437°C

+Rates expressed in gMole/gcat-sec

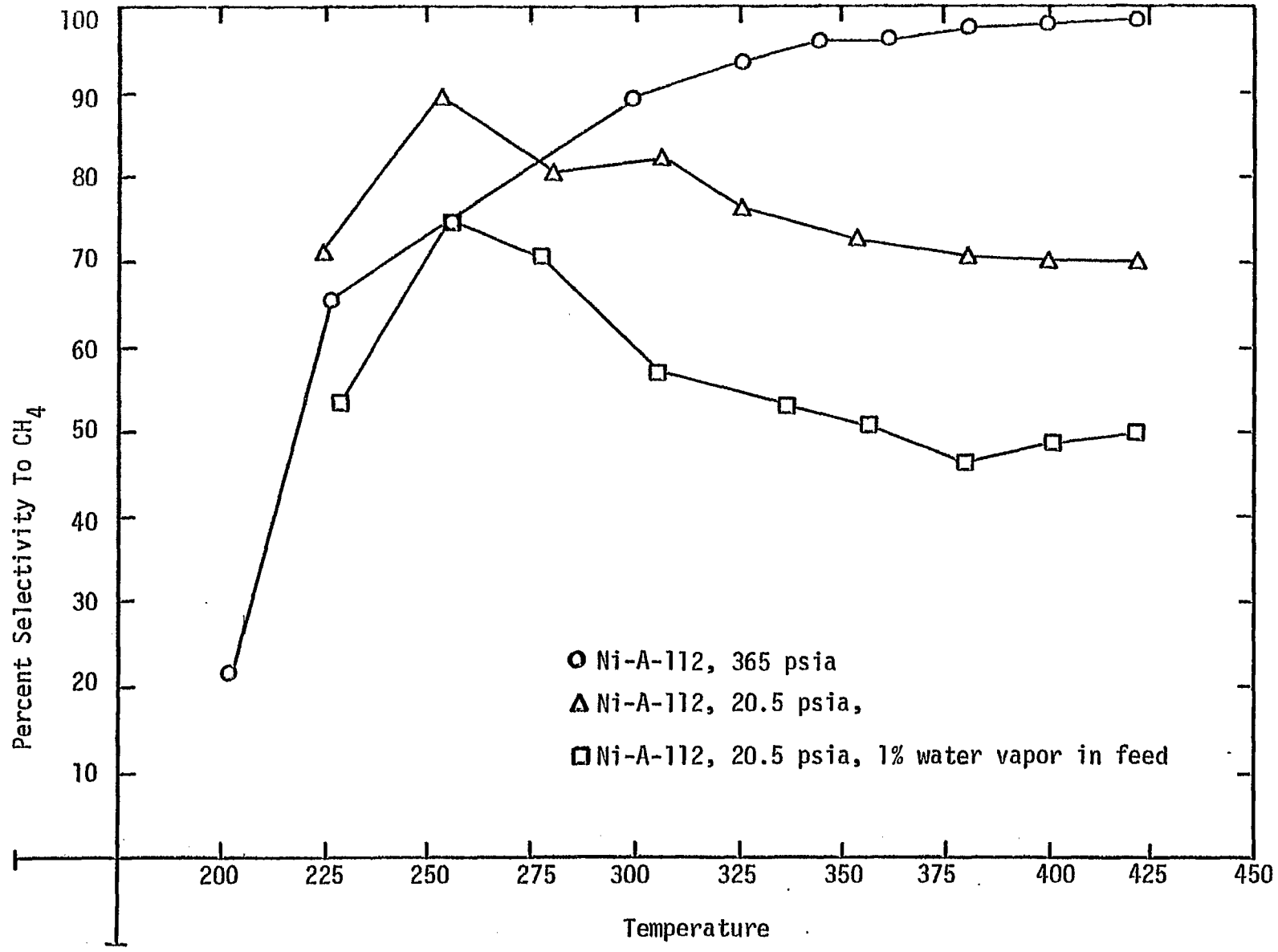

Figure 23. Selectivity vs. temperature Ni-A-112 (3%-Ni/Al_2O_3) GHSV = 30,000 hr^{-1}.

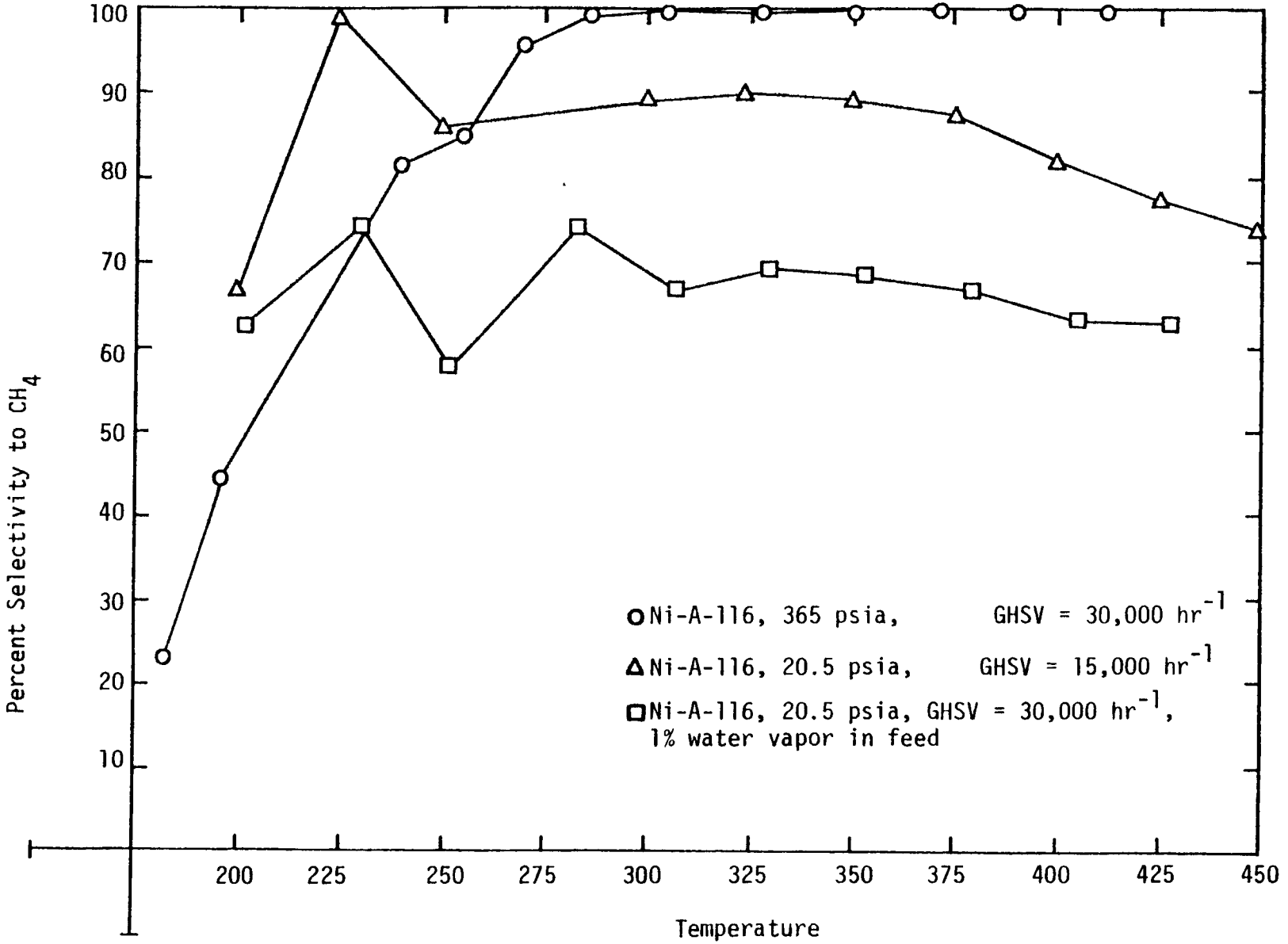

Figure 24. Selectivity vs. temperature Ni-A-116 (14% Ni/Al_2O_3).

Table 21

Turnover Numbers for Nickel and Nickel Alloys at High and Low Pressures

Catalyst	$N_{CH_4} \times 10^3$ sec^{-1}	$N_{CO} \times 10^3$ sec^{-1}	% Selectivity CH_4
	225°C, GHSV = 30,000 hr^{-1}, 365 psia		
Ni-A-112	6.3	9.6	66
Ni-MoO_3-A-101	9.1	18.8	48
Ni-Ru-A-105	0.44	1.9	23
Ni-Rh-A-100	5.9	11.7	51
	225°C, GHSV = 30,000 hr^{-1}, 20.5 psia		
Ni-A-112	1.2	1.8	67
Ni-MoO_3-A-101	1.6	2.8	57
Ni-Ru-A-105	1.5	2.2	68
Ni-Rh-A-100	1.6	2.4	67

mixtures at various temperatures and pressures to determine the equilibrium formation of ammonia, carbon, and carbon dioxide. A detailed description of these calculations and results is found in Appendix 1 of QPR-7.

Generally, we found that ammonia formation for our test mixtures would be less than 0.1 mole percent at equilibrium. Since NH_3 formation is very much kinetically limited at methanation reaction temperatures the ammonia concentration which the catalysts see can be estimated to be about 1 ppm or less.

Based on our calculations for carbon formation we found that higher pressure, lower temperatures, higher H_2/CO ratios, addition of N_2 or He diluents, and the presence of small amounts of H_2O (1%) inhibit carbon formation. Conversely, lower pressures, higher temperatures, lower H_2/CO ratios, addition of CH_4 and the absence of H_2O promote carbon formation. Carbon dioxide formation is inhibited generally by lower temperatures, higher pressures, and the absence of H_2O.

e. Steady State Carbon Deposition Tests. The work with powdered catalysts is essentially complete. Most of the problems were worked out in the eighth quarter; however, our CO tank was found to contain iron carbonyl which poisoned our catalyst during the early steady state runs. The results of the first five runs for nickel are therefore questionable (see Table 22).

In order to facilitate use of powdered samples at high space velocities the steady state runs were conducted in a glass reactor (see Figure 12). During the early runs a black substance deposited on the preheater coils from the point where the coils enter the oven to the catalyst bed. Deposits were formed at steady state temperatures from 325 to 450°C. There were no deposits downstream of the catalyst bed. After long term Run 8 for Ni-A-112 oxygen was passed through the cell at 300°C to burnoff the carbon and regenerate the catalyst. Very little of the deposited material was removed. During subsequent evacuation the sample could not be pumped down. Nevertheless, upon freezing the cell with liquid nitrogen the pressure was easily lowered. Chromic acid cleaning solution only partially removed the deposit; however, the remainder dissolved readily in hydrocholric acid. Apparently then, iron carbonyl from the CO cylinder was thermally decomposed to iron in the preheater coil, which then catalyzed formation of a volatile cabonaceous deposit.

Iron carbonyl also apparently deactivated the catalyst, i.e., the remaining iron carbonyl (not decomposed on the preheater coils) was adsorbed by the catalyst bed since there was no deposit after that point. The powdered catalysts

TABLE 22

Summary of Steady State Carbon Deposition Tests
(Reaction Mixture: 25% CO, 50% H_2, 25% N_2; $H_2/CO = 2$)

Catalyst	Run#	Space Vel.x10^{-3} (hr^{-1})	Hours above 400°C	Final Activity rate/gr poisoned/ rate/gr fresh	Selectivity % CH_4 before	Selectivity % CH_4 after
Ni-A-112	1*[a]	15	27	.73[b]	65	66
	3*[a]	5	16	.70[c]	70	75
	6*	250	25	.41	92	66
	8*	250	15	.31	85	70
	9*	250	2	.23	86	63
	10	250	9	.71	83	87
	12	250	12	.79	87	91
Ni-Co-A-101	1	165	13[d]	.34	69	13[e]
	2	165	7	.87	67	70
Ni-Ru-A-105	2	165	12	.32	88	91
	3	165	12	.81	94	97
	4	165	12	.68	83	77
Ni-Rh-A-100	1	165	12	.65	85	77
	2	165	12	.29	83	100[f]
Ni-Pt-A-101	1	165	12	.90	84	67
	2.	165	5	.75	80	81
Ni-MoO_3-A-101	1	165	3	.00	--	--
	2	165	4	.00	--	--

*iron carbonyl present

[a]pellet sample

[b]differential test at 225°C

[c]differential test at 250°C

[d]temperature excursion during startup; 500+°C; 30 min.

[e]very low conversion, CH_4 not analyzed well by GC

[f]CH_4 peak not analyzed properly by GC; reason unknown.

that were suspected to have been poisoned by the iron carbonyl all showed a decrease in selectivity to methane after the steady state run and a significant decrease in conversion on the order of 50-70%. This can be seen readily in Table 22 for Ni-A-112 long term runs 6, 8, and 9. In Runs 1 and 3 with pellets an increase in selectivity to methane and a decrease in activity of about 25% was observed. With long term Run 1 it was possible to regenerate the surface area by treating the catalyst with oxygen at 300°C. Therefore, it is reasonable to assume that the loss of surface area and activity in Runs 1 and 3 was mainly due to carbon deposition and not iron carbonyl poisoning. The difference between the two different kinds of observations in the long term runs could be caused by at least two factors: (1) geometrical effects in iron carbonyl poisoning, (2) a substantial decrease in the amount of iron carbonyl available for poisoning due to the lower space velocity used in these runs.

Following the early steady state runs a fresh molecular seive trap and a new activated carbon trap were added to the system to eliminate the iron carbonyl problem. After they were installed no deposits on the preheater coils (presumably caused by iron carbonyl) were observed.

The steady state runs were originally planned to be run at H_2/CO ratios of 3 and 2 with 25% N_2 diluent. Since the rate of carbon deposition was less than expected, the $H_2/CO = 3$ runs were eliminated. After the early $H_2/CO = 2$ tests were partially completed it was found that the actual ratio was 1.8. To keep the results comparable the same ratio was used for the remaining tests.

Various problems were encountered in early testing of small powder samples (0.2 g) at high space velocities, e.g. channeling and bypass. Therefore, slightly larger samples (0.5 g) and lower space velocities (165,000 hr^{-1}) were used for most of the runs.

Results of the steady state runs for nickel and nickel bimetallic catalysts are summarized in Table 22. The last two nickel runs and all nickel alloy runs were started at 440 to 450°C. During each of these runs as carbon deposition occurred the temperature dropped gradually, in some cases falling below the light-off temperature. The time that the runs were above 400°C is listed in Table 22. The corresponding activities (defined as the rate after carbon deposition divided by the rate of the fresh catalyst) and selectivies to methane are also listed. Since the results are somewhat varied even for a given catalyst it is difficult to draw quantitative conclusions. Nevertheless, it appears that qualitatively the Ni-Pt and Ni-Co catalysts are slightly more resistant to carbon deposition than the other catalysts. On the other hand, Ni-Rh and $NiMoO_3$ appear to be less resistant; indeed the $NiMoO_3$ catalyst is completely

deactivated after a short period of time. Since the $NiMoO_3$ catalyst is not completely reduced it is possible that molybdenum oxide accelerates cracking of synthesized hydrocarbons and the rate of coke formation. This might also be true for the Ni-Ru and Ni-Rh catalysts since they are probably not completely reduced at 450°C in H_2. Differences in state of reduction could also account for some inconsistencies in the results for the nickel catalyst, although all the catalysts were reduced in H_2 for 2 hours at 450°C.

Figure 25 shows the activity of Ni-A-112 as a function of time. It can be seen that most of the activity loss occurs during the first few hours of the run. The rate of deactivation is estimated to be 2 1/2 % of the original activity per hour for the first 10 hours. Activity data for Ni-A-112 as a function of time were measured in differential tests, which required about 1 1/2 hours for measurement of each data point, if the time to return to steady state conditions at 400°C is included. Because of the large amount of time and effort required, activity vs. time data were obtained only for the one nickel catalyst.

3. Accomplishments - Monolithic Supported Catalysts

a. Low Pressure Conversion-Temperature Tests. Conversion-temperature tests of nickel and nickel bimetallic monolithic catalysts at 20.5 psia are summarized in Table 23a. An example is shown in Figure 26. The nine nickel monoliths were prepared by the same general techique, but vary in nickel loading percent. One sample, Ni-M-101, was three inches long and the others were 1/2 inch in length. Four different nickel bimetallics are also represented in the same table. The reaction conditions included a space velocity of 30,000 hr^{-1}, a reaction mixture containing 95% N_2, 4% H_2, and 1% CO, a pressure of 20.5 psia and temperatures from 200 to 450°C. Three of the tests were conducted at 15,000 hr^{-1} to provide a comparison with the several pellet catalysts which had been tested at this lower space velocity. Turnover numbers (molecules of CH_4 formed per active site per second) were calculated from the activity tests at 225°C (see Table 23a). Turnover numbers at 225°C were chosen because at that temperature, most (but not all) of the catalysts converted less than 10% of the CO in the reactant stream. At such low conversions the effects of pore diffusion and exterior film resistance should not significantly influence the rate of reaction.

Comparison of the turnover numbers for the different monolithic catalysts shows the order of specific activity to be $Ni\text{-}MoO_3$ > Ni-Co > Ni > Ni-Pt > Ni-Ru. The order of specific activity on a mass basis (rate/g catalyst) is approximately the same. Comparison of the turnover numbers at 225°C for monolithic catalysts (Table 23a) with

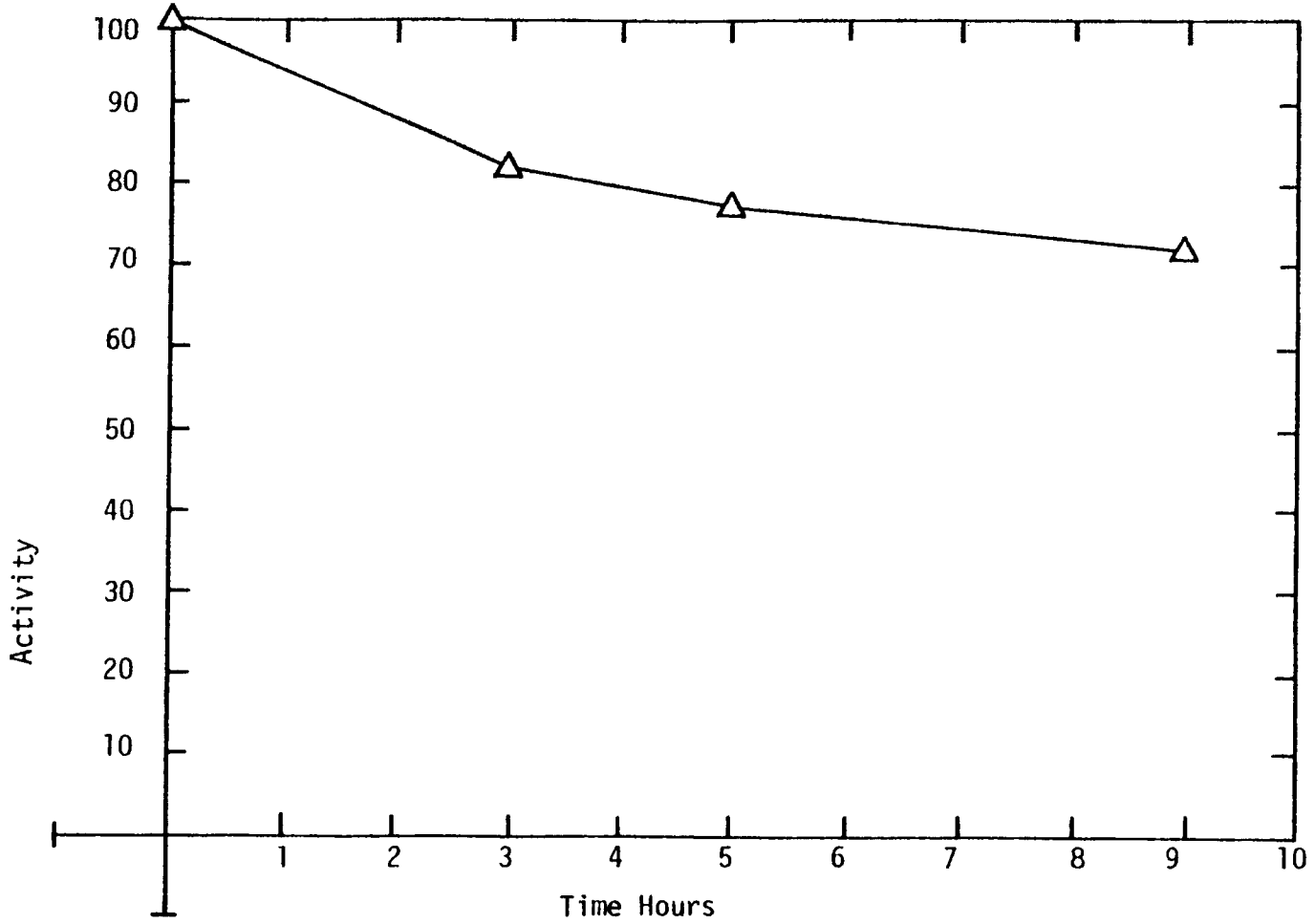

Figure 25. Carbon Deposition Steady State Run #10 (Ni-A-112).

TABLE 23

Summary of Integral Temperature Conversion Tests on Monolithic Supported Catalysts

Catalyst	Temperature for CO Conversion of 10%	50%	95%	At 95% CO Conversion % CO converted to CH_4	CO_2	At Peak CH_4 Production % CO converted to CH_4	Temperature	Rate of CH_4 Production (Moles/gram-sec x 10^7)	At 225°C Turnover Number, N_{CH_4} (molecules CH_4 per site per sec)
a. The following 17 tests were conducted at 20.5 psia, 95% N_2, 4% H_2 and 1% CO, and at 30,000 hr^{-1} GHSV									
Ni-M-101[a]	180	230	270	83	5.0	100	300	8.8[a,d]	3.4
Ni-M-101[a]	175	230	270	94	3.5	100	275	8.7[a,d]	0.9
Ni-M-107[a]	240	295	370	65	17	69	375	39.7[a,d]	12.6
Ni-M-113[a]	200	255	290	88	7.7	97	325	26.5[a,d]	3.2
Ni-M-114	215	260	325	85	12	87	350	48.0	4.3
Ni-M-115	215	275	325	76	13	81	345	53.8	4.5
Ni-M-117	220	270	320	83	11	89	365	50.8	3.7
Ni-M-118	210	265	305	84	11	88	340	46.4	2.7
Ni-M-121	225	275	320	78	16	86	355	60.4	3.8
Ni-Co-M-101	240	320	437[b](85%)	64[b]	18[b]	65	410	40.9	4.8
Ni-Co-M-104	225	270	305	71	23	85	360	53.7	4.2
Ni-MoO_3-M-100	260	315	411[b](85%)	64[b]	18[b]	65	410	40.9	3.5
Ni-MoO_3-M-103	215	270	315	85	7.8	87	320	57.6	---
Ni-MoO_3-M-106	220	270	310	85	6.9	90	345	55.5	10.
Ni-Pt-M-107	235	305	404[b](93%)	77[b]	6.2	78	390	34	1.8
Ni-Ru-M-100	315	370	440[b](82%)	64[b]	15	64	420	32.3	.93
Ni-Ru-M-108	265	375	436[b](76%)	60[b]	12	60	435	25.5	---
b. The following 7 tests were conducted at 365 psia, 30,000 hr^{-1} GHSV and same composition as above									
Ni-M-117[c]	190	245	315	92	1	98	420	91.6	10.1
Ni-M-121	<185	225	245	94	1	100	250	54	9.
Ni-Co-M-100	205	250	350	89	4	92	400	56.8	7.9
Ni-Co-M-103	200	235	275	83	5	100	350	60.	10.5

TABLE 23 continued

$Ni-MoO_3$-M-101	230‡	280	395	90	2	95	415	66.5	---
Ni-Pt-M-108	<220	240	285	90	4	98	337	42.1	2.6
Ni-Ru-M-111	270	300	360	87	2	99.6	411	46.6	<7
c. The following 6 tests were conducted at 20.5 psia, 30,000 hr^{-1} GHSV and with 1% H_2O in the reactant stream									
Ni-M-303	225	275	310	68	22	77	350	33.5	1.8
Ni-M-122	240	290	330[b]	63[b]	32[b]	71	385	50.7	2.2
Ni-Co-M-108	230	265	400[b](92%)	51[b]	28[b]	53	365	28.9	4.2
$Ni-MoO_3$-M-104	240	295	370[b](82%)	60[b]	20[b]	63	345	42.6	---
Ni-Ru-M-109	320	400	435[b](79%)	35[b]	39[b]	35	435	17.1	<0.4
Ni-Pt-M-108	240	300	420[b](92%)	55[b]	23[b]	60	370	28.1	1.8

[a]These 3 tests were conducted at 15,000 hr^{-1} GHSV

[b]These catalysts did not achieve 95% CO conversion within the temperature range studied(200-450°C). The % in parenthesis indicates the highest conversion obtained.

[c]This test only was conducted at 50,000 hr^{-1} GHSV.

[d]Ni-M-101 is twice as dense as Ni-M-113. Rates expressed per gram of catalyst.

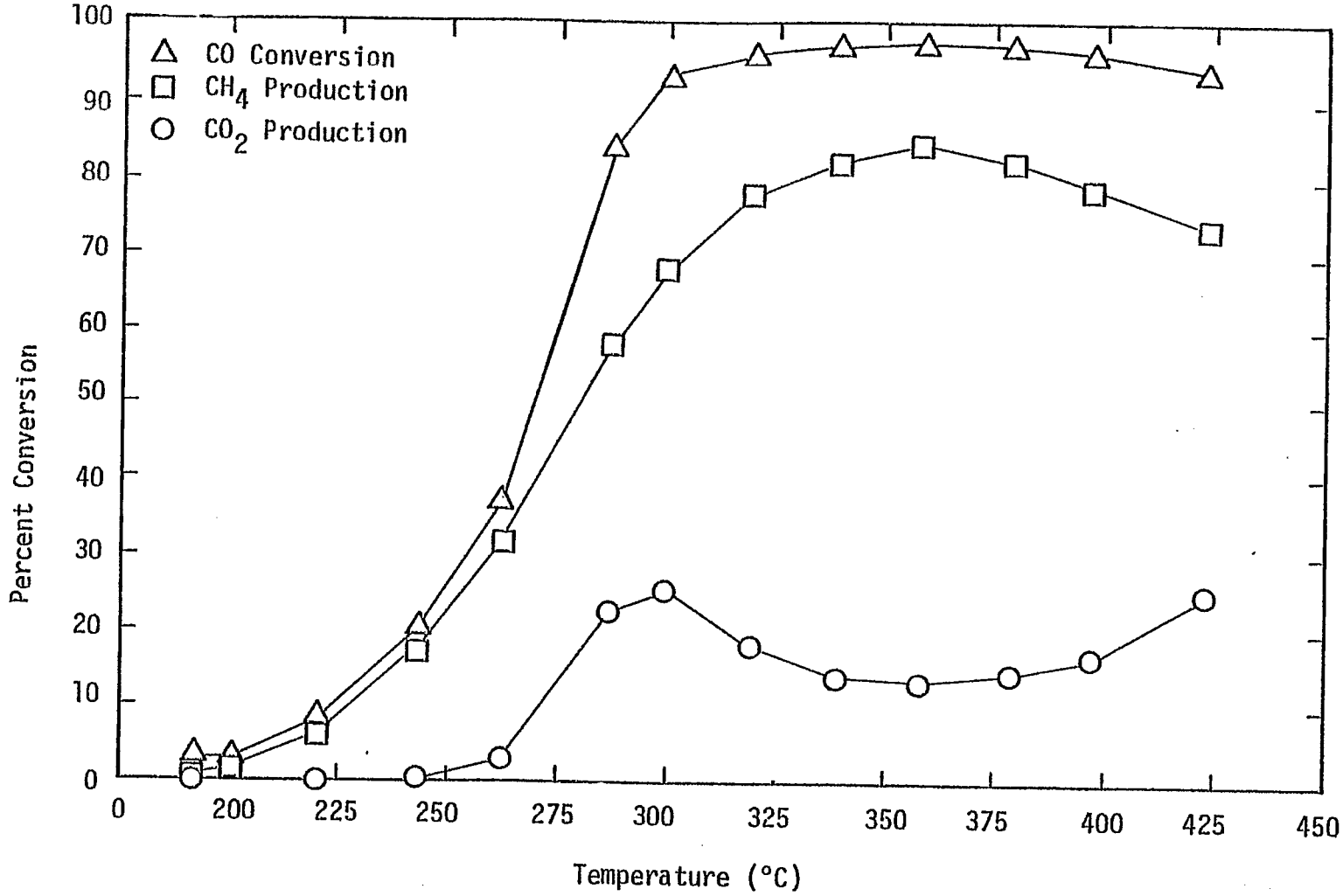

Figure 26. Conversion vesus temperature for Ni-Co-M-104 (5% Ni/5% Co/Al_2O_3/monolith) (20.5 psia, GHSV = 30,000 hr^{-1}).

those for pelleted catalysts (Table 11) reveals that the pelleted catalysts have 20-100% lower specific activities (on a per site basis). Similarly, comparison of the methane production at peak methane conversion on a per mass basis (Tables 18 and 23a) shows the monolithic catalysts to be 30-100% more active.

The Ni, Ni-Co and Ni-MoO_3 monolithic catalysts show behavior similar to that of the corresponding pelleted catalysts as far as temperature and conversion are concerned. The 50% conversion temperatures are about the same for pelleted and monolithic catalysts. The temperature at which the peak rate occurs varies between 320 and 375°C for both kinds of catalysts.

Nevertheless, certain of the monolithic catalysts do not reach a maximum conversion within the temperature range of the experiment. Particularly the Ni-Ru and Ni-Pt catalysts display a smaller conversion-temperature slope at lower temperatures and do not reach high conversion until much higher temperatures. The selectivity to methane at peak methane production is 60% for Ni-Ru and 77% for Ni-Pt and remains close to these values through most of the temperature range.

The Ni, Ni-Co, and Ni-MoO_3 monoliths, on the other hand, exhibit a steep jump in conversion around 275°C. Some of these catalyst samples show complete conversion for a wide range of temperature, as in Figure 27 for Ni-M-118. It is quite possible that those catalysts which can completely convert CO over a spread of 150 degrees or more may be able to exhibit high conversions at even higher space velocities than those studied, suggesting the monolithic catalysts may be ideal for a high throughput, recycle methanator.

Some of our data suggest that the performance of monolithic catalysts may be more sensitive to preparation technique and metal loading than to the kind of metal. Ni-M-107 was sintered in preparation and was not expected to perform well. Indeed, the conversion for Ni-M-107 is shifted towards higher temperature with respect to the other nickel monoliths, but its rate of peak methane production is comparable to the others, even though its selectivity is poor. Ni-Co-M-101 experienced a temperature excursion during reduction possibly due to the very exothermic decomposition of nitrate to ammonia. The data of Ni-Co-M-101 are similar to those for Ni-M-107. Ni-MoO_3-M-100 was simply low in metal content. In each of these three cases, the performance curves are shifted to higher temperatures, but the peak methanation rate is not affected. Thus, for the Ni, Ni-Co and Ni-MoO_3 monoliths, the differences in performance between the different catalysts are not as significant as the differences between samples of the same

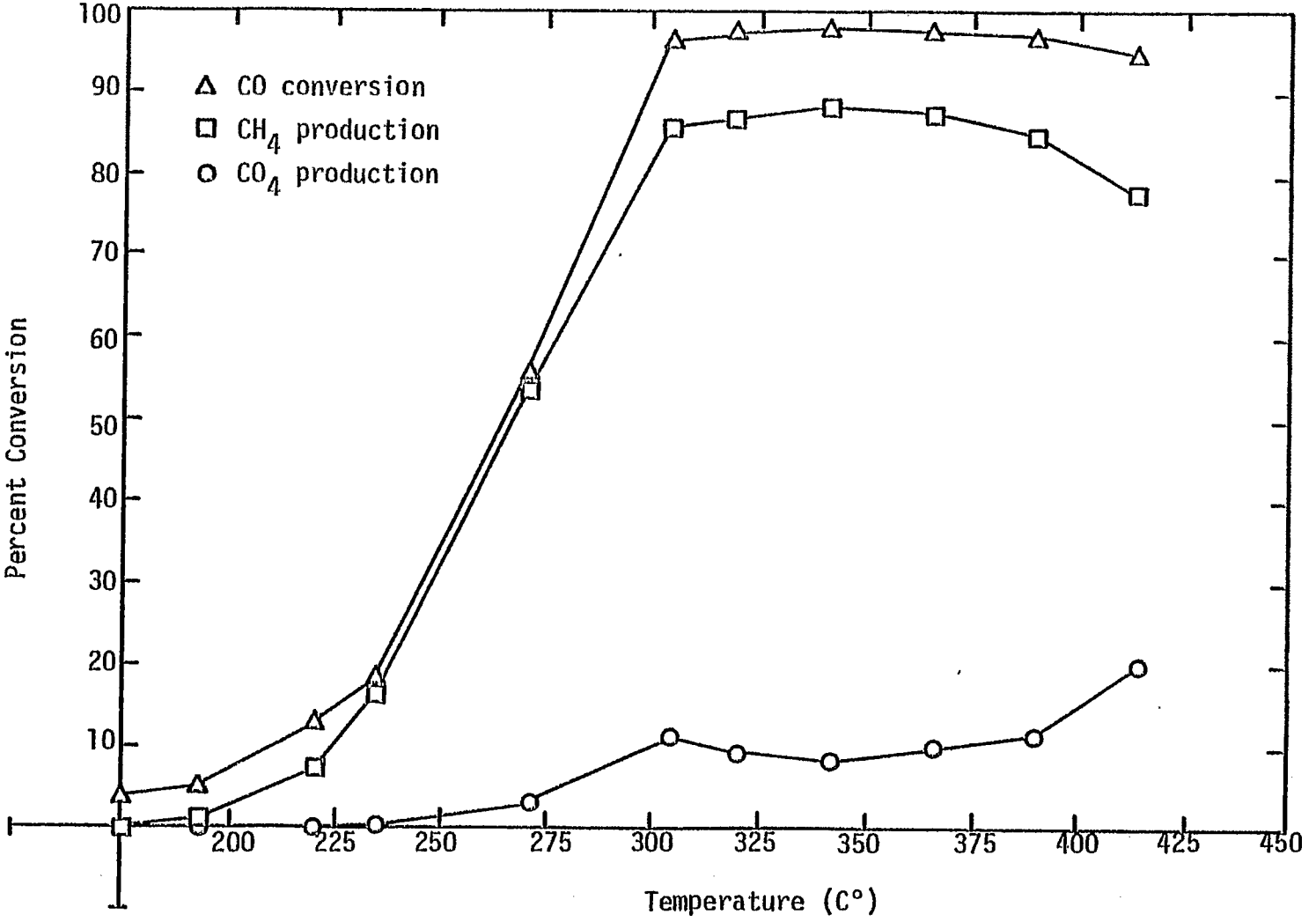

Figure 27 Conversion vs. temperature for Ni-M-118 (11% Ni/Al_2O_3/Monolith), 20.5 psia, GHSV = 30,000 hr^{-1}.

catalyst as a result of differences in preparation technique.

Nevertheless, the performance of the two Ni-Ru catalysts was surprisingly similar even though the preparation techniques were quite different. Ni-Ru-M-100 was accidentally soaked in tap water overnight and then washed in $NaCO_3$ solution, losing a significant amount of substrate in the process. Ni-Ru-M-108 was prepared using the standard preparation methods without washing to remove chloride. We had supposed that better performance might be obtained with chloride-free ruthenium. However, the data obtained thus far do not confirm our hypothesis. Nevertheless, there is a need to test a larger number of catalysts before we can be sure.

b. High Pressure Temperature-Conversion Tests. Table 23b lists the results of temperature-conversion tests conducted on nickel and nickel bimetallic monolithic catalysts at 25 atmospheres pressure. A typical conversion-temperature plot is shown in Figure 28. Generally, the effect of higher pressure is to shift the conversion curves toward lower temperatures while the selectivity to methane is improved. These data for monolithic catalysts are quite similar to those obtained for the corresponding pelleted catalysts at high pressure (compare Tables 20 and 23b). The rates of methane production at high conversions of CO are approximately the same for a given catalyst type in either pellet or monolithic form.

Ni-M-117 was tested at 50,000 hr^{-1} GHSV so as to gauge the effect of higher space velocity on conversion. The range of complete conversion was shifted to the right by about 50°C. More significantly, the rate of peak methane production was increased by about 75%. Again the potential of using monolithic catalysts in a high throughput methanator is emphasized.

Le Chatelier's principle states that at higher pressures, the reaction which decreases gas volume will be favored. Methanation reduces one volume of CO and three volumes of hydrogen to one volume each of water and methane, while the competing water gas shift, on the other hand, undergoes neither volumetric expansion nor contraction. Accordingly, the data for the high pressure tests indicate almost complete selectivity to methane. The turnover number at 225°C is two to three times higher at 25 atm than at 1 atm. As a kinetic comparison, however, one must take into account that the high pressure turnover number is based upon 30% conversion, while the low pressure turnover number was calculated for 10% conversion. Since diffusional effects would tend to lower the rate based on higher conversion, the actual difference in rates at high and low pressures could be even greater.

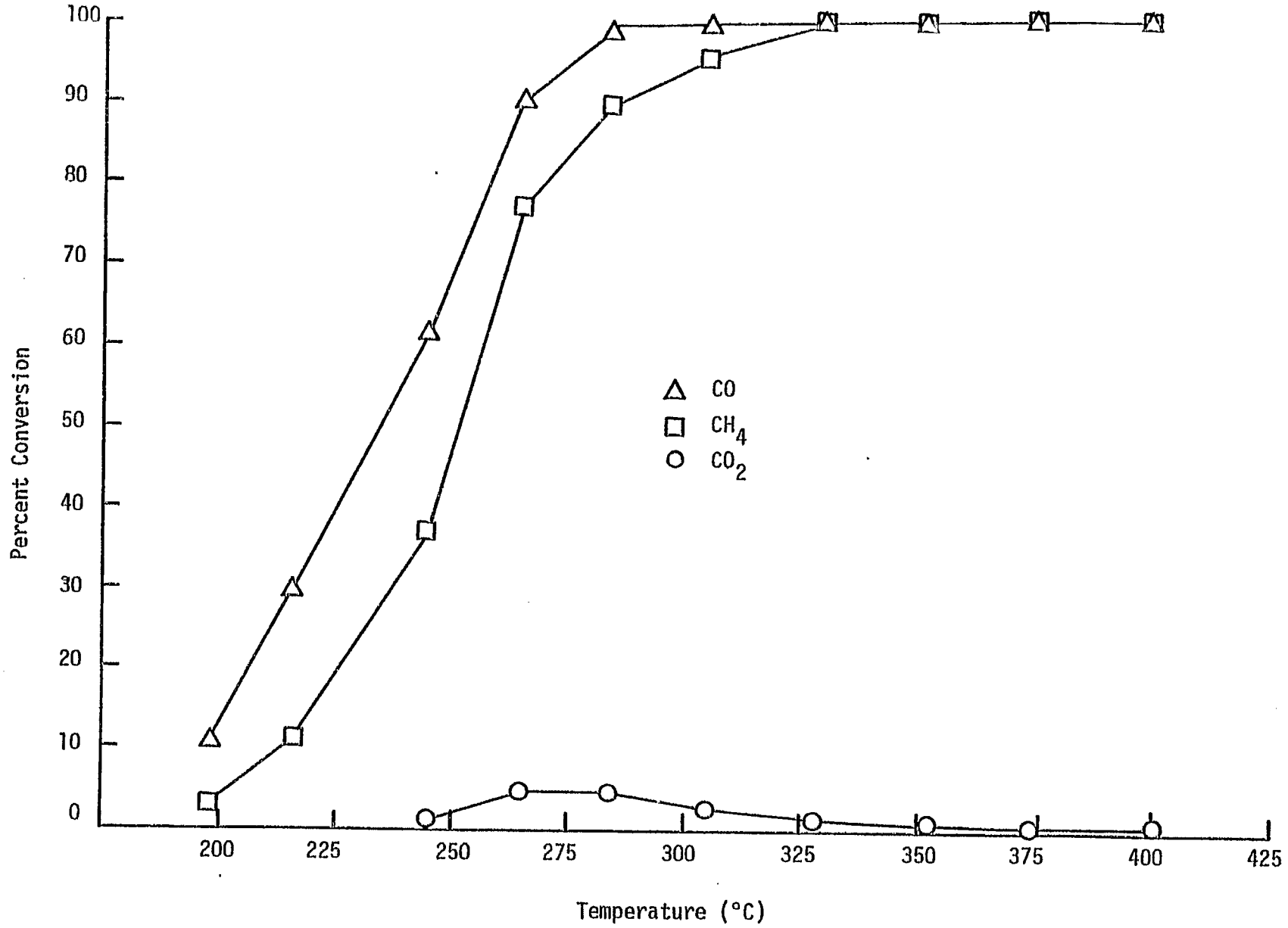

Figure 28. Conversion versus Temperature for Ni-Co-M-103 (4.5% Ni, 4.5% Co/Al_2O_3/monolith) (365 psia, 30,000 hr^{-1})

c. Integral Conversion Tests with Water Injection. Table 23c lists four tests performed on monolithic catalysts with a reactant stream composed of 95% N_2, 4% H_2, 1%CO on a dry mole basis with addition of 1% H_2O by volume. An example is shown in Figure 29. In many respects these tests were similar to the other low pressure integral tests at 30,000 hr^{-1} GHSV (Table 23c). However, upon addition of steam, the percentage of methane formed is about 25% less, and the selectivity to CO_2 is greatly increased. The methanation rate at peak production is in most cases 15-25% lower than in the absence of water and the turnover numbers at low conversions and 225°C are also lower. Again, as with the pelleted catalyst, it is surmised that much of the water reacted with carbon monoxide to form hydrogen and CO_2 by the water gas shift reaction.

In the absence of steam addition to the reactant stream, there is nevertheless some steam formed in the methanation reaction. Adding 1% steam to the reactants has the effect of holding the concentration of water vapor relatively constant in the high conversion case. That is, if 50% of the CO is changed to CO_2 and the other 50% to CH_4, as much steam is formed in methanation as is consumed in the shift reaction. Therefore the comparison between the 0% and 1% stream feed cases is actually between average concentrations of less than 0.5% and somewhat greater than 1% steam along the length of the monolith when operating at high temperatures and conversions.

d. Tests with Different Support Geometries. The purpose of this study was to provide comparisons of the performance of differently shaped monolithic supports and pellets in methanation. Cordierite ceramic supports were obtained from Corning Glass Works with three different channel geometries: 200 square channels per square inch of cross section, 300 squares per square inch and 236 triangular channels per square inch. These monoliths were prepared in a similar manner as the other Ni/Al_2O_3 monoliths. The results of methanation conversion-temperature tests for these monolithic catalysts at low pressure are given in Table 24, along with data obtained for some representative pelleted catalysts. The monolithic samples numbered 200 through 205 and 303 through 308 were prepared and tested first. However, samples in the triangular 200 series showed significant variations in nickel loading and also contained less nickel than corresponding samples of other geometries. Thus, additional samples were prepared under a more rigidly controlled technique. Each monolith (151, 154, 250, 252, 254, 350 & 351) was part of a batch handled in exactly the same manner, vis.: each alumina washcoat was dried at the same time in the same oven, each impregnation with nickel nitrate came from the same solution and the reduction in hydrogen at 450°C was carried out at the same time in the same cell. Even with these rigid controls, the conversion

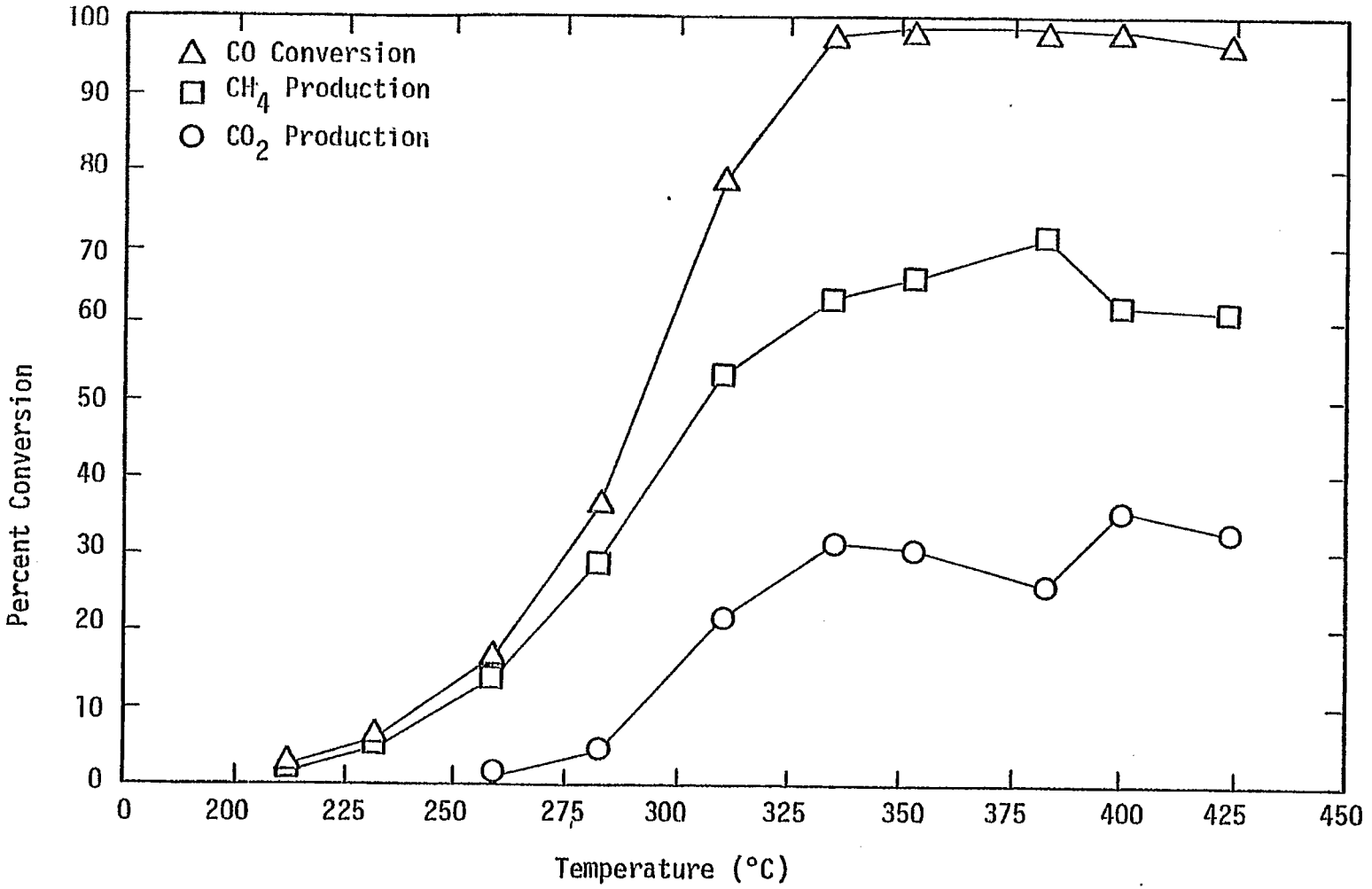

Figure 29. Conversion versus temperature for Ni-M-122 (20% Ni/Al_2O_3/monolith) (1% H_2O in feed, 20.5 psia, GHSV = 30,000 hr^{-1}).

TABLE 24

Summary of Temperature Conversion Tests of Different Catalyst Support Geometries

Catalyst	Support Geometry	Temperature for CO Conversion of 50%	Temperature for CO Conversion of 95%	At 95% CO Conversion % CO converted to CH_4	At 95% CO Conversion % CO converted to CO_2	At 325°C % CO converted to CH_4	At 325°C Rate of CH_4 Formation (Moles/gram-sec x 10)
a. The following 18 tests were conducted at 30,000 hr^{-1} GHSV of 95% N_2, 4% H_2 and 1% CO, 20.5 psia and 250 to 400°C)							
Ni-M-151	square channelled monolith,	245	295	93	6	93	36
Ni-M-154	200 /in^2	260	310	83	5	93	37
Ni-M-200	triangular channelled monolith,	285	325	76	17	76	44
Ni-M-201	236 /in^2 (loadings range 4-9%	285	350	70	12	74	46
Ni-M-204	Ni)	---	---	--	--	82	51
Ni-M-205		280	320	78	15	80	51
Ni-M-250	triangular channels (loading	250	320	87	7	86	44
Ni-M-252	22% Ni)	250	300	86	10	92	47
Ni-M-254		255	300	83	10	91	46
Ni-M-303	square channels, 300 /in^2	260	350	83	11	83	38
Ni-M-304	(20% Ni)	260	310	85	11	99.6	44
Ni-M-305		255	315	85	8	90	44
Ni-M-308		255	300	85	9	99.6	42
Ni-M-350	square channels, 300 /in^2	270	315	80	12	87	40
Ni-M-351	(19% Ni)	250	295	84	8	94	39
Ni-A-116	1/8" beads (14% Ni)	280	340	70	11	65	38
Haldor Topsoe TX-7-70-X52	extrudites, 5 mm DIA x 15 mm	305	423[a] (79%)	60[a]	17[a]	48	20
Girdler T-310	cylinders, 5mm DIA x 3 mm	325	418[a] (79%)	57[a]	18[a]	44	9.9
Girdler G-87	extrudites, 1/8" DIA x 3/8"	275	400[a] (91%)	69[a]	15[a]	63	27

TABLE 24 continued

b. The following tests were conducted at 15,000 hr^{-1} GHSV of 95% N_2, 4% H_2 and 1% CO, 20.5 psia and 200 to 400°C

Ni-M-101[b] Run 1	square channelled monolith,	230	270	83	5.0	100	8.7
Run 2	200 /in^2, 3" long	230	270	94	3.5	99.7	8.7
Ni-M-113[b]	square channelled monolith, 200 /in^2, 1/2" long	255	290	88	7.7	97	26.5
Ni-A-112	1/8" pellets with various	265	350	74	20	71	27
Ni-A-116	nickel loadings and alloy	220	280	84	10.5	90	28.6
Ni-Co-A-100	compositions	215	265	76	19	84	25
Ni-MoO_3-A-101		270	375[a](86%)	70[a]	17[a]	72	27
Ni-Pt-A-100		240	375[a](84%)	70[a]	13[a]	73	23
Ni-Rh-A-100		310	400[a](81%)	64[a]	16[a]	49	16.7
Ni-Ru-A-100		315	400[a](73%)	58[a]	16[a]	49	18.3
Co-A-100	240	305	68	26	71	22.8	
Engelhard Ru	cylinders 1/8" x 1/8"	365	425[a](82%)	60[a]	21[a]	11	8.1
Girdler G-87	extrudites, 1/8" DIA x 3/8"	190	245	81	13	79	18.0

[a] These catalysts did not acheive 95% CO conversion within the temperature range studied, (200-400°C). The % in parenthesis indicates the highest % CO conversion obtained.

[b] Ni-M-101 is twice as dense as Ni-M-113. Rates expressed per gram of catalyst.

data for both batches (except for samples 200-205) are the same within experimental error. Larger differences exist between monoliths of the same geometry than between the different geometries. The monoliths with triangular holes, however evidence significantly larger rates of methane production on a per mass basis.

Four pellet-supported catalysts were also examined under the same reaction conditions. The 14% Ni/Al_2O_3 1/8 inch beads (Ni-A-116) show a significantly lower conversion of CO to CH_4 compared to the monoliths, having a corresponding metal loading, i.e., the yield of methane at 95% CO conversion was 70% for the Ni-A-116 compared to 80-90% for most of the monolithic catalysts. The rate of methane production for the Ni/Al_2O_3 beads is comparable to that for the monoliths with 200 squares/square inch but lower than the rates observed for other geometries. Three commercial nickel catalysts were also tested and the data are included in Table 23. The first two commercial pellet samples (containing 11-12% Ni/Al_2O_3) and the commercial methanation catalyst (about 30% Ni) were significantly less active than either the monoliths or the Ni-A-116 beads. Indeed, at 325°C, the rates of methane production under conditions of high conversion were only half to one fourth of the rates obtained for the monolithic catalysts.

Table 24b contains the results of tests conducted at 15,000 hr^{-1} GHSV for both monolithic and pellet supported catalysts. The effect of halving space velocity is to halve methanation rate, as expected for the mass-transfer-limited case. The monolithic nickel catalysts show 97-100% conversion of CO to CH_4 at 325°C compared to 70-90% conversion for the two pelleted nickel catalysts. The commercial nickel catalyst (G-87) has a rate per gram about 30% lower than the monolithic nickel catalyst (Ni-M-113) and our 14% Ni/Al_2O_3 (Ni-A-116). The 0.5% Ru/Al_2O_3 is apparently the least active and selective for methane production of the catalysts tested.

E. Task 5: Technical Visits and Communication

1. Accomplishments. During the past two years the principal investigator has established technical communications with quite a number of other workers active in methanation catalysis, many of whom are listed on the Report Distribution List in Appendix B. Private communications in the form of letters, phone calls, visits, exchange of preprints, and informal discussions at meetings have been very helpful in keeping up-to-date and comparing important results while avoiding unnecessary duplication.

The principal investigator was Secretary-Treasurer of the California Catalysis Society during the first year and is presently the Task Force Leader for Metal Surface Areas on the ASTM D-32 Catalyst Committee. These professional duties bring the principal investigator directly in contact with others working in catalyst characterization, surface area measurement, and methanation catalysis, all pertinent to this present investigation.

At the beginning of the first quarter the principal investigator attended the Symposium on Catalytic Conversion of Coal held April 21-23, 1975 in Pittsburgh. The experience was valuable in terms of direct private contacts and communications with other workers in methanation catalysis and informative presentations dealing directly with methanation catalysis and other catalytic aspects of coal conversion.

During the second quarter the principal investigator and Mr. Kyung Sup Chung attended the ERDA/EPRI/NSF-RANN Contractors Conference held October 22-23, 1975 in Park City, Utah. The experience was very useful because of direct private conversations with other workers in coal conversion and informative presentations outlining other coal conversion projects. Preliminary arrangements to visit other laboratories were initiated during this meeting.

During the third quarter the principal investigator attended the California Catalysis Society Meeting held November 7-8, 1975 in Pasadena where he engaged in fruitful discussions with other investigators regarding hydrogen and carbon monoxide chemisorption on nickel. The PI also presented a paper "Chemistry of Nickel-Alumina Catalysts," at the 68th Annual AIChE meeting in Los Angeles held November 16-22, 1975 and attended a short course dealing with "Catalyst Deactivation." The short course was rigorous, informative and quite pertinent to our present poisoning work.

Dr. Bartholomew was symposium chairman for the First Rocky Mountain Fuel Symposium held January 30, 1976 at Brigham Young University. The symposium featured 24 different speakers in discussions of coal gasification, oil shale, and tar sand research and development. One of these was a talk by Mr. Blaine Barton entitled "Alloy Catalysts for Methantion of Coal Synthesis Gas." based on kinetic data from this study.

During the fourth quarter, the principal investigator, Mr. Joseph Oliphant, and Mr. Richard Pannell (both students supported by NSF) attended the Spring Meeting of the California Catalysis Society where Mr. Pannell presented a paper dealing with H_2 and CO adsorption on nickel powder. Dr. Bartholomew has also participated in the organization of the new Utah Consortium for Energy Research and is involved as a member of the catalysis committee. The committee has plans to

prepare joint University of Utah-BYU proposals in the Fossil Fuels area and to organize a center of excellence in catalysis.

During the fifth quarter Dr. Bartholomew attended the ASTM catalyst committee meeting held May 17-18 at the National Bureau of Standards in Washington D.C. The primary involvement of the PI at this meeting was in committee discussions to establish standards for measuring Pt and Ni metal surface areas. A procedure was proposed for measuring Ni areas, based on work performed in this study and the related NSF study. While at NBS Dr. Bartholomew toured the surface chemistry facilities and discussed methanation research with Dr. John Yates of NBS. While in Washington, Dr. Bartholomew visited with Dr. Mike Biallis of ERDA to discuss progress during the past year and ideas for a follow-on proposal. During the same trip the PI made one day visits to three other methanation laboratories: (1) Carnegie-Mellon University, (2) The Pittsburgh Energy Research Center, and (3) The Institute of Gas Technology (IGT).

At Carnegie-Mellon University Dr. Bartholomew discussed with Professor Anthony Dent the latter's ERDA-supported investigation of catalytic hydrocarbon synthesis (methane included) and toured his laboratory.

The visit to the Pittsburgh Energy Research Center (PERC) included discussions with Dr. Fred Steffgen, supervisor of chemical research and two members of his group, Dr. Charles Kibby and Dr. Richard Wiffenbach. The afternoon was spent in visiting with Dr. Michael Baird and Dr. Richard Schehl of Dr. Bill Haynes group and in touring screening, bench scale, and pilot plant facilities for testing methanation catalysts (mainly of the sprayed Raney-nickel variety). Because of the obvious similarity of the parallel plate configuration used at PERC to the monolithic catalysts in this study, arrangements were made with Dr. Baird and Dr. Haynes to spray Raney Ni on a parallel plate configuration to be constructed and subsequently tested at BYU.

At IGT Dr. Bartholomew visited with Mr. Tony Lee, the principal researcher in methanation. The discussion was centered on procedures for testing catalysts and on evaluations to qualify catalysts for industrial use, particularly in the Hygas process. The possibility of having catalysts from this study tested at IGT was also discussed.

The Gordon Research Conference on Catalysis held June 28 to July 2 was as usual top quality. The talks and discussions were generally very good and some quite pertinent to coal research. The PI had ample opportunity to discuss methanation catalysis with other attendees, including about a dozen who are doing methanation-related research. Arrangements were made with several of these researchers to exchange reports, papers and data. Dr.

Bartholomew also presented a minitalk (10-15 min.) dealing with adsorption stoichiometries on Ni based on the NSF work and obtained feed back useful in both the NSF and ERDA studies.

During the sixth quarter, the principal investigator, Dr. Bartholomew, presented two invited papers dealing with activities and kinetics of nickel and nickel alloys methanation catalysts at the Centennial Meeting of the American Chemical Society held August 30 - September 3 in San Francisco. One of these papers presented at the methanation symposium in the Division of Fuel Chemistry, summarized results of activity tests performed under this contract. On September 2, he visited with Henry Wise, Jon McCarty, Kenneth Sancier, and Bernard Wood at SRI in Menlo Park regarding various aspects of methanation catalysis and toured their laboratories. This was followed with a short visit to Stanford University to discuss alloy catalysis with members of Professor Boudart's research group. On September 3 and 4 Dr. Bartholomew participated in the ERDA sponsored University Contractors' Conference in Golden, Colorado.

On October 14, Dr. Bartholomew was invited by the Department of Fuels Engineering at the University of Utah to present a seminar on Methanation Studies performed at BYU. While at the University of Utah he also visited with Professors Massoth and Oblad, toured the catalysis research laboratories of Professor Oblad, discussed plans for the 2nd Rocky Mt. Fuel Symposium with Professors Massoth and Wood, and attended a Seminar given in the Chemistry Dept. by Professor Michel Boudart of Stanford. The following day Professor Boudart visited BYU; an informal seminar was held in which recent studies at both BYU and Stanford were discussed.

Other visitors to BYU included Mr. Tony Lee of IGT (September 22), Mr. Bill Boyer of Corning Glass Works (October 27) and Mr. Robert Wade of Ventron Corporation (October 28). Mr. Lee presented a seminar in which he discussed testing of methanation and water-gas-shift catalysts. Possible testing at IGT of catalysts developed at BYU was also discussed. The visit with Mr. Boyer focused on continued cooperative efforts between Corning Glass Works and BYU. Arrangements were made to obtain additional monolithic supports. The discussion with Mr. Wade focused on sulphur-resistant catalysts such as nickel and cobalt borohydrides.

Also during the sixth quarter, a publication based on work performed during the 2nd quarter, "Methanation Activity of Suported Nickel Alloys" was published in the Preprints of the ACS Divsion of Fuel Chemistry (Vol. 21, No. 4). A proposal to continue this contract work an additional two years was completed and submitted during the sixth quarter. The preparation of the proposal involved extensive

searches of the literature dealing with methanation catalysis, sulphur poisoning, carbon deposition, and sintering.

During the seventh quarter the principal investigator, Dr. Bartholomew, attended the ASTM D-32 Catalyst Committee Meeting held November 15 and 16 in Oakridge, Tennessee where he presented a summary of nickel surface area measurements obtained at Brigham Young University and other laboratories. On November 17, Dr. Bartholomew visited with Drs. Larry Campbell and Robert Farrauto of Catalyst and Chemicals Research, Engelhard Industries, Edison, New Jersey where he presented a seminar on "Methanation - Alloys and Sulfur Poisoning." The seminar was followed by a tour of the catalyst research laboratories and discussions regarding characterization of catalysts.

On November 18, Dr. Bartholomew was the guest of Mr. Ralph Beaty, Director of Engineering Research, Continential Oil Company, Ponca City, Oklahoma where he also toured research facilities, visited with Paul Poynor, Research Group Leader, Joseph Kleinpeter, Manager of Liquifaction Research, and John Dew, Director of Fuels Technology Development, and presented a seminar entitled "Methanation Catalyst Activities of Alumina-Supported Nickel and Alloys."

Dr. Bartholomew was also invited by the Department of Chemical Engineering, University of Idaho (Moscow) to visit and present a research seminar on December 9, 1976. In addition to the seminar on "Kinetic Studies of Alloy Methanation Catalysts," he held discussions with faculty members including Professor Bill Thomson, who is actively pursuing methanation research.

Also, during the seventh quarter, a paper entitled, "The Stoichiometry and Poisoning by Sulfur of Hydrogen, Oxygen, and Carbon Monoxide Chemisorption on Unsupported Nickel," was accepted by the Journal of Catalysis. A note entitled "Crystallite Size, Support, and Alloying Effects in Methanation on Nickel," was also submitted to the same journal. Both papers are based on research supported by NSF and this contract. Two large publications dealing with effects of H_2S on CO and H_2 adsorption and with methantion activities of alloy catalysts are still in preparation.

During the eighth quarter the principal investigator and six students attended the 2nd Rocky Mountain Fuel Symposium held February 17 and 18 at the Salt Lake Hilton. Dr. Bartholomew was symposium co-chairman and Mr. George Jarvi presented a paper entitled "Investigation of Nickel and Nickel-Alloy Monolithic Methanation Catalysts" based on research supported by this contract. A business meeting was held on February 17 to organize the Rocky Mountain Fuel Society, and Dr. Bartholomew was elected to the organizing committee with Dr. Frank Massoth and Dr. Ralph Coates.

On February 24, 1977, Dr. Bartholomew participated in a faculty lecture series by presenting an address entitled: "What Can Be Done About the Energy Crisis,". Copies of this address were sent to Utah Senators, Congressmen, the Governor of Utah, Dr. James Schlesinger and President Jimmy Carter.

On March 16, Dr. Bartholomew visited by invitation the Department of Chemical Engineering at the University of Wisconsin at Madison where he visited with faculty members and presented a seminar on methanation kinetics and catalyst poisoning based on work supported by NSF and this contract. Discussions were held with Professor James Dumesic, active in catalysis research.

At the Spring meeting of the California Catalysis Society (Menlo Park, Calif.) March 31 - April 1, Dr. Bartholomew presented a paper on "Magnetic Studies of Supported Platinum-Iron Alloys" based on research performed during his graduate studies at Stanford. Several other papers of pertinance to methanation and alloy catalysis were presented.

At the end of the eighth quarter, Mr. Richard Pannell and Dr. Bartholomew attended the North American Catalysis Society Meeting in Pittsburgh (April 26-28) where they presented papers on sulfur adsorption and methanation kinetics and poisoning studies based on NSF and ERDA-supported research. There were also many other interesting and pertinent papers and private discussions relating to our research too.

While in Pittsburgh, Dr. Bartholomew participated in the April 28-29 meeting of the ASTM D-32 Catalysts Committee. The following Monday (May 2) Dr. Bartholomew visited the Ventron Corporation where he was invited to present a seminar on methanation catalysis research and tour research facilities. He discussed with Ventron research personnel the possibilities of a joint research program in the study of Ni and Co borides for methanation. He was also recently in telephone communication with personnel at Climax Molybdenum Corporation about obtaining some new Co and Mo alloys for testing.

On July 1, Dr. Gerald Krulik of Borg-Warner chemicals visited BYU and presented a seminar on electroless plating of nickel and its possible application to catalysis. He left some plating solution which was used to coat nickel metal on monolithic and pellet supports. These catalyst samples will be tested for methanation activity.

Mr. Erek Erekson, Ph.D. candidate, attended a Gas Chromatography Short Course on July 27-29 at the University of Utah. He learned gas chromatographic techniques that will be useful in the continuation of this study. During the week of August 1-5, Dr. Bartholomew attended a special conference of Chemical Engineering Educators in Snowmass,

Colorado, where he discussed curriculum relating to kinetics, catalysis and surface chemistry.

On August 24, Dr. Bartholomew visited with personnel at Bituminous Coal Research regarding a program to test fluidized methanation catalysts. While in Pittsburgh he attended the ERDA/EPRI University Contractors Meeting (August 25-26) where he presented a summary of accomplishments during the past two years of this study.

He later attended the 174th National Meeting of the American Chemical Society held August 28 to Septmber 2 in Chicago, at which he presented a paper entitled, "Sintering of Nickel-Alumina Catalyst." He also visited with research personnel at the Institute of Gas Technology and the IIT Research Institute while in Chicago. While at IGT he discussed recent developments in methanation catalysis with Mr. Tony Lee.

Recent visitors to our laboratory included Drs. Ed Tucci and George McQuire of Matthey-Bishop, Inc. (August 17) who discussed with Dr. Bartholomew the potential application of noble metal catalysts in methanation. Apparently there is not a shortage of ruthenium for such applications. Arrangements were made for our laboratory to obtain chloride free salts of the noble metals and to test some of the MBI catalysts for methanation.

Professor Alex Bell of Berkeley (Dept. of Chemical Engineering) visited our department on September 8, visited with faculty, toured our laboratories and presented a seminar on I.R. Applications in Catalyst Study. This also provided an opportunity for Drs. Bell and Bartholomew to bring each other up-to-date on their respective methanation programs. Mr. Fred Hoover and Dr. Larry Guilbault visited on September 14 to review our investigation of borohydride reduced catalysts for methanation.

Altogether the visits, meetings, presentations, and interactions with other workers have stimulated many useful interchanges of up-to-date, pertinent information regarding the project. We have recently received quite a number of requests for copies of our quarterly reports and are presently in close communication with more than 20 other methanation laboratories in the United States and Europe.

2. Student Participation. During the first two years and the four month contract extension period, eight graduates and seven undergraduates have contributed to progress of this project. Three students have completed master thesis research on this project, three other students have master's thesis research in progress, and two students have Ph.D. dissertation research in progress.

IV. CONCLUSIONS

1. Hydrogen adsorption at 25°C is generally a reliable means of measuring metal surface area and the number of active sites for methanation. However, in the case of Ni-Mo/Al_2O_3 catalysts, the nickel sites adsorb both H_2 and CO, whereas the MoO_3 sites do not. Hence, H_2 and CO adsorption techniques are not useful for measuring the active molybdenum oxides sites.

2. Carbon monoxide adsorption on nickel is an unreliable technique for measuring nickel surface area in view of (1) considerable variation in adsorption uptakes resulting from modest variations in equilibration pressure and temperature, (2) formation of $Ni(CO)_4$ causing significant loss of nickel from the catalyst, and (3) extensive physical and chemical adsorption of carbon monoxide on the alumina support requiring large corrections to the data with corresponding losses in accuracy.

3. Data for CO adsorption on a nickel powder at 25°C show a CO/H value of 1.74 suggesting surface carbonyl formation. After evacuation at 25°C, however, the ratio decreases to 0.76, showing that reversible adsorption-desorption occurs. A value of CO/H of 0.76 is also obtained at -83°C before and after pumping at the low temperature indicating no reversible adsorption. Our procedure of measuring CO adsorption at -83°C avoids complications due to either carbonyl formation or reversible CO adsorption.

4. Hydrogen adsorption data at 25°C show that alumina-supported nickel and nickel bimetallic catalysts prepared in this study generally have higher surface areas and dispersions than commercial methanation catalysts. Since these catalysts were prepared by reduction at 450°C for 12-16 hours, they are quite thermally stable over a period of hours (in some instances days) under typical reaction conditions (225-450°C).

5. The effect of exposure to 10 or 25 ppm H_2S in H_2 at 450°C of nickel or ruthenium catalysts is to lower the amount of H_2 adsorbed at 25°C. The observed decrease in hydrogen adsorption for a catalyst after exposure to H_2S may be a qualitative measure of its resistance to sulfur poisoning. Generally the loss of metal surface area during exposure to H_2S is linear with time. However, Ni-MoO_3/Al_2O_3 shows unusual behavior by adsorbing within 3-6 hours enough H_2S to block 40-45% of the hydrogen adsorption sites after which there is no further significant adsorption of H_2S within the next 6-12 hours. Ni-Pd, Ni-Co, and Pd-Ru catalysts lose a smaller percentage of surface area after exposure to 10 ppm H_2S for 12 hours than other nickel or ruthenium containing catalysts possibly indicating higher resistance

to sulfur poisoning in terms of adsorption capacity.

6. The effect of exposure to 10 or 25 ppm H_2S in H_2 at 450°C on nickel catalysts is to increase the amount of CO adsorbed at -83°C. The increase in carbon monoxide adsorption after exposure to H_2S may be explained by either $Ni(CO)_4$ formation or the formation of a $(CO)_xS$ complex which after formation migrates to the support. Our observations favor the formation of $Ni(CO)_4$, possibly catalyzed by surface sulfur.

7. X-ray diffraction measurements to determine phase composition and crystallite sizes of alumina-supported nickel and nickel alloys are feasible if a sensitive instrument is available and if the signal-to-noise ratio is increased by runnng at very slow rate or by counting at fixed angles. Diffraction data for nickel and ruthenium alloys suggest that the metals are probably in solid solution (i.e., exist as alloys). Particle sizes calculated from x-ray line broadening are generally 10-30% smaller than those calculated from hydrogen chemisorption data for nickel and nickel alloys. This observation may be explained by considering that some of the nickel or other metal sites are not reduced completely to the metal. Comparison of nickel crystallite diameters calculated from H_2 chemisorption, x-ray diffraction line broadening and transmission electron microscopy shows good agreement for 15 and 25% Ni/Al_2O_3. This confirms that hydrogen adsorbs dissociatively on supported nickel with a stoichiometry of one hydrogen atom per nickel surface atom.

8. Steady-state conversions measured at 225 and 250°C, 1 atm and space velocities of 30,000 and 60,000 hr^{-1} indicate that very nearly differential (low conversion) conditions obtain only for low (3-6 wt.%) metal loading catalysts. Activity data for 15-20 wt.% metal/Al_2O_3 catalysts are influenced by pore diffusional limitations. Nevertheless, the turnover numbers for both 3 and 14% Ni/Al_2O_3 agree to within a factor of 2 with data from the literature for 5% Ni/Al_2O_3.

9. Alumina-supported Co, Ni-Co, Ni-Mo and Ni are the most active catalysts on a per surface area basis. A 14 wt. % Ni/Al_2O_3 prepared in this study is the most active catalyst on a per mass basis--even more active than a commercial 32 wt.% Ni/Al_2O_3 catalyst, probably because the 14% catalyst has a higher nickel surface area.

10. Conversion versus temperature data indicate that a commercial nickel catalyst (G-87) attains a maximum methane production of 80% at 250-300°C compared to a production of 90% for a 14 wt.% Ni/Al_2O_3 catalyst prepared in this laboratory. The higher selectivity for the latter catalyst is possibly a result of its higher state of reduction to

metallic nickel.

11. In comparison with pellet-supported nickel catalysts, monolithic supported nickel catalysts are 30-40% more active on a per mass basis at high conversions and approximately twice as active on a turnover number basis at low conversions. Moreover the monolithic nickel catalysts are significantly more selective for production of methane. Thus, monolithic-supported catalysts are especially attractive for achieving high conversions of CO to CH_4 in a high throughput recycle methanator.

12. Turnover numbers at 225 and 250°C for nickel and nickel bimetallic catalysts show that alloying other catalytic metals with nickel has a relatively modest but nevertheless significant effect on activity. Increases or decreases in specific activity generally range from 0 to 200%. However, a factor of 2 increase in rate can be translated into a factor of 2 decrease in reactor size, resulting in substantial savings for a 50 million dollar methanation plant. The key consideration, moreover, is stability, i.e. how the different bimetallic catalysts maintain their activity over long periods of time relative to nickel catalysts. There could be orders of magnitude difference in rates after a period of days under severe reaction conditions. The objectives of the next two years of investigation include a more thorough investigation of stability for the most promising bimetallics of nickel and ruthenium.

13. The effect of a 12-24 hour preexposure to 10 ppm H_2S in H_2 is to increase the specific catalytic activity (turnover number) based upon the remaining unpoisoned sites for 20 wt.% Ni-Co, Ni-Ru, and Ni-MoO_3 catalysts. These results model the behavior of these catalysts in response to a plant upset in which the catalyst bed is exposed to 10 ppm H_2S over a period of hours sufficient to poison a portion of the bed. Of course, these results will be followed up with long term activity tests with H_2S in the reactant stream.

14. Addition of steam to reactants for methanation ($H_2O/CO = 1$) substantially increases the rate of CO conversion to CO_2 while lowering the production of methane by 30-40%. Presumably steam serves to increase the rate of the water gas shift reaction relative to the methanation reaction.

15. Steady state activity tests over a period of 12-24 hours at 400-450°C ($H_2/CO = 2$) show that alumina-supported Ni, Ni-Co, Ni-Pt, Ni-Rh, and Ni-Ru lose 30-50% of their activity, presumably due to deposition of carbonaceous material. Ni-Pt and Ni-Co may be slightly more resistant than nickel to carbon deposition. Ni-MoO_3/Al_2O_3 completely deactivates within a few hours.

16. The effects on methanation reaction rate of increasing pressure from 1 to 25 atmospheres are reasonably modest. The rate per gram of catalyst at high conversion is increased for most nickel containing catalysts by factors of 2 to 2 1/2. Turnover numbers at low conversions are increased by factors of 4 to 5. Nevertheless these effects are clearly large enough to warrent industrial operation at higher pressures.

V. REFERENCES

1. M. Greyson, "Methanation" in "Catalysis" Vol. IV., ed. P.H. Emmett, Rheinhold Pub. Corp., New York, 1956.

2. G.A. Mills and F.W. Steffgen, "Catalytic Methanation," Catalysis Reviews 8, 159 (1973).

3. C.H. Bartholomew, "Alloy Catalysts with Monolith Supports for Methanation of Coal-Derived Gases," Quarterly Technical Progress Report Fe-1790-1 (ERDA), August 6, 1975.

4. C.H. Bartholomew, "Alloy Catalysts with Monolith Supports for Methanation of Coal-Derived Gases," Quarterly Technical Progress Report FE-1790-2 (ERDA). Nov. 6, 1975.

5. C.H. Bartholomew, "Alloy Catalysts with Monolith Supports for Methanation of Coal-Derived Gases," Quarterly Technical Progress Report FE-1790-3 (ERDA), Feb. 6, 1976.

6. C.H. Bartholomew, "Alloy Catalysts with Monolith Supports for Methanation of Coal-Derived Gases," Annual Technical Progress Report FE-1790-4 (ERDA) May 6, 1976.

7. C.H. Bartholomew, "Alloy Catalysts with Monolith Supports for Methanation for Coal-Derived Gases," Quarterly Technical Progress Report FE-1790-5 (ERDA) Aug. 6, 1976.

8. C.H. Bartholomew, "Alloy Catalysts with Monolith Supports for methanation of Coal-Derived Gases," Quarterly Technical Progress Report FE-1790-6 (ERDA), Nov. 6, 1976.

9. C.H. Bartholomew, "Alloy Catalysts with Monolith Supports for Methanation of Coal-Derived Gases," Quarterly Technical Progress Report FE-1790-7 (ERDA), Feb. 6, 1977.

10. C.H. Bartholomew, "Alloy Catalysts wtih Monolith Supports for Methanation of Coal-Derived Gases," Quarterly Technical Progress Report FE-1790-8 (ERDA), May 6, 1977.

11. R.J. Farrauto, "Determination of Catalytic Surface Area Measurements," AIChE Symposium Series, 70, No. 143, 9-22 (1975).

12. C.H. Bartholomew and R.J. Farrauto, " Chemistry of Ni/Al_2O_3 Catalysts," J. Catal. 45, 41 (1976).

13. C.H. Bartholomew, "New Catalysts for Methanation," NSF Final Report, ENG-75-00254.

14. C.H. Bartholomew and M. Boudart, "Surface Composition and Chemistry of Supported Platinum-Iron Alloys," J. Catal. 29, 178 (1973).

15. C.E. O'Neill, Ph.D. Thesis, Columbia University, 1961.

16. A.W. Aldag and L.D. Schmidt, J. Catal., 22, 260 (1971).

17. J.J.F. Scholten, and A. Van Montfoort, J. Catal., 1, 85 (1962).

18. J. Freel, J. Catal., 25, 149 (1972).

19. T.A. Dorling and R.L. Moss, J. Catal., 7, 378 (1967).

20. D. Cormack and R.L. Moss, J. Catal., 13, 1 (1969).

21. W.B. Pearson, "A Handbook of Lattice Spacings and Structures of Metals and Alloys," Pergamon Press, New York, N.Y. (1956).

22. D. Stowell, Master's Thesis, Brigham Young University, 1976.

23. M.A. Vannice, "The Catalytic Synthesis of Hydrocarbons form H_2/CO Mixtures Over the Group VIII Metals," J. Catal. 37, 449 (1975).

24. R.A. Dalla Betta, A.G. Piken, and M. Shelef, "Heterogeneous Methanation: Steady-State Rate of CO Hydrogenation on Supported Ruthenium, Nickel, and Rhenium," J. Catal., 40, 173 (1975).

U.S. DEPARTMENT OF COMMERCE
Technology Administration
National Technical Information Service
Springfield, VA 22161 (703) 605-6000